Investigation of Standing Up Strategies and Considerations for Gait Planning for a Novel Three-Legged Mobile Robot

Ivette M. Morazzani

Thesis submitted to the Faculty of the
Virginia Polytechnic Institute and State University
in partial fulfillment of the requirements for the degree of

Master of Science
in
Mechanical Engineering

Dennis W. Hong, Chair
Alfred L. Wicks
Corina Sandu

April 30, 2008
Blacksburg, Virginia

Keywords: Three-Legged Robot, Robot Locomotion, Standing Up Strategies, Gait Planning, Stability, Kinematics

Investigation of Standing Up Strategies and Considerations for Gait Planning for a Novel Three-Legged Mobile Robot

Ivette M. Morazzani

(ABSTRACT)

This thesis addresses two important issues when operating the novel three legged mobile robot STriDER (Self-excited Tripedal Dynamic Experimental Robot); how to stand up after falling down while minimizing the motor torques at the joints and considerations for gait planning. STriDER uses a unique tripedal gait to walk with high energy efficiency and has the ability to change directions. In the first version of STriDER, the concept of passive dynamic locomotion was emphasized; however, for the new version, all joints are actively controlled for robustness. The robot is inherently stable when all three feet are on the ground due to its tripod stance, but it can still fall down if it trips while taking a step or if unexpected external forces act on it. The unique structure of STriDER makes the simple task of standing up challenging for a number of reasons; the high height of the robot and long limbs require high torque at the actuators due to its large moment arms; the joint configuration and length of the limbs limit the workspace where the feet can be placed on the ground for support; the compact design of the joints allows limited joint actuation motor output torque; three limbs do not allow extra support and stability in the process of standing up. This creates a unique problem and requires novel strategies to make STriDER stand up. This thesis examines five standing up strategies unique to STriDER: three feet pushup, two feet pushup, one foot pushup, spiral pushup, and feet slipping pushup. Each strategy was analyzed and evaluated considering constraints such as static stability, friction at the feet, kinematic configuration and joint motor torque limits to determine optimal design and operation parameters. Using the findings from the analysis, experiments were conducted for all five standing up strategies to determine the most efficient standing up strategy for a given prototype using the same design and operation parameters for each method. Also, a literature review was conducted for human standing from a chair and human pushup exercises and the conclusions were compared to the analysis presented in this thesis.

Many factors contribute to the development of STriDER's gait. Several considerations for gait planning as the robot takes a step are investigated, including: stability, dynamics, the body's maximum and minimum allowable heights, the swing legs foot clearance to the ground, and the range of the subsequent swing foot contact positions. A static stability margin was also developed to asses the stability of STriDER. This work will lay the foundation for future gait generation research for STriDER. Additionally, guidelines for future work on single step gait generation based on kinematics and dynamics are discussed.

The findings presented will advance the capabilities and adaptability of the novel robot STriDER. By studying standing up strategies and gait planning issues, the most efficient control methods can be implement for standing up and preparing to take a step and lay out the foundations for future research and development on STriDER.

Acknowledgments

I would first like to thank God for blessing me with a loving, supportive, and caring family. Without Him nothing I do would be possible. I want to thank my parents, for their unconditional support and for always being the best role models, *los quiero mucho*. Thank you for always believing in me and for always being there when I needed you the most. Your advice is priceless and I admire you both so much. I am where I am because of YOU. I also want to thank my sisters, Elaine, Jeanette, and Lizette (Gugu), for all of their support and encouragement, you are the best sisters! To my grandparents, aunt, uncle, cousins and all of my family members that believed in me, I can't say how much it means to me to have you all in my life. To my friends, close and far, thank you for always being just a phone call away and for all the great memories we've made! I will always take them with me!

I would like to thank my advisor Dr. Hong for letting me be part of the number one robotics lab in the world! Thank you for an amazing opportunity and for being a great mentor. I would also like to acknowledge my committee members, Dr. Wicks and Dr. Sandu, for their contribution to this work. Thank you Derek Lahr and Nick Milo for all of your hard work and help in the design, fabrication, and testing of STriDER. Without your help I wouldn't have a robot! Also, a big thank you to Karl Muecke for developing a great interface program for testing robots. Finally, I would like to thank all of my labmates for helping me along the way and for making the lab so much fun!

This thesis is dedicated to my parents, Jorge and Lizette Morazzani.

Contents

List of Figures

List of Tables

Chapter 1

Introduction

STriDER (Self-excited Tripedal Dynamic Experimental Robot) is a novel three-legged walking robot that utilizes a unique tripedal gait to walk [1–6]. To initiate a step, two of its legs are oriented to push the center of gravity outside a support triangle formed by the three foot contact points, using a unique abductor joint mechanism [2]. As the robot begins to fall forward, the middle leg or swing leg, swings in between the two stance legs and catches the fall. Simultaneously, the body rotates 180 degrees preventing the legs from tangling up.

The first version of STriDER [1, 3, 4] emphasizes the passive dynamic nature of its gaits. Passive dynamic locomotion utilizes the natural built in dynamics of the robot's body and limbs to create the most efficient natural walking motion [1,7,8]. In the new version, STriDER 2.0, all of its joints are actuated for robustness. STriDER was developed for deploying sensors rather than task manipulations. The robot's tall stance is ideal for surveillance and setting cameras at high positions [1].

The current research focuses on standing up strategies, posturing, gait synthesis, and trajectory planning for which the concept of passive dynamics is not emphasized. The robot is inherently stable with its tripod stance, but it can still fall if it trips while walking or if external forces act on it. Thus, a number of standing up strategies have been investigated for STriDER and are presented in this thesis. Design and operation parameters were varied and the effects of these parameters on the efficiency of standing up were studied. Since STriDER is a non-linear, under-actuated mechanical system in nature, where there is no actuator between the foot and the ground, dynamics is a key factor in the planning of gaits. Recent research on the optimization of bipedal gait with dynamic constraints includes the work of Sangwan and Agrawal [9, 10]. The technical approaches discussed in these studies can be utilized as the source of reference for the novel tripedal gait in this study. This thesis also presents considerations for gait planning strategies based on kinematics and lay out the foundation and guidelines for future work on a single step gait generation based on both kinematics and dynamics.

1.1 Motivation

The design and locomotion strategies of robots are often inspired by nature; however, STriDER utilizes an innovative tripedal gait not seen in nature. Unlike common bipeds, quadrupeds, and hexapods, STriDER, shown in Fig. 1.1, is an innovative three-legged walking machine that can incorporate the concept of actuated passive dynamic locomotion. Thus, the proper mechanical design of a robot can provide energy efficient locomotion without sophisticated control methods [11]. However, STriDER is inherently stable with its tripod stance and can easily change directions. This makes it uniquely capable to handle rugged terrain where the path planning, turning, and positioning strategies studied here are crucial. Although this thesis will not focus on the passive dynamic locomotion capabilities of STriDER, as discussed in [1], it is still a desirable trait of the robot. There are many advantages to the design of STriDER. The robot can be launched to difficult to access areas while its long legs absorb the shock of landing. Also, the robot's tall stance is useful for surveillance since it is capable to see above bushes.

Figure 1.1: STriDER 2.0 prototype on right of its predecessor, STriDER.

The overall motivation of this research is advancing the capabilities of this adaptable and novel robot. If the robot falls, it is important for it to be able to stand up to finish accomplishing its tasks or continue walking. Thus, it is crucial to study different standing up strategies that will be both energy efficient and easy to implement. Different parameters can effect the required torque at the motors and total power consumption as the robot stands. So, by investigating the effects of these parameters on several standing up strategies, one can determine the appropriate design and/or operation parameters for different scenarios (terrains, elevations, inclines, etc). Also, in order for the robot to properly take a step, different factors can contribute to the efficiency of gait planning. Thus, this thesis will consider stability, body height, body twisting, and swing leg's clearance and landing position, as several of the constraints that contribute to kinematically based gait planning.

1.2 Background and Previous Research

This section presents background information on STriDER, a description of the novel tripedal walking gait and gaits for changing directions, an introduction to a unique rotator aligning joint mechanism, and a brief discussion on how STriDER can be modeled as a parallel manipulator. In addition, literature review findings on human standing from a chair and human pushup exercise analysis are discussed.

1.2.1 Novel Tripedal Gait

The novel tripedal gait (patent pending) is implemented, as shown in Fig. 1.2, for a single step. Fig. 3 in Section 3 shows the joint and link names for STriDER. During a step, two legs act as stance legs while the other acts as a swing leg. STriDER begins with a stable tripod stance (Fig. 1.2(a)), then, the hip links are oriented to push the center of gravity forward by aligning the stance legs' pelvis links (Fig. 1.2(b)). As the body of the robot falls forward (Fig. 1.2(c)), the swing leg naturally swings in between the two stance legs (Fig. 1.2(d)) and catches the fall (Fig. 1.2(e)). As the robot takes a step, the body needs to rotate 180 degrees to prevent the legs from tangling up. Once all three legs are in contact with the ground, the robot regains its stability and the posture of the robot is reset in preparation for the next step (Fig. 1.2(f)) [1, 3].

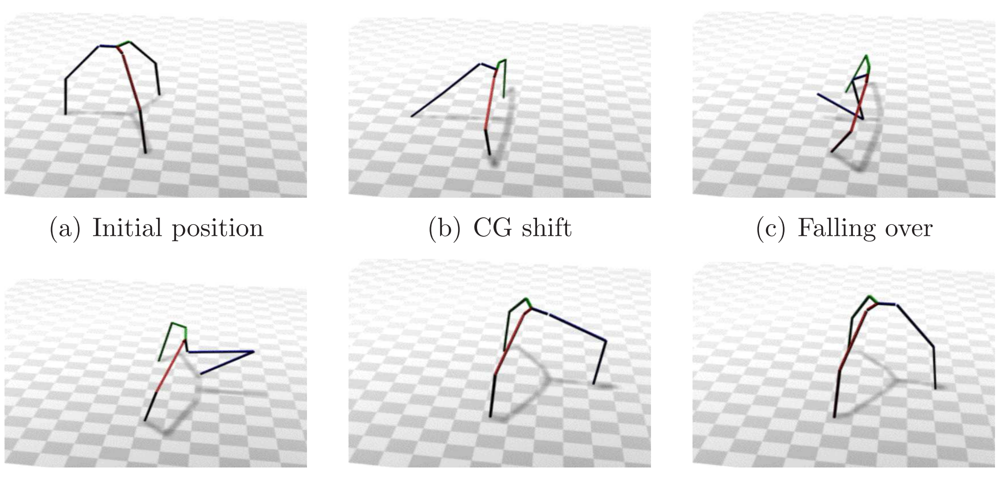

(a) Initial position (b) CG shift (c) Falling over

(d) Leg swing (e) Catches the fall (f) Reset position

Figure 1.2: The motion of a single step [1].

1.2.2 Changing Directions

Gaits for changing directions can be implemented in several ways, one of which is illustrated in Fig. 1.3. By changing the sequence of choice of the swing leg, the tripedal gait can move the robot in 60 degree interval directions for each step [6]. Alternatively, the step direction can be modified such that the stance momentarily changes to an iscoceles or scalene triangle as opposed to an equilateral. This will then change the orientation of the following stance legs from the customary 60 degree angle and, therefore, the direction of the robot's travel as well. This method is of particular interest because of the inherent flexibility which is more conducive to rugged environments [1].

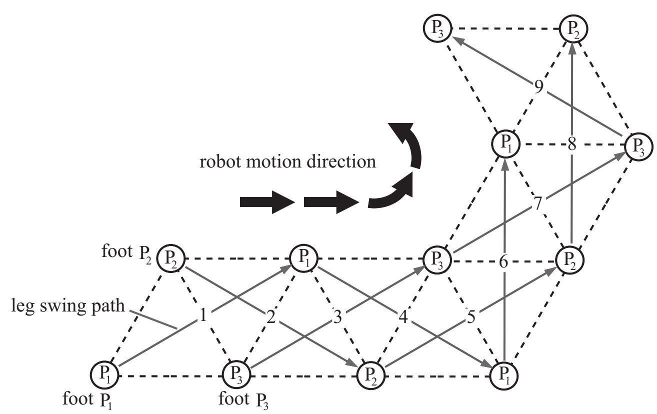

Figure 1.3: Gait for changing directions [6].

1.2.3 Rotator Joint Aligning Mechanism

STriDER is actuated using DC servo motors through distributed control with position feedback. Because of the continuous inverting motion inherent to the locomotion strategy of this robot, slip rings were built into each of the three rotator joints [1]. It is necessary then to remove the actuators away from the rotation axis of the joint such that wires could be routed through the rotator shaft. In both the first version and new version of STriDER, this is accomplished using a spur gear pair [2, 6].

The tripedal gait requires the entire body of STriDER to rotate about the two hip rotator joints of the stance legs as the swing leg swings between them. Since any one of the three legs can be chosen as the swing leg, any two of the three hip rotator joints need to be able to align to each other. The hip abductor joints perform this motion by changing the angle of the hip rotator joints so that the axis of one hip rotator joint can be aligned to another while the third is set to be perpendicular to this axis. In addition to the three orientations in which a pair of rotator joints is aligned, it is also desirable that all rotator axes intersect in the center of the body. In the first prototype of STriDER, the three hip abductor joints (shown in Fig. 3 in Section 3) were independently actuated and controlled with three separate DC motors. While this approach worked, the size and weight of the two additional motors made the design undesirable, as it essentially requires only a single degree of freedom motion to successfully align the rotator joints in the four desired configurations [6]. In [2], a new abductor joint mechanism is presented which aligns the rotator joints using only one actuator which can replace the three motors of STriDER's abductors. This mechanism uses an internal gearset to generate a special trifolium curve with a pin which guides the hip rotator joints via slotted arms through the four specific positions shown in Fig. 1.4.

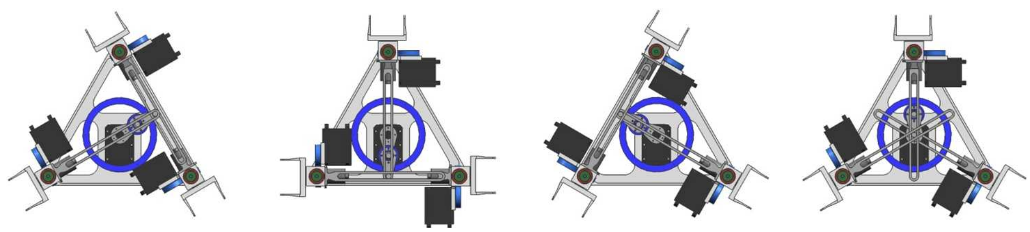

(a) (b) (c) (d)

Figure 1.4: Four positions of the rotator joint aligning mechanism with internal gear set [2,6].

1.2.4 STriDER Modeled as a Parallel Manipulator

When all three feet of STriDER are on the ground, the kinematic structure of the robot behaves like an in-parallel manipulator. Forward and inverse displacement analysis for STriDER is presented in [5]. This analysis may be used to plan and control the change in posture of the robot, while keeping the three feet in contact with the ground. Note that by assuming no slipping at the feet, each foot contact point can be treated as a spherical joint.

In [5], kinematic analysis methods for in-parallel manipulators are adopted for the forward and inverse displacement analysis for this mobile robot. Both loop-closure equations based on geometric constraints and the intersection of the loci of the feet are utilized to solve the forward displacement problem. Closed-form solutions are identified and discussed in the cases of redundant sensing with displacement information from nine, eight, and seven joint angle sensors. For the non redundant sensing case using information from six joint angle sensors, it is shown that closed-form solutions can only be obtained when the displacement information is available from non-equally distributed joint angle sensors among the three legs. As for the case when joint angle sensors are equally distributed among the three legs, it will result in a 16th-order polynomial of a single variable. Finally, results from the simulations are presented for both inverse displacement analysis and the non-redundant sensing case with equally distributed joint angle sensors. It was found that at most sixteen forward displacement solutions exist if displacement information from two joint angle sensors per leg are used and one is not used [5].

1.2.5 Human Standing and Pushup Exercise Research Findings

A variety of research has been conducted for human sitting to standing motion, as presented in [12–16]. In particular, Hutchison et al. completed a dynamic analysis of joint forces and torques while rising from a chair [12]. Their goal was to determined if quasi-static models (assume the body segments are in static equilibrium at any instant) are valid for chair-rise or if dynamic analysis is necessary. They used inverse kinematics and ten adult subjects to calculate joint torques of twenty chair-rise trials at different rising speeds per subject. Their results concluded that the effect of segmental dynamics can be neglected for the ankle and knee joints since they contribute to only 1% of the total ankle and knee forces and torques [12]. However, the effects of the segmental dynamics on the hip joints contributed to 10% of the hip forces and torques. Hutchinson also concluded that static loads dominate joint forces and torques as a subject rises from a sit position; however, dynamics becomes more important as the speed increases. From Hutchison's findings [12], it was concluded that for the study of STriDER's standing up strategies, dynamics can be ignored and the analysis will be solely statically based, assuming the robot is not standing up at high speeds.

Schenkman et. al. studied whole-body movements during rising to standing from sitting [15]. They included nine test subjects in their rising from a chair controlled condition experiments. They divided the rising motion into four phases. The four phases included: a flexion-momentum phase used to initiate the initial momentum for rising, a phase when the subject rises from the chair and ends at maximal ankle dorsiflexion, an extension phase where the subject rises to its full upright position, and a stabilization phase [15]. The goal of this study was to gain a brighter insight on the rising from a chair motion to facilitate identifying impairments of people who have trouble standing. Schenkman's results, can be applied to STriDER's standing up study by dividing the standing up motion into different phases. Although this was not implemented in this thesis, it may be applied to future research. However, for the presented work, it was important to keep some trends consistent for each strategy. For example, similar initial and final conditions were chosen for all standing up strategies, as will be presented later.

In [13], an analysis of the sit-stand-sit movement cycle was done with normal subjects. Although research has been conducted for sit to stand movements, the idea of stand to sit has not been thoroughly analyzed. Kerr et al. have obtained a basis of descriptive data for sit-stand-sit movement cycle from fifty normal subjects of various ages and both sexes [13]. They believe this data will result in a better understanding of the sit-stand-sit motion. As mentioned, this thesis focuses on standing but the findings in Kerr's work can be applied to STriDER. More specifically, the motion of the body moving upwards and downwards can relate to the research of parallel manipulators. As previously mentioned, when all of

STriDER's three feet are on the ground, the robot can me modeled as a parallel manipulator.

Next, a synthesis of standing up trajectories using dynamic optimization was presented in [14]. Kuželiĉki et al. investigated dynamic optimization as a tool to compute standing-up trajectories. Sit-to-stand manouvers in five intact persons and five trans-femoral amputees were measured [14]. During the experiments, movements and ground reaction forces on the body were recorded. From this data, a three dimensional dynamic model of standing-up was developed. Optimal trajectories were computed by minimizing cost functions with five main quantities. These quantities included; jerk (derivative of acceleration) of cartesian coordinates, jerk of joint angles, derivative of joint torques, joint torques, and muscle forces and force derivatives [14]. The results indicated that dynamic optimization can be used to compute trajectories for standing up taking into account solely the body dynamics and kinematics without modeling muscle behavior [14]. Similar to Kuželiĉki, a cost function was developed for STriDER's standing up strategies to optimize design and operation parameters specific to STriDER, as will be discussed in later sections.

In addition to rising and standing findings, pushup exercise analysis was also considered in the research findings. First, Kai-Nan et. al investigated intersegmental loading patterns on the elbow joint during a push-up exercise [17]. Sensors and a piezoelectric plate were used to record upper body forces during push-ups in six different hand positions [17]. They found that the hand position had a statistically significant effect on the axial force on the elbow. Kai-Nan et al. believe that the data collected in their studies may aid in determining factors for optimal rehabilitation for injuries or prosthetic replacement [17]. Some of the standing up strategies investigated for STriDER have motions similar to human pushups. Thus, the effects of different foot positions on the actuator torques as STriDER stands will be investigated. In fact, optimal foot positions for each strategy will be discussed in this thesis given design parameters (link length ratio, robot weight, etc).

Another study was conducted on hand position effects on the elbow joint during a pushup exersice by Donkers et al. In [18] they found that as the distance between the hand position increased the peak forces exerted on the elbow joint along a forearm axis decreased. Thus, it is easier to do a pushup when the hands are father apart on the floor. In the case of STriDER, each leg will be analyzed individually and the total weight of the robot will be assumed to be located in the center of the body. Since five strategies will be studied and different design parameters yield different optimal foot positions, a general conclusion on the optiml foot position cannot be made. Thus, a cost function will be computed to obtain optimal foot positions given design parameters.

A complete kinematic and kinetic analysis of a push-up was analyzed by Kai-Nan et al. They discussed that the location of the palm relative to the shoulder, the plane of arm movement and the relative foot positions are three major factors that affect the intersegmental loads (force and moment generated at the joint from external and inertial loads) on the joint [19]. The load across the wrist, elbow and shoulder were experimentally measured and analytically determined in their paper. Kai-Nan's study on the plane of arm movement relates to the different standing up strategies investigated for STriDER when comparing the three feet pushup and two feet pushup. The three feet pushup simply lifts the body straight upwards without translating the body in the horizontal direction. The two feet pushup for STriDER has the same motion as a human pushup. These strategies are analyzed in detail in later sections.

In order to adequately compare the results of the literature review findings and the work presented in this thesis it is important to know basic body segment length ratios. Thus in [20], a book that focuses on biomechanics and human movements, Winter lists body segment lengths as a fraction of body height. From this data, the upper arm ratio to the total height was 0.188 and lower arm segment ratio to the total height was 0.253. Thus, the upper arm to lower arm ratio is approximately 0.74. Also, the lower body (hip to feet) length ratio to the total height is 0.53 for a typical male.

As noted, the results of the literature review findings influenced the steps for the investigation of STriDER's standing up methods. In particular, it was concluded that dynamics would not have a large effect on the results thus, all analysis was statically based. Also, it was found that foot position is an important constraint when optimizing actuator torques.

Chapter 2

Forward and Inverse Kinematics

A full three-dimensional kinematic model was developed to aid in the inverse and forward displacement analysis process using Mathematica. This model will help examine standing up strategies and transitions between gaits. Also, the graphical simulation developed is beneficial for visualizing the motion of STriDER's links and joints.

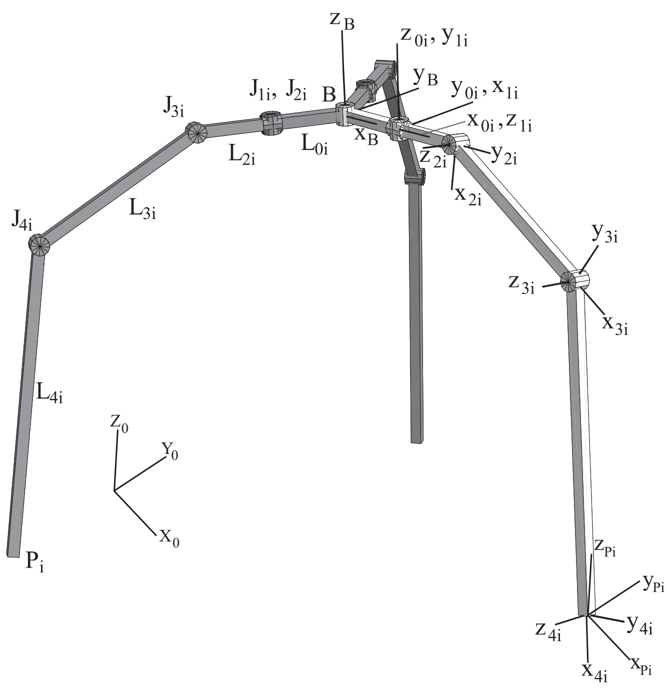

Figure 2.1: Coordinate frames and joint definitions for STriDER [5].

2.1 Kinematic Configuration

The definition of the coordinate systems for each leg is shown in Fig. 2.1. The configuration for all three legs of STriDER is the same thus, the analysis for one leg is presented here as the other two legs will follow the same procedure. The subscript i denotes the leg number (i.e. i=1, 2, 3) in the coordinate frames, links, and joint labels.

Table 2.1: Nomenclature

i	Leg number (i=1,2,3)
j	Link number (j=1,2,3,4)
$\{X_0, Y_0, Z_0\}$	Global fixed coordinate system
$\{x_B, y_B, z_B\}$	Body center coordinate system
J_{1i}	Hip abductor joint for leg i
J_{2i}	Hip rotator joint for leg i
J_{3i}	Hip flexure joint for leg i
J_{4i}	Knee joint for leg i
P_i	Foot contact point for leg i
L_{0i}	Body link for leg i
L_{1i}	Hip link for leg i (length=0)
L_{2i}	Pelvis link for leg i
L_{3i}	Thigh link for leg i
L_{4i}	Shank link for leg i

Table 2.1 lists the nomenclature used to define the coordinate frames, joints and links. First, a global coordinate system, $\{X_0, Y_0, Z_0\}$, is established and used as the reference for positions and orientations where the negative Z_0 vector is in the same direction as gravity. Next, the body coordinate frame $\{x_B, y_B, z_B\}$ is defined as shown in Fig. 2.1. Each leg is separated by 120 degrees, leg one, leg two, and leg three are 0 degrees, 120 degrees, and 240 degrees from the positive x_B axis, respectively. Each leg includes four actuated joints, J_{1i}, J_{2i}, J_{3i}, and J_{4i}. The hip abductor joint, J_{1i}, allows the stance legs' rotator joints to align during a step. In the first prototype of STriDER, developed in [1, 21], three independent abductor joints are used to accomplish the alignment. Later in [2], a new abductor joint mechanism to align the rotator joints driven by only one motor is used to replace the three abductor motors. Thus, J_{1i}, is not treated as an active joint. Next, J_{2i}, the hip rotator joint, allows the legs to rotate around the z_{1i} axis. J_{3i}, the hip flexure joint and J_{4i}, the knee joint are both revolute joints that rotate around the z_{2i} and z_{3i} axes, respectively. Two coordinate frames $\{x_{4i}, y_{4i}, z_{4i}\}$ and $\{x_{Pi}, y_{Pi}, z_{Pi}\}$ are established at each foot. The three unit vectors in frame $\{x_{Pi}, y_{Pi}, z_{Pi}\}$ are defined to be parallel to the global vector units. The foot contact points denoted by P_i are treated as spherical joints between the foot and the ground during analysis and $\{x_{4i}, y_{4i}, z_{4i}\}$ relates to $\{x_{Pi}, y_{Pi}, z_{Pi}\}$ with three Euler angles. Finally, the links listed as L_{0i}, L_{1i}, L_{2i}, L_{3i}, and L_{4i} are clearly labeled in Fig. 2.1 and represent the body

link, hip link (equal to zero), pelvis link, thigh link and shank link. Furthermore, links L_{0i}, L_{1i}, and L_{2i} are constant values that form the body triangle.

Table 2.2: Link parameters

Link	a_{ji}	α_{ji}	d_{ji}	θ_{ji}
1	$L_{1i} = 0$	$90°$	0	$\theta_{1i} + 90°$
2	0	$90°$	L_{2i}	$\theta_{2i} - 90°$
3	L_{3i}	0	0	θ_{3i}
4	L_{4i}	0	0	θ_{4i}

The coordinate systems are defined following the standard Denavit-Hartenbergs convention [22] and the link parameters are listed in Table 2.2, where j is the link number ($j = 1, 2, 3, 4$) and i is the leg number ($i = 1, 2, 3$). Additionally, a_{ji} equals the distance along x_{ji} from J_{ji} to the intersection of the x_{ji} and $z_{(j-1)i}$ axes and d_{ji} is the distance along $z_{(j-1)i}$ from $J_{(j-1)i}$ to the intersection of the x_{ji} and $z_{(j-1)i}$ axes. Also, α_{ji} is the angle between $z_{(j-1)i}$ and z_{ji} measured about x_{ji} and θ_{ji} is the angle between the $x_{(j-1)i}$ and x_{ji} measured about $z_{(j-1)i}$. Note, when all θ_{ji} are equal to zero, the legs form a right angle between L_{2i} and L_{3i}.

2.2 Forward Kinematics

Each of STriDER's legs can be represented as a simple kinematic chain. In this case, the goal of the forward kinematic analysis is to determine the global foot position for each leg given the body position and orientation based on the global coordinates, $\{X_0, Y_0, Z_0\}$, and all joint angles. As discussed in [22], a homogenous matrix, A_i, transforms the coordinates of a point from frame $i-1$ to frame i. The matrix A_i, consists of two main parts, as shown in Equation 2.1,

$$\mathbf{A}_i = \begin{bmatrix} \mathbf{R}_{i-1}^{i} & \mathbf{d}_{i-1}^{i} \\ 0 & 1 \end{bmatrix} \tag{2.1}$$

where $\mathbf{R}_{i-1}^{i}$ expresses the orientation of frame i relative to frame $i-1$ and $\mathbf{d}_{i-1}^{i}$ expresses the position. For a kinematic chain, T_i^j is known as the transformation matrix where the position and orientation of coordinate i is described in relation to coordinate j. Thus, the transformation matrix for one leg of STriDER from global coordinates to the foot position is defined using Equation 2.2,

$$\mathbf{T}_0^P = \mathbf{A}_0^B \mathbf{A}_B^1 \mathbf{A}_1^2 \mathbf{A}_2^3 \mathbf{A}_3^4 \mathbf{A}_4^P \tag{2.2}$$

where $\mathbf{A}_0^B$ is the transformation from global coordinates to the center of the body given the body position and orientation. Note, the position and orientation of the body will always be known in the analysis presented in this thesis.

2.3 Inverse Kinematics

The inverse displacement analysis is important for calculating the unknown internal angles θ_{2i}, θ_{3i}, and θ_{4i} for the hip rotator, hip flexure and knee joints, respectively. As previously mentioned, the angle between the positive x_B axis and leg one, leg two and leg three is 0 degrees, 120 degrees, and 240 degrees, respectively. The angle between x_{0i} and x_{1i}, θ_{1i}, measured about z_{0i}, is set equal to zero and treated as a constant in these calculations. Also, the orientation and position of the body in relation to the global coordinates are known. So, the unknown angles θ_{2i}, θ_{3i}, and θ_{4i} are calculated from the global body position and orientation, the angle between x_B and each leg, θ_{1i}, and global foot positions. By treating the system as an elbow manipulator, as shown in Fig. 2.2 , the unknown joint angle values can be determined. Note, in this figure, the leg is rotated 90 degrees about the x_{1i} axis for the ease of viewing [5].

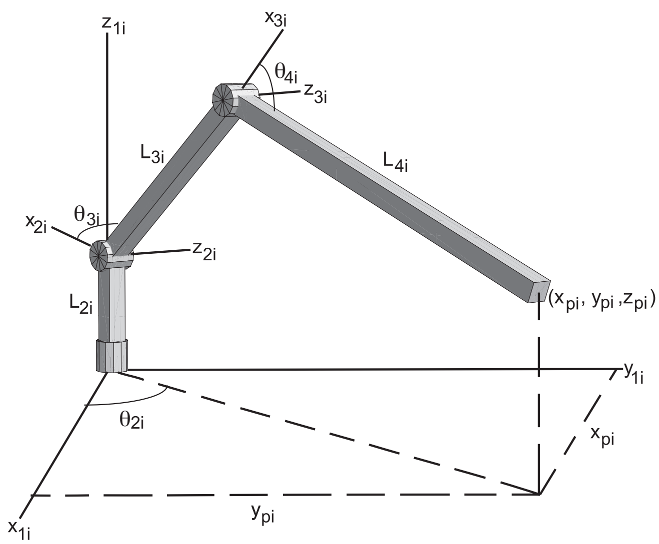

Figure 2.2: One leg represented as an elbow manipulator.

Following the coordinate systems in Fig. 2.1, a homogeneous transformation from the global coordinate to the hip rotator joint was derived, as shown in Equation 2.3,

$$\mathbf{H}_0^{1i} = \mathbf{H}_0^{B}\mathbf{H}_B^{0i}\mathbf{H}_{0i}^{1i} = \underbrace{\begin{bmatrix} \mathbf{R}_0^{1i} & \mathbf{d}_0^{1i} \\ 0 & 1 \end{bmatrix}}_{4\times 4} \tag{2.3}$$

where $\mathbf{R}_0^{1i}$ and $\mathbf{d}_0^{1i}$ specify the orientation and translation of $O_{x_{1i},y_{1i},z_{1i}}$ relative to O_{X_0,Y_0,Z_0} respectively. Next, the orientation and translation of O_{X_0,Y_0,Z_0} relative to $O_{x_{1i},y_{1i},z_{1i}}$ were found using Equations 2.4 and 2.5,

$$\mathbf{R}_{1i}^0 = \left[\mathbf{R}_0^{1i}\right]^T \tag{2.4}$$

$$\mathbf{d}_{1i}^0 = -\mathbf{R}_{1i}^0\mathbf{d}_0^{1i} \tag{2.5}$$

The orientation matrix, $\mathbf{R}_{1i}^0$, and translation vector, $\mathbf{d}_{1i}^0$, are used to find the translational vector, $\mathbf{d}_{1i}^{Pi}$, to relate the position of $O_{x_{Pi},y_{Pi},z_{Pi}}$ to $O_{x_{1i},y_{1i},z_{1i}}$, as shown in Equation 2.6,

$$\mathbf{d}_{1i}^{Pi} = \mathbf{R}_{1i}^0\mathbf{d}_0^{Pi} + \mathbf{d}_{1i}^0 \begin{bmatrix} x_{Pi} \\ y_{Pi} \\ z_{Pi} \end{bmatrix} \tag{2.6}$$

where $\mathbf{d}_0^{Pi}$ is the foot position in relation to the global coordinates and vector $[x_{Pi}\ y_{Pi}\ z_{Pi}]^T$ represents the foot position relative to the local hip rotator coordinates, which is also the base of the elbow manipulator shown in Fig. 2.2. This now becomes a common elbow manipulator problem [22].

The angle at the hip rotator joint, θ_{2i}, is found using Equation 2.7,

$$\theta_{2i} = ArcTan2\left(x_{Pi}, y_{Pi}\right) + \frac{\pi}{2} \tag{2.7}$$

where x_{Pi} and y_{Pi} are the x and y foot positions relative to the elbow manipulator base. Notice that 90 degrees are added to this value due to the link parameter definition listed in Table 2.2. Next, the angle at the knee joint, θ_{4i}, is calculated, as shown in Equation 2.8,

$$\theta_{4i} = ArcTan2\left(D, \pm\sqrt{1-D^2}\right) \tag{2.8}$$

where D is a constant term determined from Equation 2.9,

$$D = \frac{{x_{Pi}}^2 + {y_{Pi}}^2 + \left(z_{Pi} - L_{2i}\right)^2 - {L_{3i}}^2 - {L_{4i}}^2}{2L_{3i}L_{4i}} \tag{2.9}$$

where L_{2i}, L_{3i}, and L_{4i} are link lengths and z_{Pi} is the z foot position relative to the base. As shown, with $\pm$ in Equation 2.8 there will be two values for θ_{4i}, each corresponds to an elbow up or elbow down case. Thus, there will also be two corresponding values for θ_{3i}, as calculated in Equation 2.10,

$$\theta_{3i} = ArcTan2\left(\sqrt{{x_{Pi}}^2 + {y_{Pi}}^2}, z_{Pi} - L_{2i}\right) - ArcTan2\left(L_{3i} + L_{4i}cos\theta_{4i}, L_{4i}sin\theta_{4i}\right) \quad (2.10)$$

Thus, if the body global position and orientation, the hip abductor joint angle, θ_{1i}, and the global foot positions are known, then the internal joint angles (hip rotator joint angle, θ_{2i}, hip flexure joint angle, θ_{3i}, and knee joint angle, θ_{4i}) can be calculated by modeling the legs as elbow manipulators where the base is at the hip rotator joint and all link lengths are known and constant.

Chapter 3

Standing Up Strategies

STriDER can often fall down if it trips while walking or if external forces act on it. Thus, it is important to investigate a variety of standing up strategies specific to STriDER in order for the robot to stand up and complete its tasks. The unique structure and operation of STriDER makes the simple task of standing up challenging for a number of reasons; the tall height and long limbs of the robot require high torque from the actuators due to large moment arms; the joint configuration and length of the limbs limit the workspace where the feet can be placed on the ground for support; the compact design of the joints allows for limited actuator torque; and the number of limbs (three) does not allow extra support and stability in the process of standing up. In this research, the mechanics of five strategies have been studied; a three feet pushup, two feet pushup, one foot pushup, spiral pushup and feet slipping pushup. A detailed analysis for each strategy is presented in this section considering constraints such as, static stability, friction at the feet, kinematic configuration, link length ratios, and actuator torque limits. The objective of this analysis is to determine optimal design and operation parameters that will minimize actuator torques as the robot stands up. By minimizing actuator torque less power is consumed and the robot can stand more efficiently. In addition, due to the size and weight limitations of the robot, it is difficult to find powerful and compact motors for STriDER. Thus, finding the parameters for minimum torque is important. Also as discussed in the research findings, it was assumed that dynamics will not have a large effect on the results thus, all the analysis was based on static equilibrium assumptions [12]. Experiments are also presented in this section to validate the analysis and determine the most efficient standing up strategy for a specific experimental platform.

In this section a number of important joints and links will often be referred to in the analysis. Fig. 3 shows the joint and link names for STriDER. The rotator, flexure and knee joints will often be addressed in this section as well as the flexure and shank links.

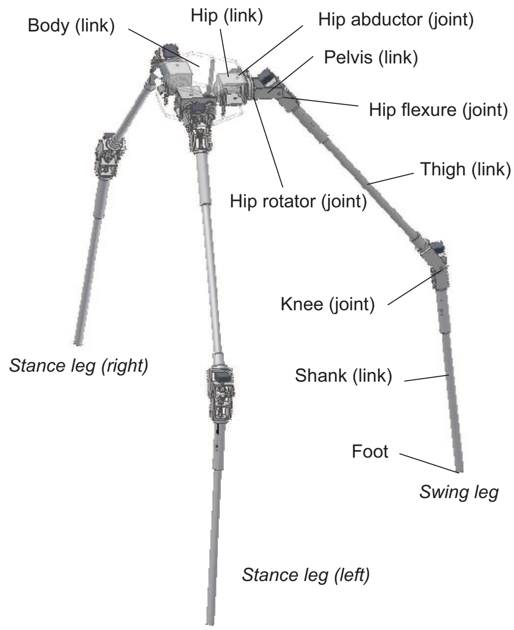

Figure 3.1: Joint and link labels [1].

3.1 Three Feet Pushup

Beginning with the robot flat on the ground with all three legs extended outwards, as shown in Fig. 3.2(a), the three feet pushup method moves the three legs inwards towards the body to position the three feet to their final desired positions, in this case forming an equilateral triangle. A distance d for one leg, shown in Fig. 3.3, is defined as the distance between the projected center of the body to the ground and the foot contact point. For this example, the distance d for all three legs is equal since the three contact points form an equilateral triangle. The value of d will play an important role in the motor torque calculations of the required motor torques at the joints. Once the feet reach their desired foot positions, the body begins to move upwards by pushing against the ground until it reaches its desired height (Fig. 3.2). The maximum body height is achieved when the thigh and shank links are aligned, as shown in Fig. 3.2(f).

This method is probably one of the first standing up methods that would come to mind for STriDER. Its symmetrical approach allows for simpler analysis and guarantees static stability since the center of gravity is always located in the center of the body. The configuration for all three legs in the three feet pushup standing up method is the same thus, a detailed analysis for only one leg is presented here as the other two legs will follow the same procedure. A kinematic and quasi-static torque analysis is presented for the portion when the body begins to move upward and reaches its maximum height (Fig. 3.2(b) to Fig. 3.2(f)). The effect of d values, link length ratios ($\alpha = \frac{r_3}{r_4}$) and allowable tangential friction forces between the feet

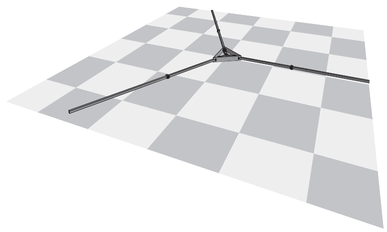

(a) Initial position

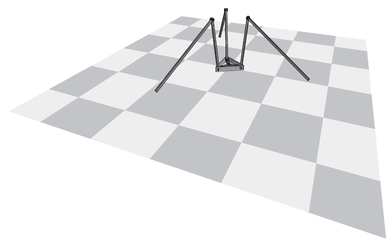

(b) Desired foot position

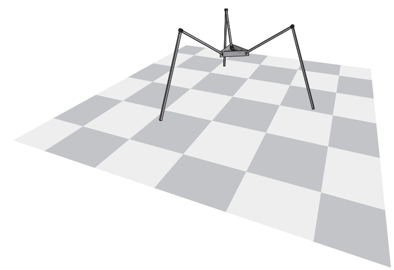

(c) Begins to move upwards

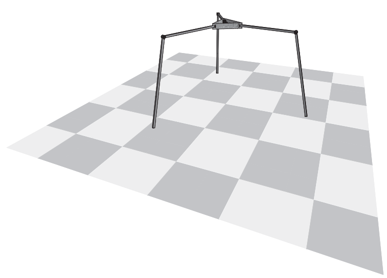

(d) Continues to move upwards

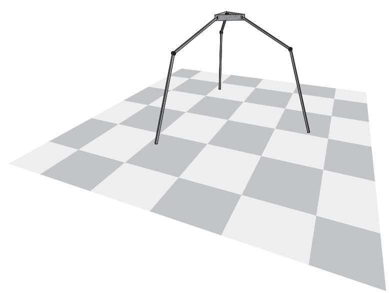

(e) Continues to move upwards

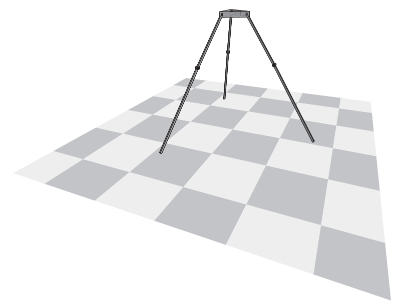

(f) Maximum height reached

Figure 3.2: The motion of the three feet pushup.

and the ground on the motor torques will be investigated in the analysis.

The minimum allowable d is the difference between the thigh and shank link length plus the body link ($L_b = L_0 + L_1 + L_2$) length. The maximum allowable d is the added length of the thigh, shank, and L_b. For the analysis presented in this research, the thigh and shank link length ratio, α, is optimized for standing up; however, it is crucial that the link lengths are adequate for walking. Thus, it is more important to optimize link length for walking rather than standing up. The range of tangential contact force between the foot and the ground is defined by the friction coefficient and the normal contact force due to gravity. Thus, the minimum tangential contact force is zero (no friction force) and the maximum tangential contact force is the normal force times the friction coefficient. As long as the tangential contact forces, at the three feet, satisfy these conditions and the force balance is satisfied, the tangential forces can be adjusted by force control of the actuators of the robot [23, 24]. The choice of the tangential force will effect the motor torque requirements at the joints.

3.1.1 Kinematic Analysis for the Three Feet Pushup

To find the leg's joint angles as the robot stands up, the body and links may be modeled as a slider-rocker mechanism, where the body is the slider link moving vertically, the thigh is the coupler link, and the shank is the rocker, as shown in Fig. 3.3. For a no slip condition, the foot contact point can be modeled as a revolute joint, between the shank link and the ground.

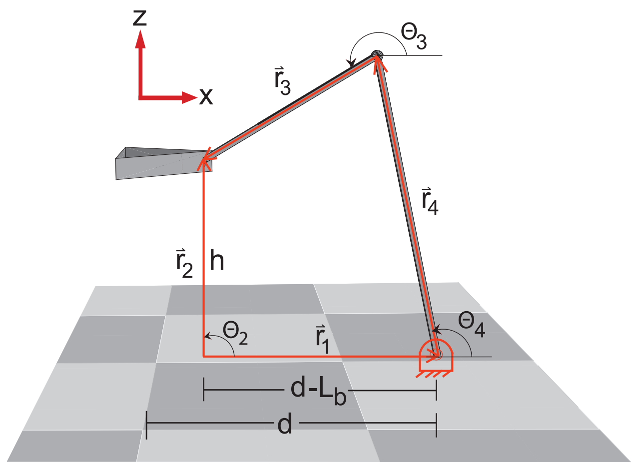

Figure 3.3: Body and one leg modeled as a slider-rocker mechanism.

As the body moves upward in the positive z direction, the joint angles, θ_3 and θ_4 are calculated given the body height, h, and using the vector loop equation, shown in Equation 3.1. The angle of vector $\vec{r_1}$, θ_1, equals zero and θ_2 equals 90 degrees, when the body is moving straight up perpendicular to the ground. The value of d is predefined, L_b is the constant body link length ($L_b = L_0+L_1+L_2$) (Fig. 2.1) and h is the input variable. With these values, Equation 3.1 is simplified, thus θ_3 and θ_4 can be calculated using Equation 3.2. Also, the maximum height of the body, or the height when the thigh and shank link are aligned, is calculated with Equation 3.3.

$$\begin{aligned} x &: r_2 cos\theta_2 - r_3 cos\theta_3 - r_4 cos\theta_4 - r_1 cos\theta_1 = 0 \\ z &: r_2 sin\theta_2 - r_3 sin\theta_3 - r_4 sin\theta_4 - r_1 sin\theta_1 = 0 \end{aligned} \tag{3.1}$$

$$\begin{gathered} x : -r_3 cos\theta_3 - r_4 cos\theta_4 - (d - L_b) = 0 \\ z : h - r_3 sin\theta_3 - r_4 sin\theta_4 = 0 \end{gathered} \tag{3.2}$$

$$h_{max} = \sqrt{(r_3 + r_4)^2 - (d - L_b)^2} = \sqrt{(r_{tot})^2 - (d - L_b)^2} \tag{3.3}$$

3.1.2 Static Force Analysis for the Three Feet Pushup

A free body diagram for the links of one leg is shown in Fig. 3.4. A friction force was added at the feet to account for different tangential forces, F_T. For example, if STriDER was attempting to stand up on ice, where there is very limited friction (small allowable tangential forces), the motor torque requirements at the joints would be different than those when standing up on a rough surface, where relatively larger tangential forces can exist.

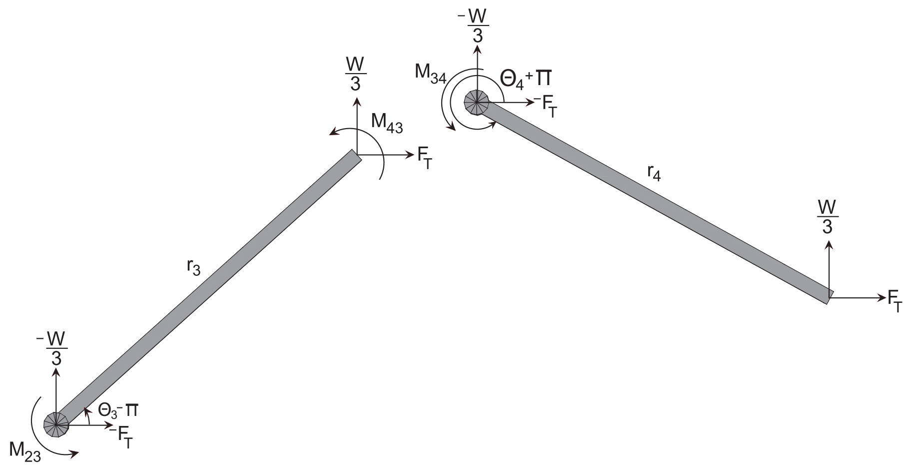

Figure 3.4: Free body diagram for one leg of the three feet pushup.

Another example is the different force requirements of the arm muscles when lifting a bar with two hands and lifting a set of dumbbells, as shown in Fig. 3.5. When lifting a set of dumbbells straight up, one on each hand, the arm muscles need to exert forces such that the resultant forces are vertically upwards against gravity, as shown in Fig. 3.5(a). However, when lifting a bar with two hands, interaction forces between the hands are allowed through the bar as long as they are equal and opposite in direction to each other thus, canceling each other, as shown in Fig. 3.5(b). In such case, the arm muscles could exert less net forces thus, it is generally easier to bench press than lift a set of dumbbells with the same total weight. Using this concept, the tangential forces at the foot contact points could be adjusted to minimize the joint torque requirements.

(a) Lifting dumbbells (b) Lifting a bar

Figure 3.5: Forces when lifting dumbbells and lifting a bar.

A maximum friction coefficient, μ, of 0.3 was chosen for this analysis and the total weight of the robot was set to 28.42 N. A tangential force, F_T, can be chosen for any value less than the normal force times the friction coefficient. Since only one leg is being analyzed the maximum tangential force is one third of the weight of the body times μ. The maximum magnitude of F_T is 2.84 N and can act in both the positive and negative direction, $-2.84N \leq F_T \leq 2.84N$.

The minimum magnitude of the F_T is equal to zero. The positive and negative values of F_T account for an outwards and inwards reactive force at the feet.

The moment at the flexure joint, M_{23}, and at the knee joint, M_{34}, are calculated from Equations 3.4 and 3.5, respectively. The legs were assumed to be weightless for the torque analysis since they would be negligible compared to the weight of the body. Also, $\theta_4 + \pi$ and $\theta_3 - \pi$ are the angles from the positive x-axis to the shank and thigh links, respectively. By combining the kinematic analysis using the slider-rocker mechanism and force analysis using the FBD equations, the torque at the flexure and knee joints can be calculated.

$$M_{34} = r_4 sin\left(\theta_4 + \pi\right) F_T - r_4 cos\left(\theta_4 + \pi\right) \frac{W}{3} \tag{3.4}$$

$$M_{23} = r_3 sin\left(\theta_3 - \pi\right) F_T - r_3 cos\left(\theta_3 - \pi\right) \frac{W}{3} + M_{34} = -hF_T - \left(d - L_b\right) \frac{W}{3} \tag{3.5}$$

3.1.3 Actuator Torque for Three Feet Pushup

This section will investigate the effects of d, link length ratio ($\alpha = \frac{r_3}{r_4}$), and F_T on the actuator torques. First, the effects of d and α on the actuator torques when F_T equals zero will be considered independently. Then, d and α will be coupled and the maximum actuator torques will be calculated when F_T equals zero. Once the relationships between d and α on the actuator torques are investigated, the effects of F_T on the actuator torques will be studied. A total link length (r_{tot}= r_3 + r_4) of 1.2 m, body link length, L_b, ($=L_0 + L_1 + L_2$, shown in Fig. 2.1) equal to 0.18 m, a friction coefficient, μ, of 0.3 and total body weight, W, of 28.42 N were chosen for the entire actuator torque analysis.

Effects of d on Actuator Torques

The effects of the value of d on the actuator torques were studied. The parameters chosen for the analysis were as follows: $r_3 = 0.45$ m, $r_4 = 0.75$ m, (or $\alpha = 0.6$) and d ranged from $(r_4 - r_3) + L_b$ and $(r_3 + r_4 + L_b)$. Fig. 3.6 shows the knee and flexure joint torques as the body lifts upwards for different values of d and F_T equal to zero.

Note that as the value of d increases the maximum height of the body (h_{max}) decreases since the stance of the robot is larger. The flexure joint torque, shown in Fig. 3.6(b), decreases as d decreases. Also, when F_T is equal to zero the flexure joint torque is constant for each value of d ($M_{23} = \frac{-(d-L_b)W}{3}$).

However, the knee joint torque significantly changes as d changes. For this example, the maximum knee joint torque occurs when d equals the minimum allowable value (0.48 m)

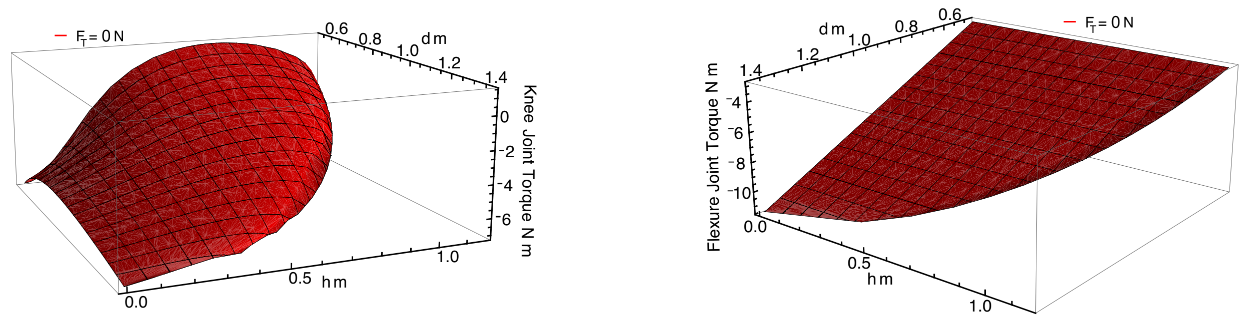

(a) Knee joint torque

(b) Flexure joint torque

Figure 3.6: Joint torques for various d values and F_T =0 for the three feet pushup.

and h=0. The maximum knee joint torque does not always occur when h equals zero as will be later discussed.

Effects of Link Length Ratio on Actuator Torques

The effects of the link length ratio, α, were studied given a d value of 0.65 m and a total link length, r_{tot}, of 1.2 m and F_T equal to zero. Fig. 3.7 shows the actuator torque results as the body moves upward for different link length ratios. The minimum and maximum allowable values of α given r_{tot}, d and L_b are calculated from Equations 3.6 and 3.7. Note that if α_{min} equals zero then d equals $r_{tot} + L_b$ where r_{tot} equals r_4.

$$\alpha_{min} = \frac{-d + L_b + r_{tot}}{d - L_b + r_{tot}} \tag{3.6}$$

$$\alpha_{max} = -\frac{-d + L_b - r_{tot}}{-d + L_b + r_{tot}} \tag{3.7}$$

As shown in Fig. 3.7(b) the flexure joint torque is not affected by the various link length ratios when a value for d is specified and F_T equals zero. From Equation 3.5, the flexure joint torque can be defined in terms of F_T, h, $d - L_b$, and W thus, for a given d value and total link length value, r_{tot}, the different link length ratios will not affect the flexure joint torque. The knee joint torque, however, is affected by α, as shown in Fig. 3.7(a). For this specific example, as α increases and the robot stands up the knee joint experiences a smaller range of torques. Note that the maximum knee joint torque occurs at different heights for each α. In this case, the maximum knee joint torque occurs when α equals α_{min} and h equals 0.

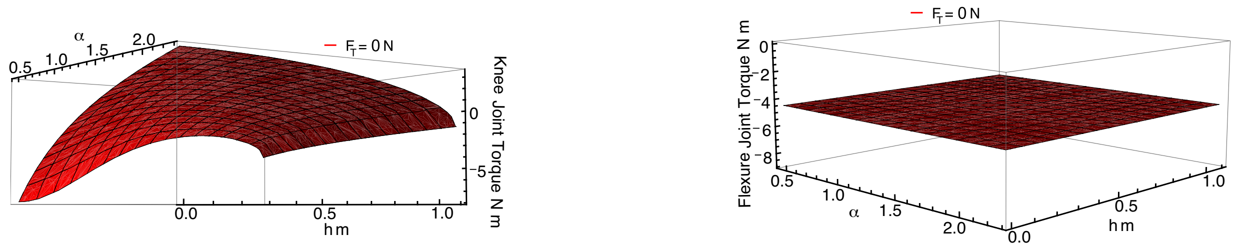

(a) Knee joint torque

(b) Flexure joint torque

Figure 3.7: Joint torques for different link length ratios ($\alpha = \frac{r_3}{r_4}$) and F_T=0 for the three feet pushup.

Maximum Actuator Torques for Various d and α Combinations

After studying how d and α independently affect the actuator torques, the results show that it is important to minimize the maximum torque. Thus, this section first discusses three distinct cases where the knee joint torque is maximum. Recall that the flexure joint torque is only affected by d when F_T equals zero and the torque is smallest with smaller d values. Thus, the knee joint torque will be studied more closely. Next, relationships between d and α will be established for each of the three cases. Finally, an expression for the optimal d value that will minimize the maximum knee joint torque given α will be presented.

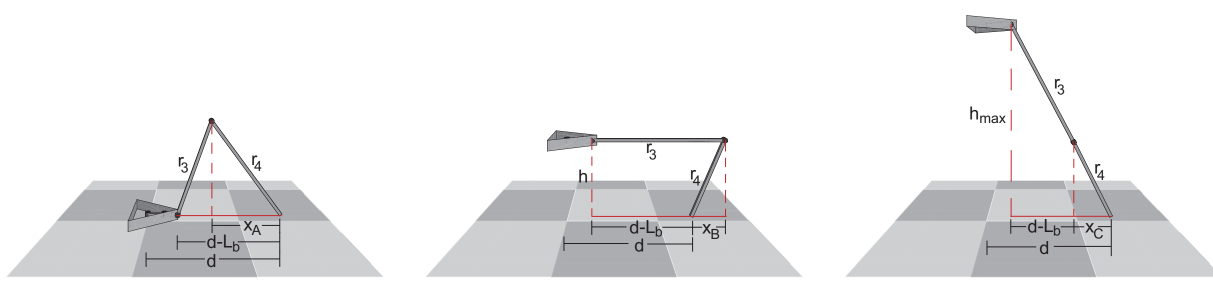

(a) Case A: height equals zero

(b) Case B: height when r_3 is parallel to the ground

(c) Case C: maximum Height

Figure 3.8: Cases for maximum height for the three feet pushup

As mentioned, the maximum knee joint torque when F_T equals zero occurs at three specific cases depending on the value of d and α, as shown in Fig. 3.8. *Case A*, shown in Fig. 3.8(a), is defined when the maximum knee joint torque occurs at the initial standing position (i.e. h=0). *Case B*, shown in Fig. 3.8(b), is defined when the maximum knee joint torque occurs when r_3 is parallel to the ground. This is also the maximum allowable range of the shank link. Finally *Case C*, shown in Fig. 3.8(c), is defined when the maximum knee joint torque occurs when the robot reaches its maximum height (thigh and shank links are aligned). Thus, for each case the maximum knee joint torque can be calculated from Equation 3.8, where x_A, x_B, and x_C are calculated using Equations 3.9, 3.10, and 3.11, respectively and are shown in Fig. 3.8.

$$M_{34max} = \frac{-W}{3} x_{A,B,orC} \tag{3.8}$$

$$x_A = \frac{1}{2}\left(d - L_b + \frac{(-1+\alpha){r_{tot}}^2}{(1+\alpha)(-d+L_b)}\right) \tag{3.9}$$

$$x_B = -d + L_b + \frac{\alpha r_{tot}}{(1+\alpha)} \tag{3.10}$$

$$x_C = \frac{d - L_b}{1+\alpha} \tag{3.11}$$

Now that equations for x_A, x_B, and x_C have been expressed in terms of d and α, *Cases A*, *B* and *C* can be defined also in terms of d and α. More specifically, when $|x_A| > |x_B|$ and $|x_A| > |x_C|$ then, *Case A* is satisfied and the relationships between d and α are listed in Table 3.1. On the other hand, when $|x_B| > |x_A|$ and $|x_B| > |x_C|$ then, *Case B* is satisfied and the relationships between d and α are listed in Table 3.2. Finally, when $|x_C| > |x_A|$ and $|x_C| > |x_B|$ then, *Case C* is satisfied and the relationships between d and α are listed in Table 3.3. Thus, for each of these cases, given α the ranges of d that will yield a maximum knee joint torque can be found.

Table 3.1: *Case A*: Relationship between d and α that yields a maximum knee joint torque for the three feet pushup.

α	d *range*
$0 < \alpha \leq \frac{\sqrt{3}}{2}$	$L_b + \frac{(r_{tot}-\alpha r_{tot})}{(1+\alpha)} \leq d < L_b + r_{tot}$
$\frac{\sqrt{3}}{2} < \alpha < 1$	$L_b + \frac{(r_{tot}-\alpha r_{tot})}{(1+\alpha)} \leq d \leq L_b + \frac{(\alpha r_{tot})}{3(1+\alpha)} - \frac{1}{3}\sqrt{\frac{(-3+4\alpha^2){r_{tot}}^2}{(1+\alpha)^2}}$ or $\frac{1}{3}\left(3L_b + \frac{\alpha r_{tot}}{(1+\alpha)} + \sqrt{\frac{(-3+4\alpha^2){r_{tot}}^2}{(1+\alpha)^2}}\right) \leq d < L_b + r_{tot}$
$\alpha = 1$	$L_b + \frac{r_{tot}}{3} \leq d < L_b + r_{tot}$
$\alpha > 1$	$d = L_b + \frac{(-1+\alpha)r_{tot}}{(1+\alpha)}$

Fig. 3.9 summarizes the results of *Cases A*, *B*, and *C* for α ranging from 0 to 3 and the corresponding d values. For this analysis, a total link length, r_{tot}, was chosen to be 1.2 m, L_b

Table 3.2: *Case B*: Relationship between d and α that yields a maximum knee joint torque for the three feet pushup.

α	$d\ range$
$\alpha = \frac{\sqrt{3}}{2}$	$d = L_b + (-1 + \frac{2}{\sqrt{3}})r_{tot}$
$\frac{\sqrt{3}}{2} < \alpha < 1$	$L_b + \frac{(\alpha r_{tot})}{3(1+\alpha)} - \frac{1}{3}\sqrt{\frac{(-3+4\alpha^2){r_{tot}}^2}{(1+\alpha)^2}} \leq d \leq \frac{1}{3}\left(3L_b + \frac{\alpha r_{tot}}{(1+\alpha)} + \sqrt{\frac{(-3+4\alpha^2){r_{tot}}^2}{(1+\alpha)^2}}\right)$
$\alpha = 1$	$L_b < d \leq L_b + \frac{r_{tot}}{3}$
$\alpha > 1$	$L_b + \frac{(-1+\alpha)r_{tot}}{(1+\alpha)} \leq d \leq L_b + \frac{\alpha r_{tot}}{(2+\alpha)}$

Table 3.3: *Case C*: Relationship between d and α that yields a maximum knee joint torque for the three feet pushup.

α	$d\ range$
$\alpha \geq 1$	$L_b + \frac{\alpha r_{tot}}{(2+\alpha)} \leq d < L_b + r_{tot}$

was set to 0.18 m and F_T was equal to zero. Fig. 3.9(a) represents the maximum knee joint torques given α and d. Note that for $\alpha \geq 1$ the minimum maximum knee joint torque occurs for values of d that satisfy x_B equal to x_C. Also, for $\alpha < 1$ the minimum maximum torque occurs for d values for when the derivative of x_A equals zero. Thus, given a link length ratio, α, the optimal d, d_{opt}, that will yield the minimum maximum knee joint torque can be found using Equation 3.12. Also, it can be concluded that given a d value the largest α will yield the minimum maximum knee joint torque.

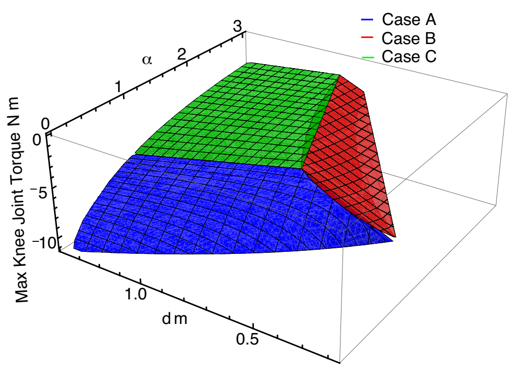

(a) Knee joint torque

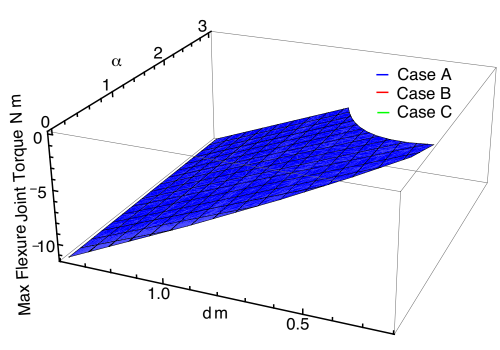

(b) Flexure joint torque

Figure 3.9: Maximum joint torques for different d and α values when F_T =0 for the Three Feet Pushup

$$d_{opt} = \begin{cases} L_b + \frac{\sqrt{-(-1+\alpha^2){r_{tot}}^2}}{(1+\alpha)} & \alpha < 1 \\ L_b + \frac{\alpha r_{tot}}{(2+\alpha)} & \alpha \geq 1 \end{cases} \tag{3.12}$$

Fig. 3.9(b) shows the maximum flexure joint torque for different d and α values when F_T equals zero. As previously noted, α does not affect the flexure joint torque when F_T equals zero. Thus, in order to minimize the flexure joint it is best to choose the smallest d value.

Effects of the Tangential Force on Actuator Torques

The effects of a friction force at the feet on the actuator torques were studied. As mentioned in Section 3.1.2, a range of $-2.84N \leq F_T \leq 2.84N$ was considered given a maximum magnitude of 2.84 N ($\frac{\mu W}{3}$) acting in positive and negative directions at the feet. For this analysis, the three feet pushup can be divided in two other cases: *Case* 1 and *Case* 2 (separate from Case A, B and C, previously discussed), as shown in Fig. 3.10. *Case* 1 is defined as the case when $\frac{\pi}{2} < \theta_4 < \pi$ (Fig. 3.10(a)) during the entire standing motion and $r_3 < d - L_b$. *Case* 2 is defined as the case when θ_4 will equal $\frac{\pi}{2}$ at least once as the robot stands and $r_3 \geq d - L_b$ (Fig. 3.10(b)). The chosen parameters for *Case* 1 were $r_3 = 0.45$ m, r_4=0.75 m, and $d = 0.65$ m. For this case $d - L_b = 0.47$ m. On the other hand, the chosen parameters for *Case* 2 were $r_3 = 0.45$ m, r_4=0.75 m, and $d = 0.55$ m, where $d - L_b = 0.37$ m. In order to adequately compare the two cases the same link length ratio ($\alpha = 0.6$) was selected.

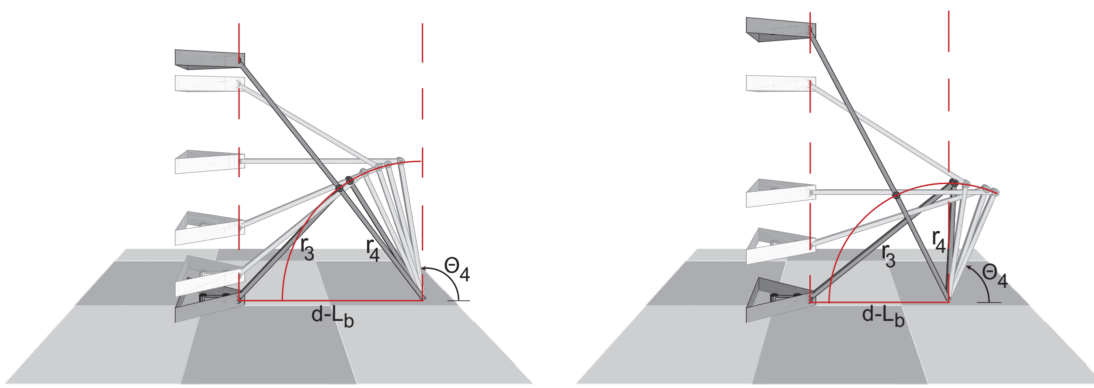

(a) *Case* 1: $r_3 < d - L_b$ (b) *Case* 2: $r_3 \geq d - L_b$

Figure 3.10: Case study of the three feet pushup standing up method.

Case 1 knee and flexure joint torque results for the allowable friction force range are shown in Figs. 3.11(a) and 3.11(b). It was found that a tangential force acting inwards toward the center of the body results in lower actuator torques than a tangential force acting outwards. Also, the magnitude of the knee joint torque for *Case* 1 and F_T equal to zero will always be

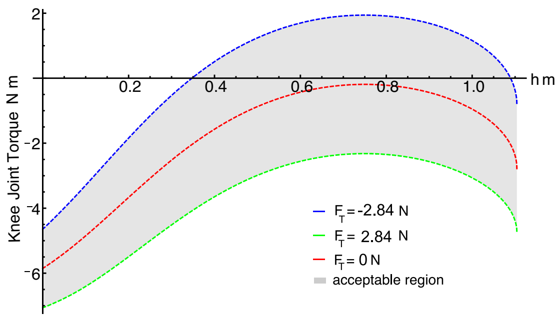

(a) *Case* 1: Knee joint torque range

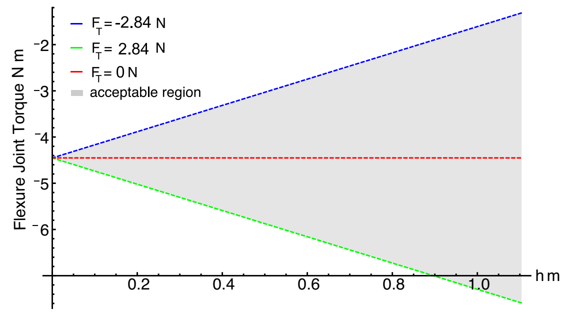

(b) *Case* 1: Flexure joint torque range

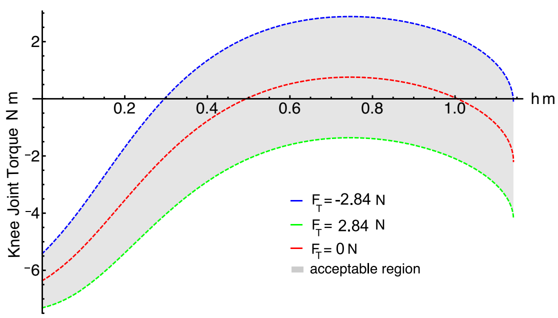

(c) *Case* 2: Knee joint torque range

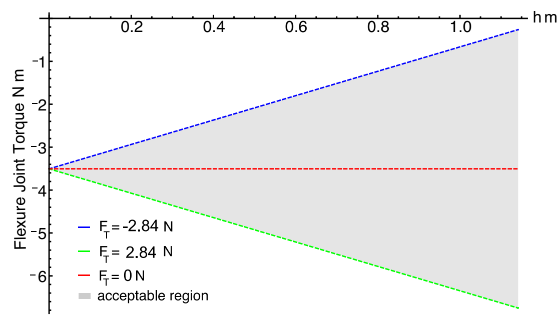

(d) *Case* 2: Flexure joint torque range

Figure 3.11: Joint torque region defined by a maximum and minimum F_T for the three feet pushup.

greater than zero since the shank link will never be perpendicular to the flat surface because $r_3 < d - L_b$. The local maximum of the knee joint torque curve occurs when the thigh link is parallel to the ground. The magnitude of the flexure joint torque linearly decreases when the F_T pushes inwards towards the center of the body and linearly decreases when F_T pushes outwards. The positive direction of F_T is shown in Fig. 3.4. When no tangential forces exist the flexure joint is constant and equal to $\frac{-(d-L_b)W}{3}$.

Case 2 knee and flexure joint torque results for the allowable friction force range are shown in Figs. 3.11(c) and 3.11(d). For this case, it was also concluded that a tangential force pushing inwards towards the center of the body will result in less actuator torques than a tangential force pushing outwards. The knee joint torque will equal zero when F_T equals zero and the shank link, r_4, is perpendicular to the ground. Also, the local maximum of the knee joint torque plots occurs when the thigh link, r_3, is parallel to the ground. The same flexure joint torque trends as *Case* 1 occur for *Case* 2. The flexure joint torque linearly decreases in magnitude when F_T pushes inwards and linearly increases in magnitude when F_T pushes outwards. Also, the flexure joint torque is constant when F_T equals zero.

After comparing the actuator joint torque results given an allowable friction force range, defined by a friction coefficient and normal force, it was concluded that a maximum tangential force acting inwards towards the body will result in the lowest actuator torques as the body lifts using the three feet pushup.

3.1.4 Overall Conclusions of the Three Feet Pushup

The three feet pushup is one of the considered standing up methods for STriDER. It symmetrically uses its three legs to lift the body. First, the feet of the robot are placed to the desired final foot positions and the body is then lifted upwards by pushing the feet against the ground. Since the three legs act in the same way one leg can individually be analyzed and modeled as a slider-rocker mechanism. The effects of three important parameters on the actuator torques as the robot stands up were investigated. These parameters included, a distance d defined by the distance between the projected center of the body on the ground and foot position, a thigh and shank link length ratio, α, and friction force F_T at the feet. The effects of all three parameters were considered given a total link length value of, r_{tot} equal to 1.2 m, L_b equal to 0.18m, and total body weight, W, of 28.42 N.

First, the effects of d and α on the actuator torques were investigated individually ignoring the tangential forces. Then, d and α were coupled and the maximum actuator torques were analyzed for F_T equal to zero. Three distinct cases were defined where the maximum knee joint torque may occur depending on the values of d and α. In order to minimize the knee joint torque, a relationship between d and α was established to determine the minimum maximum knee joint torque. It was found that for a given link length ratio, α, an optimal d value, d_{opt}, can be calculated using Equation 3.12. Also, for a given d value, the largest α will yield a minimum maximum knee joint torque. Although a maximum α yields lower actuator torques when F_T equals zero, it is important to note that link lengths will most likely be optimized for walking and not standing. Thus, optimizing d, in this case, is more beneficial than optimizing α. It was also found that the flexure joint torque is not affected by different link length ratios and a minimum d value will yield the lowest flexure joint torque. The literature review findings concluded that for human pushups, the elbow joint torque decreases as the distance between the hand positions increases. For STriDER, a human elbow is the same as its knee joint thus, from the three feet pushup knee joint torque results it was found that for a range of low d values as d increases and the body moves upwards the maximum knee joint torque does decrease. However, for a range of high d values the maximum knee joint torque increases as d increases.

Finally, the effects the tangential forces, F_T, were studied. Two cases were presented ($Case$ 1 and $Case$ 2) where $Case$ 1 is defined when $r_3 < d - L_b$ and $Case$ 2 is defined when $r_3 \geq d - L_b$. It was found that a tangential force acting inwards towards the center of the body will yield lower actuator torques than a tangential force acting outwards.

3.2 Two Feet Pushup

The two feet pushup begins with the robot flat on the ground with all three legs extended outwards (Fig. 3.12(a)) then, two of its legs move inwards toward the body to their final desired position, defined by d, leaving one leg extended (Fig. 3.12(b)). d is the distance from the center of the body to the desired final foot positions for the two bending legs. Once the two legs reach their desired foot positions, the body is pushed upwards by the two legs pushing against the ground until it reaches its maximum height (Fig. 3.12(c) to 3.12(f)). Note that the flexure joint of the straight leg follows an arc defined by the thigh and shank links as the robot stands. The maximum body height is achieved when the thigh and shank links of the bending legs are aligned. Although this method is statically stable always since all three feet are touching the ground and the projected center of gravity lies inside the support triangle, it requires high torques at the actuators due to the large moment arms.

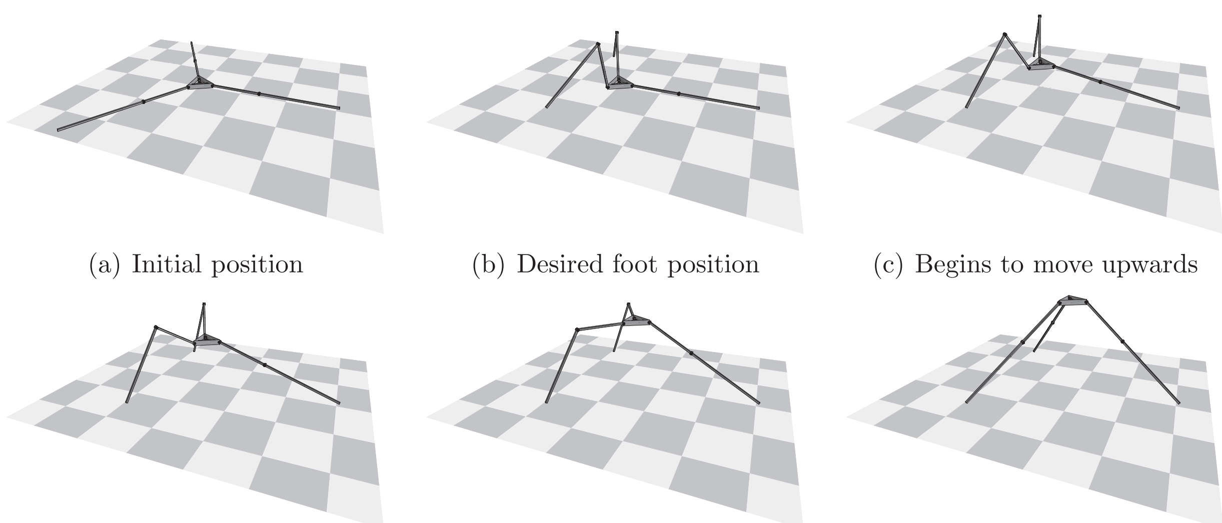

(a) Initial position (b) Desired foot position (c) Begins to move upwards

(d) Continues to move upwards (e) Continues to move upwards (f) Maximum height reached

Figure 3.12: The motion of the two feet pushup.

This method follows the same motion as a human pushup thus, the research findings will be more relative for this standing up strategy. Note that the foot positions do not form an equilateral triangle for the two feet pushup because two of the legs bend and the third leg must remain straight. Also it was preferred not to actuate the rotator aligning mechanisms for simplicity, so an equilateral triangle is not formed due to this choice. Thus, the two feet pushup and three feet pushup methods cannot be directly compared. The configuration of the two bending legs in the two feet pushup standing up method is the same, while the third leg (straight leg) keeps the thigh and shank links aligned as the robot stands. Thus, the analysis of the two feet pushup is divided in two parts: analysis of the bending leg and analysis of the straight leg. A kinematic and torque analysis is presented for the portion when the body begins to move upwards and reaches its maximum height (Fig. 3.12(b) to 3.12(f)).

A range of d values, various link length ratios ($\alpha = \frac{r_3}{r_4}$) and a range of allowable tangential friction forces between the feet and the ground will also be investigated in the analysis. As stated in Section 3.1, the minimum allowable d is the difference between the thigh and shank link length plus the body link ($L_b = L_0 + L_1 + L_2$) length. The maximum allowable d is the added length of the thigh, shank, and L_b. The range of tangential contact force between the foot and the ground is defined by the friction coefficient and the normal contact force due to gravity. Thus, the minimum tangential contact force is zero (no friction force) and the maximum tangential contact force is the normal force times the friction coefficient for a non-slip condition. As long as the tangential contact forces, at the three feet, satisfy these conditions and the force balance is satisfied, the tangential forces can be adjusted by force control of the actuators of the robot. The choice of the tangential force will effect the motor torque requirements at the joints.

3.2.1 Kinematic Analysis for the Two Feet Pushup

The inverse kinematics procedure discussed in Section 2.3 will be used to find the joint angles of the bending and straight leg as the body moves upwards. In order to use the inverse kinematics method to find the rotator, flexure and knee joint angles, the global body position and orientation and global foot positions as the robot stands must be known. The global foot position in global coordinates, assuming the global coordinates are located in the initial center of the body location, for the straight leg are $\mathbf{d}_0^{P_1} = [(L_B + r_{tot})\ \ 0\ \ 0]^T$ and for the bending legs $\mathbf{d}_0^{P_2} = \left[\frac{-d}{2}\ \ \frac{\sqrt{3}d}{2}\ \ 0\right]^T$ and $\mathbf{d}_0^{P_3} = \left[\frac{-d}{2}\ \ \frac{-\sqrt{3}d}{2}\ \ 0\right]^T$. Note that the feet positions do not move as the robot stands up. The global body orientation as the robot stands, $\mathbf{R}_0^B$, is always zero since the body does not rotate about the X_0, Y_0, or Z_0 axis. The body position in global coordinates changes in both the X_0 and Z_0 directions. The body height (body position in $+Z_0$ direction) is assumed to be an input from zero to a maximum height, calculated from Equation 3.13. Note that the maximum height is calculated from a constant d value, L_b, and r_{tot}, where r_{tot} equals the total thigh and shank link lengths. Once the height of the body is known, the X_0 position of the body is calculated using Equation 3.14. Now the global body position, orientation and foot positions are known given d, L_b, and r_{tot}, so inverse kinematics can be used on each leg to find the rotator, flexure and knee joint angles ($\theta_{2i}, \theta_{3i}, \theta_{4i}$) as the body stands up.

$$h_{max} = \frac{\sqrt{-\left(d - L_b - r_{tot}\right)\left(d - L_b + r_{tot}\right)\left(\left(d - L_b\right)^2 + 2\left(d - L_b\right)r_{tot} + 3{r_{tot}}^2\right)}}{\left(d - L_b + 2r_{tot}\right)} \tag{3.13}$$

$$B_{X_{0_{pos}}} = r_{tot} - \sqrt{-h^2 + r_{tot}^2} \tag{3.14}$$

3.2.2 Static Force Analysis for the Two Feet Pushup

Once the rotator, flexure and knee joint angles are calculated for each leg using the inverse kinematics method, a static force analysis can be completed to calculate the actuator torques. Notice that as the body lifts using the two feet pushup method, the weight distribution for each leg changes. Fig. 3.13 shows the forces at the feet for each leg and Equations 3.15 and 3.16 are used to calculate the normal forces at the feet. Recall that d is the distance between the bending legs foot positions and the projected center of the body, r_{tot} is the sum of the thigh and shank link lengths, h is the height of the body, L_b is the body link length $(L_0 + L_1 + L_2)$, shown in Fig. 2.1, and W is the total weight of the body. In order for the forces to be balanced in the z-direction the sum of the normal forces at the feet must equal the total weight of the robot.

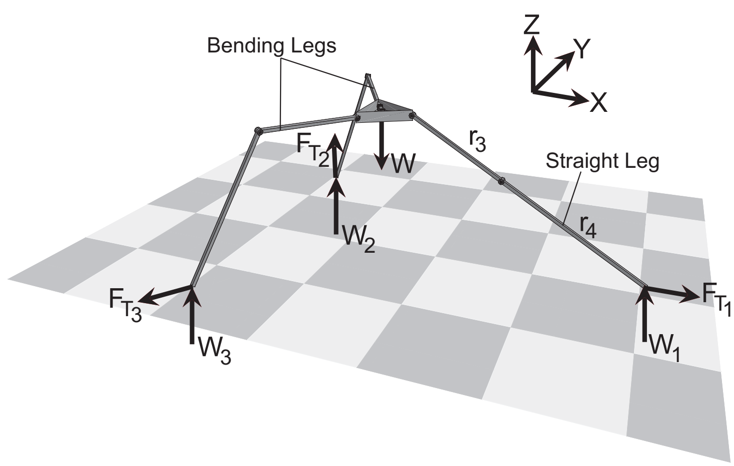

Figure 3.13: Forces at the feet for the two feet pushup.

$$W_1 = \frac{(d + 2r_{tot} - 2\sqrt{-h^2 + r_{tot}^2})W}{d + 2(L_b + r_{tot})} \tag{3.15}$$

$$W_2 = W_3 = \frac{(L_b + \sqrt{-h^2 + r_{tot}^2})W}{d + 2(L_b + r_{tot})} \tag{3.16}$$

The x and y components of the maximum friction force at the feet are calculated using Equations 3.17, 3.18, and 3.19. The maximum allowable tangential force at each foot is the friction coefficient, μ, times the normal force at the foot. Thus, for the straight leg, leg 1, the maximum tangential force, F_{T_1} is equal to μW_1 and for bending legs, legs 2 and 3, the maximum tangential force at the feet, F_{T_2} and F_{T_3} are μW_2 and μW_3, respectively. Since both bending legs act the same as the robot stands, only leg 2 will be analyzed and leg 1 will be used for the straight leg torque analysis.

$$F_{T_1} = \begin{bmatrix} F_{T_{x_1}} \\ F_{T_{y_1}} \end{bmatrix} = \begin{bmatrix} \mu W_1 \\ 0 \end{bmatrix} \tag{3.17}$$

$$F_{T_2} = \begin{bmatrix} F_{T_{x_2}} \\ F_{T_{y_2}} \end{bmatrix} = \begin{bmatrix} -\frac{\mu W_1}{2} \\ \frac{1}{2}\sqrt{-(\mu W_1)^2 + 4(\mu W_2)^2} \end{bmatrix} \tag{3.18}$$

$$F_{T_3} = \begin{bmatrix} F_{T_{x_3}} \\ F_{T_{y_3}} \end{bmatrix} = \begin{bmatrix} -\frac{\mu W_1}{2} \\ -\frac{1}{2}\sqrt{-(\mu W_1)^2 + 4(\mu W_2)^2} \end{bmatrix} \tag{3.19}$$

Straight Leg Joint Torque Equations

The joint torques for the straight leg, labeled in Fig. 3.13, will first be discussed. A general torque expression, shown in Equation 3.20, will be used to find the individual joint torque equations. This equation shows that torque can be calculated by taking the cross product of a distance vector from the feet to the joint with a force vector at the feet and then taking the dot product of that result with the a unit vector at the desired joint. Since the equations for the forces at the feet have been discussed, the next step is to determine the vectors from the feet to the rotator, flexure and knee joints. Note that the rotator joint does not experience any torque for the straight leg since the leg does not rotate as the body stands up.

$$Torque = \left[\{dx_P^j, dy_P^j, dz_P^j\} \times \{F_x, F_y, F_z\}\right] \cdot \vec{n_j} \tag{3.20}$$

The vectors from the feet to the flexure and knee joints are found using Equations 3.21 and 3.22, where $B_{X_{0pos}}$ is the current body position from the $+X_0$ axis, r_{tot} is the sum of the thigh and shank link lengths ($r_3 + r_4$), and θ_{31} is the flexure joint angle for leg 1 calculated using the inverse kinematics method discussed in Section 3.2.1.

$$\mathbf{d}_{P_1}^2 = \begin{bmatrix} dx_{P_1}^2 \\ dy_{P_1}^2 \\ dz_{P_1}^2 \end{bmatrix} = \begin{bmatrix} B_{X_{0pos}} - r_{tot} \\ 0 \\ h \end{bmatrix} \tag{3.21}$$

$$\mathbf{d}_{P_1}^3 = \begin{bmatrix} dx_{P_1}^3 \\ dy_{P_1}^3 \\ dz_{P_1}^3 \end{bmatrix} = \begin{bmatrix} B_{X_{0pos}} - r_{tot} + r_3 sin(\theta_{31}) \\ 0 \\ h - r_3 cos(\theta_{31}) \end{bmatrix} \tag{3.22}$$

Now that the distance and force vectors are know for the flexure and knee joints the joint torques for the straight leg can be calculated from Equations 3.23 and 3.24, respectively. Note the the unit vector for the flexure and knee joint torque is the same ($\{0, -1, 0\}$).

$$M_{23_S} = -dz^2_{P_1} F_{Tx_1} + dx^2_{P_1} W_1 \quad (3.23)$$

$$M_{34_S} = -dz^3_{P_1} F_{Tx_1} + dx^3_{P_1} W_1 \quad (3.24)$$

Bending Leg Joint Torque Equations

Similar to the straight leg, the distance between the feet and the rotator, flexure, and knee joints were found for the bending leg and can be calculated using Equations 3.25, 3.26, and 3.27, respectively. As previously mentioned, $B_{X_{0pos}}$ is the current body position from the $+X_0$ axis, L_0 is the distance between the center of the body to the rotator joint, r_{tot} is the sum of the thigh and shank link lengths (r_3+r_4), and θ_{22}, θ_{32}, and θ_{42} are the rotator, flexure and knee joint angles for leg 2 calculated using the inverse kinematics method discussed in Section 3.2.1.

$$\mathbf{d}^1_{P_2} = \begin{bmatrix} dx^1_{P_2} \\ dy^1_{P_2} \\ dz^1_{P_2} \end{bmatrix} = \begin{bmatrix} B_{X_{0pos}} + \frac{d}{2} - \frac{1}{2}L_0 \\ \frac{\sqrt{3}}{2}(-d + L_0) \\ h \end{bmatrix} \quad (3.25)$$

$$\mathbf{d}^2_{P_2} = \begin{bmatrix} dx^2_{P_2} \\ dy^2_{P_2} \\ dz^2_{P_2} \end{bmatrix} = \begin{bmatrix} B_{X_{0pos}} + \frac{d}{2} - \frac{L_b}{2} \\ \frac{\sqrt{3}}{2}(-d + L_b) \\ h \end{bmatrix} \quad (3.26)$$

$$\mathbf{d}^3_{P_2} = \begin{bmatrix} dx^3_{P_2} \\ dy^3_{P_2} \\ dz^3_{P_2} \end{bmatrix} = \begin{bmatrix} B_{X_{0pos}} + \frac{1}{2}(d - L_b - r_3 sin(\theta_{32}) - \sqrt{3} r_3 cos(\theta_{32}) sin(\theta_{22}) \\ \frac{1}{2}\left(\sqrt{3}d + \sqrt{3}L_b + \sqrt{3} r_3 sin(\theta_{32}) - r_3 cos(\theta_{32}) sin(\theta_{22})\right) \\ h - r_3 cos(\theta_{32}) cos\theta_{22} \end{bmatrix} \quad (3.27)$$

From the distance and force vectors, the rotator, flexure and knee joint torque can be calculated from Equations 3.28, 3.29, and 3.30, where W_2 is the the normal force at the foot of leg 2. The general torque expression (Equation 3.20) was used to determine the individual joint torques.

$$M_{12_B} = \frac{1}{2}(dz^1_{P_2}(\sqrt{3}F_{Tx_2} + F_{Ty2}) - (\sqrt{3}dx^1_{P_2} + dy^1_{P_2})W_2) \quad (3.28)$$

$$\begin{aligned} M_{23_B} = \tfrac{1}{2}(dz^2_{P_2}(F_{Tx_2} - \sqrt{3}F_{Ty_2}) - dx^2_{P_2} W_2 + \sqrt{3} dy^2_{P_2} W_2) cos\,(\theta_{22}) + \\ (dy^2_{P_2} F_{Tx_2} - dx^2_{P_2} F_{Ty_2}) sin\,(\theta_{22}) \end{aligned} \quad (3.29)$$

$$M_{34_B} = \frac{1}{2}(dz^3_{P_2}(F_{Tx_2} - \sqrt{3}F_{Ty_2}) - dx^3_{P_2}W_2 + \sqrt{3}dy^3_{P_2}W_2)cos\,(\theta_{22}) + (dy^3_{P_2}F_{Tx_2} - dx^3_{P_2}F_{Ty_2})sin\,(\theta_{22}) \tag{3.30}$$

3.2.3 Actuator Torque for Two Feet Pushup

This section will investigate the effects of d, link length ratio ($\alpha = \frac{r_3}{r_4}$), and F_T on the actuator torques. Similar to the three feet pushup analysis, first, the effects of d and α on the actuator torques when F_T equals zero will be considered independently. Then, d and α will be coupled and an optimization will be completed to determine an optimized α and d combination that will minimize the joint torques when F_T equals zero. The effects of F_T on the actuator torques will also be studied. A total link length (r_{tot}= r_3 + r_4) of 1.2 m, body link length, L_b, (=L_0 + L_1 + L_2, shown in Fig. 2.1) equal to 0.18 m, a friction coefficient, μ, of 0.3 and total body weight, W, of 28.42 N were chosen for the entire actuator torque analysis.

Effects of d on Actuator Torques

The effects of the value of d on the actuator torques were studied. The parameters chosen for the analysis were as follows: r_3 = 0.45 m, r_4 = 0.75 m, (or α = 0.6) and d ranged from $(r_4 - r_3) + L_b$ and $(r_3 + r_4 + L_b)$. Figs. 3.14 and 3.15 show the rotator, flexure and knee joint torques for the straight leg and bending leg.

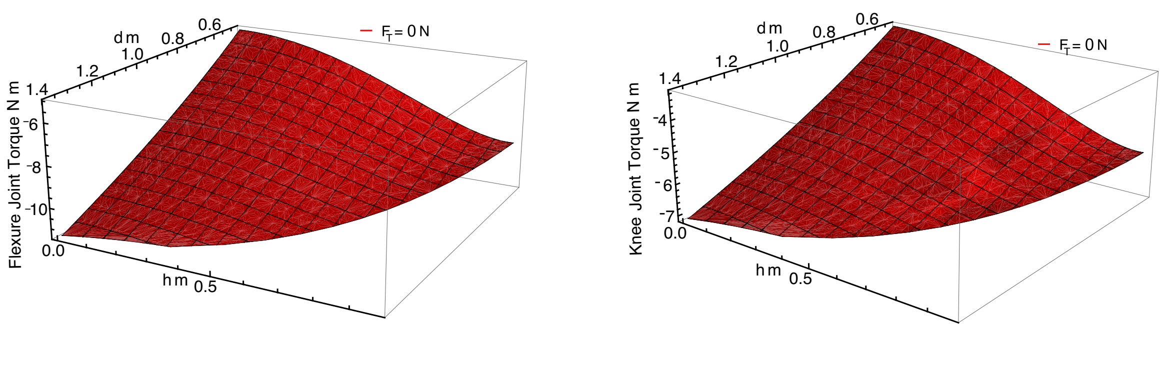

(a) Flexure joint torque

(b) Knee joint torque

Figure 3.14: Straight leg joint torques for various d values and F_T =0 for the two feet pushup.

As shown in Fig. 3.14, the flexure joint of the straight leg experiences a much higher torque than the knee joint. This is because the moment arm for the flexure joint is much longer than for the knee joint. However, for both joints a smaller d will reduce the joint torques for the straight leg. Note, that the rotator joint experiences no torque since the straight leg does not rotate as the robot stands using the two feet pushup.

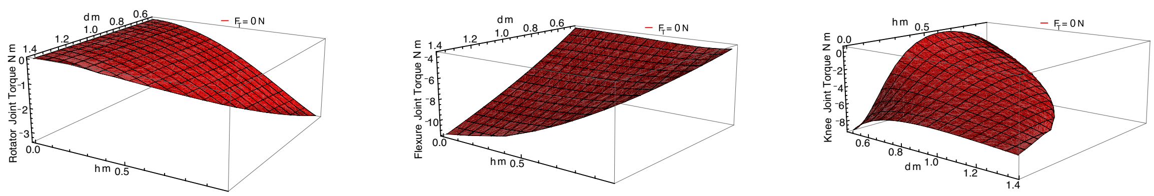

(a) Rotator joint torque (b) Flexure joint torque (c) Knee joint torque

Figure 3.15: Bending leg joint torques for various d values and F_T =0 for the two feet pushup

The rotator joint of the bending leg does rotate as the robot stands up, as shown in Fig. 3.15(a). The rotator joint torque is initially zero for any d value. As the value of d increases, the allowable maximum height decreases so, the support triangle of the robot is much larger. For smaller d values the robot can stand up to a higher height and the torque at the rotator joint increases. Thus, in order to reduce the torque at the rotator joint for the bending leg it is best to have a larger d value so the allowable maximum height of the robot is minimized. Next, the flexure joint torque for the bending leg, shown in Fig. 3.15(b) was analyzed. It is evident that smaller d values yield lower torques at the flexure joint. Finally, the knee joint torque for the bending leg, shown in Fig. 3.15(c) was analyzed. It was found, for this example, that the largest torque for a given d occurs when the robot is flat on the ground. In fact, the minimum maximum knee joint torque occurs when d equals 0.94 m.

Effects of Link Length Ratio on Actuator Torques

The effects of the link length ratio, α $(= \frac{r_3}{r_4})$, on the joint torques for the straight and bending leg were investigated given a d value of 0.65 m and F_T equal to zero, as shown in Figs. 3.16 and 3.17.

For the straight leg, it was found that the link length ratio, α, does not affect the flexure joint torque. However, the knee joint torque is affected by α, as shown in Fig. 3.16(b). It may be concluded that for a given d value and F_T equal to zero, the knee joint torque for the straight is minimized when α is large.

Next, the joint torques for the bending leg were investigated. It was found that neither the rotator joint nor the flexure joint of the bending leg are affected by the link length ratio, as shown in Figs. 3.17(a) and 3.17(b). Thus, for both the straight and bending leg, the knee joint is the only joint affect by α when d is specified and F_T equals zero. The α value that

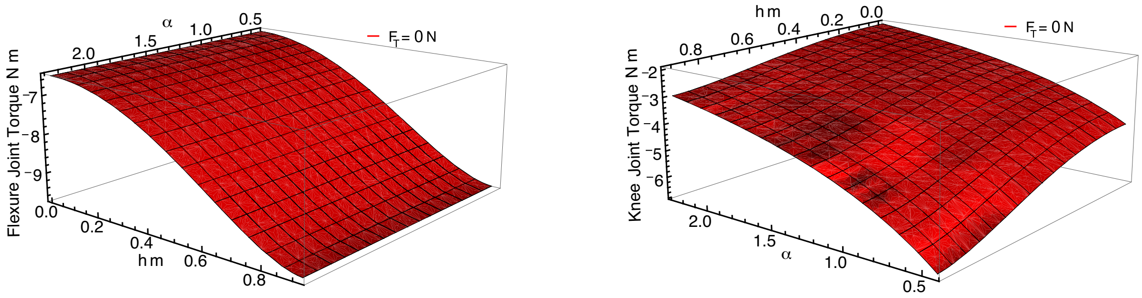

(a) Flexure joint torque (b) Knee joint torque

Figure 3.16: Straight leg joint torques for different link length ratios ($\alpha = \frac{r_3}{r_4}$) and F_T=0 for the two feet pushup.

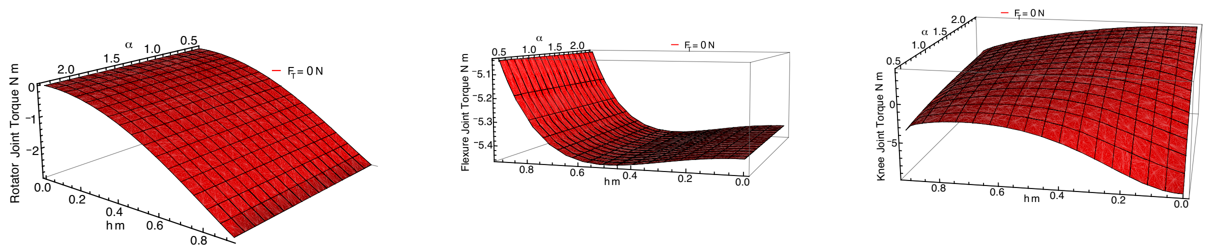

(a) Rotator joint torque (b) Flexure joint torque (c) Knee joint torque

Figure 3.17: Bending Leg joint torques for different link length ratios ($\alpha = \frac{r_3}{r_4}$) and F_T=0 for the two feet pushup.

yields the minimum maximum torque as the robot stands is considered to be the optimal α for this case. An optimization is presented in the next section.

Actuator Torques Optimization for Various d and α Combinations

Once the effects of d and α on the actuator torques were studied individually for both the straight leg and the bending leg, when F_T equals zero, a better understanding of these values was obtained. A cost function was developed to study the effects of d and α together on both legs. The cost function is calculated from Equation 3.31, where M_{23_S} and M_{34_S} are the flexure and knee joint torques for the straight leg and M_{12_B}, M_{23_B}, and M_{34_B} are the rotator, flexure and knee joint torques for the bending leg.

$$Cost = {M_{23_S}}^2 + {M_{34_S}}^2 + {M_{12_B}}^2 + {M_{23_B}}^2 + {M_{34_B}}^2 \tag{3.31}$$

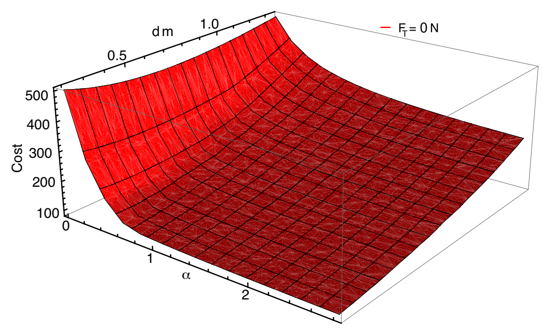

Figure 3.18: Two feet pushup d and α optimization.

Fig. 3.18 shows the results of the optimization. This plot was generated by plotting the maximum cost for a variety of d and α values as the robot stands. For example, the maximum cost as h goes from zero to h_{max} when d equals 0.65 m and alpha equals 0.6 is 170.5. From the optimization results, it was found that for a given α a d that will minimize the cost function is the smallest allowable d. Also it can be concluded that for a given d value the largest α will yield the lowest cost.

Effects of the Tangential Force on Actuator Torques

The effects of the tangential forces on the actuator torques were also considered for the straight and bending leg. The straight leg was first analyzed and the flexure and knee joint torque results are shown in Fig. 3.19. It was found that the flexure joint experiences a larger torque than the knee joint. Also, a tangential force acting inwards towards the body yields a lower torque than a tangential force acting outwards.

Next, the rotator, flexure and knee joint torques for different tangential forces were studied for the bending leg. As shown in Fig. 3.20(a), the rotator joint torque has a unique response to the tangential forces at the feet. At first, as the robot stands a tangential force acting outwards reduces the rotator joint torque. However, when the tangential force vector is parallel to the thigh link, the torque is equal for any tangential force. As the body continues to stand up, the rotator joint torque is now minimized when the tangential force acts inwards towards the center of the body. The flexure and knee joint torque results are shown in Figs. 3.20(b) and 3.20(c). Similar to the three feet pushup, both the flexure and knee joint torques are minimized for tangential forces acting inwards.

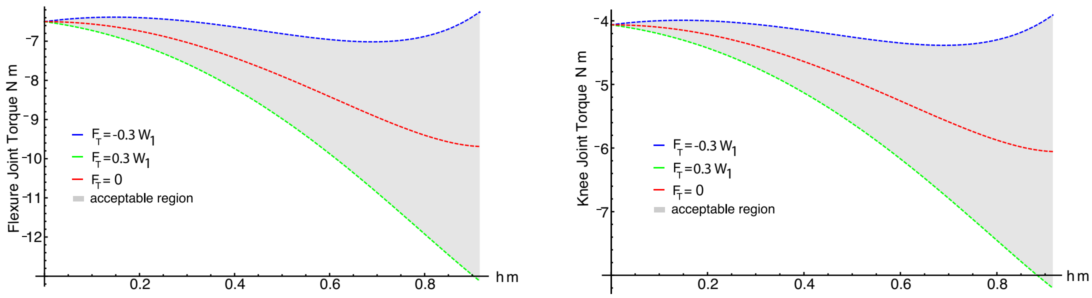

(a) Flexure joint torque (b) Knee joint torque

Figure 3.19: Straight leg joint torque region defined by a maximum and minimum F_T for the two feet pushup

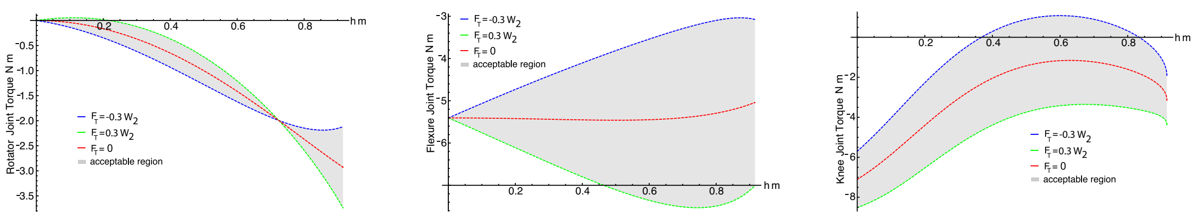

(a) Rotator joint torque (b) Flexure joint torque (c) Knee joint torque

Figure 3.20: Bending leg joint torque region defined by a maximum and minimum F_T for the two feet pushup

3.2.4 Overall Conclusions of the Two Feet Pushup

The two feet pushup is the second standing up strategy method considered for STriDER. It uses two of its legs to stand the robot while the third leg remains straight. First, two of the feet of the robot are placed at a desired final foot position and the body is then lifted upwards by pushing the feet against the ground. Note that the foot positions do not form an equilateral triangle. Since two of the legs act the same and the third remains straight, the analysis of the two feet pushup can be divided in two parts: straight leg and bending leg. This method uses the same motion as a human pushup, where two arms push the body upwards while the legs are kept straight. The effects of three important parameters on the actuator torques as the robot stands up were investigated. These parameters included, a distance d defined by the distance between the projected center of the body on the ground and foot position, a thigh and shank link length ratio, α, and friction force, F_T, at the feet. The effects of all three parameters were considered given a total link length value of, r_{tot} equal to 1.2 m, L_b equal to 0.18m, and total body weight, W, of 28.42 N.

First, the effects of d and α on the actuator torques were investigated individually ignoring the tangential forces (F_T=0). Then, d and α were coupled and a cost function was analyzed for F_T equal to zero. From the cost function it was determined that for a given link length ratio, α, a minimum allowable d would minimize the actuator torques. Also, for a given d value a maximum α would minimize the actuator torques. As mentioned in the research findings, Donkers et al. [18] found that as the distance between the hand position increased the peak forces exerted on the elbow joint along a forearm axis decreased. For STriDER it was found that as d increased the peak forces decreased when α and d are small and F_T equals zero, as shown in the cost functions results (Fig. 3.18). For large values of α and no tangential forces, as d increased the peak torque also increased. The difference in this findings might be due to the fact that for STriDER's analysis all three legs have the same total length. For humans, the arm length (shoulder to finger) and lower body length (hip to foot) is not the same, as mentioned in [20]. Also, as discussed in [19], the plane of arm movement is a major factor in the forces and torque at the joints; this was shown in the two feet pushup analysis. Note that the body translates in the $+Z_0$ and $+X_0$ directions as the robot stand using the two feet pushup.

Finally, the effects of the tangential forces on the actuator torques were studied. It was found that for the rotator joint torque of the bending leg a tangential force acting outwards minimizes the torque; however, once the thigh link is parallel to the tangential force vector at the feet then, any tangential force will yield the same torque. Once that position has passed, a tangential force acting inwards towards the body will minimize the rotator joint torque for the bending leg. Lastly, the flexure and knee joint torques for both the straight and bending leg are minimized when the tangential force at the feet acts inwards toward the center of the body.

3.3 One Foot Pushup

The one foot pushup begins with all three legs straight and flat on the ground, as shown in Fig. 3.21(a). Then, one leg moves inwards toward the body to a final desired final foot position as the other two legs remain straight on the ground (Fig. 3.21(b)). The distance between the bending leg's desired foot position and the center of the body is defined as d. Next, the body is pushed upwards by the bending leg until it reaches a maximum height (Fig. 3.21(c) to 3.21(f)). Note that the feet do not move once the bending leg's foot is in the desired position. As noted before, the maximum height is reached when the thigh and shank links of all three legs are aligned. This method is also always statically stable since all three feet are touching the ground and the projected center of gravity lies inside the support triangle.

The configuration of the two straight legs (Fig. 3.21(b)) in the one foot pushup is the same, while the third leg (bending leg) is positioned at a desired foot position defined by d. Thus, the analysis of the one foot pushup is divided in two parts: analysis of the straight legs and analysis of the bending leg. A kinematic and torque analysis is presented for the portion when the body begins to move upwards and reaches its maximum height (Fig. 3.21(b) to 3.21(f)). A range of d values, various link length ratios ($\alpha = \frac{r_3}{r_4}$) and a range of allowable

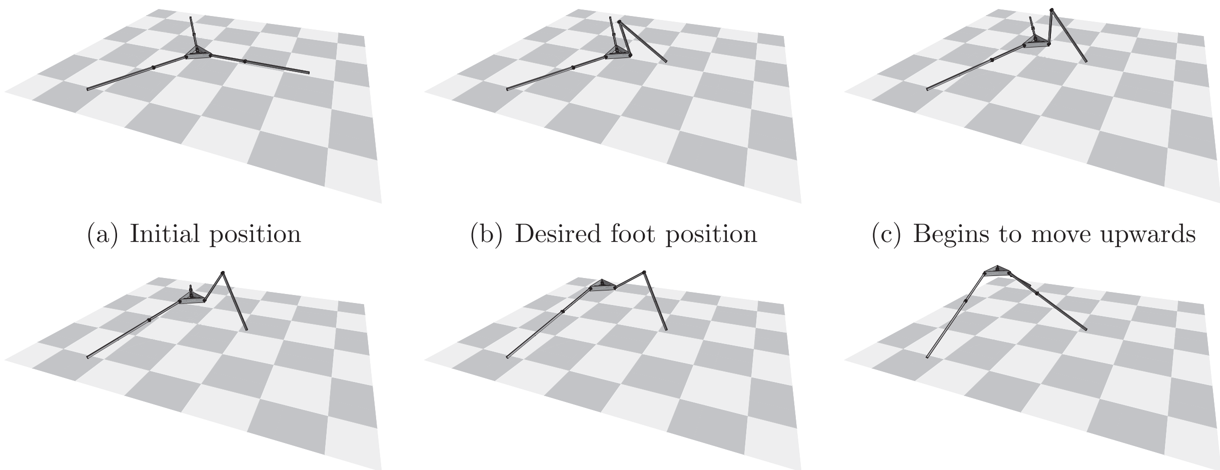

(a) Initial position (b) Desired foot position (c) Begins to move upwards

(d) Continues to move upwards (e) Continues to move upwards (f) Maximum height reached

Figure 3.21: The motion of the one foot pushup.

tangential friction forces between the feet and the ground will also be investigated in the analysis. As stated in Section 3.1 and Section 3.2, the minimum allowable d is the difference between the thigh and shank link length plus the body link length. The maximum allowable d is the added length of the thigh, shank, and L_b. The range of tangential contact force between the foot and the ground is defined by the friction coefficient and the normal contact force due to gravity. Thus, the minimum tangential contact force is zero (no friction force) and the maximum tangential contact force is the normal force times the friction coefficient for a non-slip condition. As long as the tangential contact forces, at the three feet, satisfy these conditions and the force balance is satisfied, the tangential forces can be adjusted by force control of the actuators of the robot. The choice of the tangential force will effect the motor torque requirements at the joints.

3.3.1 Kinematic Analysis for the One Foot Pushup

As discussed in the inverse kinematics section, Section 2.3, if the global body position and orientation and the global foot positions are known, the rotator, flexure and knee joint angles can be calculated. For the kinematic analysis, the global coordinate is assumed to be located at the initial center of the body position. First the global foot position for the bending leg is defined by d, where the foot position is $\mathbf{d}_0^{P_1} = [d \ 0 \ 0]^T$. The global foot positions for the two legs that are initially straight are $\mathbf{d}_0^{P_2} = \left[\frac{-(L_B+r_{tot})}{2} \ \frac{\sqrt{3}(L_B+r_{tot})}{2} \ 0\right]^T$ and $\mathbf{d}_0^{P_3} = \left[\frac{-(L_B+r_{tot})}{2} \ \frac{-\sqrt{3}(L_B+r_{tot})}{2} \ 0\right]^T$. Now that all three global foot positions have been defined, the global body position and orientation must be found. Note that the body does not change its orientation during the one foot pushup thus, the body orientation, $\mathbf{R}_0^B$, is always 0. However, the body's global position does change in the X_0 and Z_0 directions as the robot stands up. The maximum allowable height given d, L_b, and r_{tot} is calculated using Equation 3.32. The X_0 body position as the robot stands is found from Equation 3.33 where h is the given body height and ranges from zero to the maximum height. Now that the foot positions and body position and orientation are known based on global coordinates, the rotator, flexure and knee joint torques can be calculated using the equations in Section 2.3.

$$h_{max} = \frac{\sqrt{-(d - L_b)(d - L_b - r_{tot})(d - L_b + r_{tot})(d - L_b + 2r_{tot})}}{(2d - 2L_b + r_{tot})} \tag{3.32}$$

$$B_{X_{0_{pos}}} = \frac{1}{2}\left(-r_{tot} + \sqrt{-4h^2 + r_{tot}^2}\right) \tag{3.33}$$

3.3.2 Static Force Analysis for the One Foot Pushup

Using the rotator, flexure and knee joint angles calculated from the inverse kinematics, a static force analysis can be completed to calculate the actuator torques. Similar to the two feet pushup, as the robot stands the weight distribution between the three legs changes. A friction force and normal force will be applied at each foot, as shown in Fig. 3.22. Leg 1 is the bending leg in this case, while legs 2 and 3 remain straight at all times. The normal force at the feet, W_1, W_2, and W_3 can be calculated using Equations 3.34 and 3.35.

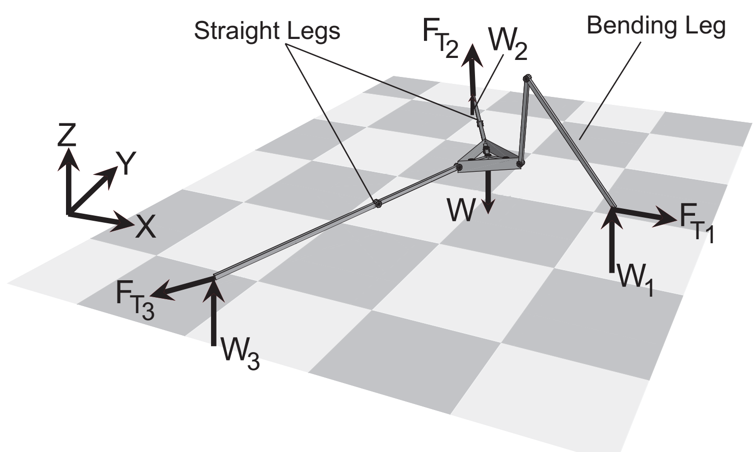

Figure 3.22: Forces at the feet for the one foot pushup.

$$W_1 = \frac{\left(L_b + \sqrt{-4h^2 + (r_{tot})^2}\right) W}{2d + L_b + r_{tot}} \tag{3.34}$$

$$W_2 = W_3 = \frac{\left(2d + r_{tot} - \sqrt{-4h^2 + (r_{tot})^2}\right) W}{2(2d + L_b + r_{tot})} \tag{3.35}$$

Next, the x and y components of the friction forces at the feet (F_{T_1}, F_{T_2}, and F_{T_3}) are calculated using Equations 3.36, 3.37, and 3.38. The maximum allowable tangential force at each foot is the friction coefficient, μ, times the normal force at the foot. Thus, for the bending leg, leg 1, the maximum tangential force, F_{T_1} is equal to μW_1 and for the straight legs, legs 2 and 3, the maximum tangential force at the feet, F_{T_2} and F_{T_3} are μW_2 and μW_3, respectively. Since both straight legs act the same as the robot stands, only leg 2 will be analyzed and leg 1 will be used for the bending leg torque analysis.

$$F_{T_1} = \begin{bmatrix} F_{T_{x_1}} \\ F_{T_{y_1}} \end{bmatrix} = \begin{bmatrix} \mu W_1 \\ 0 \end{bmatrix} \tag{3.36}$$

$$F_{T_2} = \begin{bmatrix} F_{T_{x_2}} \\ F_{T_{y_2}} \end{bmatrix} = \begin{bmatrix} -\frac{\mu W_1}{2} \\ \frac{1}{2}\sqrt{-(\mu W_1)^2 + 4(\mu W_2)^2} \end{bmatrix} \tag{3.37}$$

$$F_{T_3} = \begin{bmatrix} F_{T_{x_3}} \\ F_{T_{y_3}} \end{bmatrix} = \begin{bmatrix} -\frac{\mu W_1}{2} \\ -\frac{1}{2}\sqrt{-(\mu W_1)^2 + 4(\mu W_2)^2} \end{bmatrix} \tag{3.38}$$

Bending Leg Joint Torque Equations

Similar to the two feet pushup the static force analysis of the one foot pushup was divided in two parts: bending leg and straight leg. In the case of the one foot pushup, only one leg bends to a desired final foot position and pushes the body upwards while legs 2 and 3 (straight legs) also lift but do not change their initial foot positions. The same general torque expression (Equation 3.20) used in the two feet pushup static force analysis, Section 3.2.2, will be used for the one foot pushup actuator torque analysis. As mentioned, from the general torque analysis, torque can be calculated by taking the cross product of a distance vector from the feet to the joint with a force vector at the feet and then taking the dot product of that result with the unit vector at the desired joint. Since the equations for the forces at the feet have been discussed, the next step is to determine the vectors from the feet to the rotator, flexure and knee joints. Note that the rotator joint does not experience any torque for the bending leg since the leg does not rotate as the body stands up.

The distance vector components (x, y, z) from the foot positions to the flexure and knee joints are calculated using Equations 3.39 and 3.40, where $B_{X_{0pos}}$, calculated from Equation 3.33, is the body position relative to the X_0 axis (assumed to be located in the initial center of the body position), d is the initial distance between the global coordinates and the desired final foot position of leg 1, L_b is the body link ($= L_0 + L_1 + L_2$), r_3 is the thigh link length, and θ_{31} is the flexure joint angle as the body stands up.

$$\mathbf{d}_{P_1}^2 = \begin{bmatrix} dx_{P_1}^2 \\ dy_{P_1}^2 \\ dz_{P_1}^2 \end{bmatrix} = \begin{bmatrix} B_{X_{0pos}} - d + L_b \\ 0 \\ h \end{bmatrix} \tag{3.39}$$

$$\mathbf{d}^3_{P_1} = \begin{bmatrix} dx^3_{P_1} \\ dy^3_{P_1} \\ dz^3_{P_1} \end{bmatrix} = \begin{bmatrix} B_{X_{0pos}} - d + L_b + r_3 sin(\theta_{31}) \\ 0 \\ h - r_3 cos(\theta_{31}) \end{bmatrix} \tag{3.40}$$

By combining the force vector, distance vector and unit vector equations for the flexure and knee joints, the actuator torque equations can be found. Equations 3.41 and 3.42 represent the flexure and knee joint torque equations, where W_1 is the normal force at the foot of the bending leg.

$$M_{23_B} = -dz^2_{P_1} F_{Tx_1} + dx^2_{P_1} W_1 \tag{3.41}$$

$$M_{34_B} = -dz^3_{P_1} F_{Tx_1} + dx^3_{P_1} W_1 \tag{3.42}$$

Straight Leg Joint Torque Equations

The straight leg actuator torque equations were found following the same procedure as the bending leg. First, the distance vector components (x, y, z), defined by the distance from leg 2 foot position to the joints, were found. Equations 3.43, 3.44, and 3.45 are used to calculated the distance vectors to the rotator, flexure, and knee joint, respectively. Recall that $B_{X_{0pos}}$ is the center of the body position relative to X_0 (calculated using Equation 3.33), L_2 is the link between the rotator and flexure joint, r_{tot} is the total link length of the thigh and shank links, h is the height of the body, r_3 is the thigh link length, θ_{32} is the flexure joint angle for leg 2 as the robot stands, and θ_{22} is the rotator joint torque for leg 2.

$$\mathbf{d}^1_{P_2} = \begin{bmatrix} dx^1_{P_2} \\ dy^1_{P_2} \\ dz^1_{P_2} \end{bmatrix} = \begin{bmatrix} B_{X_{0pos}} + \frac{1}{2}\left(L_2 + r_{tot}\right) \\ \frac{-\sqrt{3}}{2}\left(L_2 + r_{tot}\right) \\ h \end{bmatrix} \tag{3.43}$$

$$\mathbf{d}^2_{P_2} = \begin{bmatrix} dx^2_{P_2} \\ dy^2_{P_2} \\ dz^2_{P_2} \end{bmatrix} = \begin{bmatrix} B_{X_{0pos}} + \frac{r_{tot}}{2} \\ \frac{-\sqrt{3} r_{tot}}{2} \\ h \end{bmatrix} \tag{3.44}$$

$$\mathbf{d}^3_{P_2} = \begin{bmatrix} dx^3_{P_2} \\ dy^3_{P_2} \\ dz^3_{P_2} \end{bmatrix} = \begin{bmatrix} B_{X_{0pos}} + \frac{1}{2}(r_{tot} - r_3 sin(\theta_{32}) - \sqrt{3} r_3 cos(\theta_{32}) sin(\theta_{22}) \\ \frac{1}{2}\left(-\sqrt{3} r_{tot} + \sqrt{3} r_3 sin(\theta_{32}) - r_3 cos(\theta_{32}) sin(\theta_{22})\right) \\ h - r_3 cos(\theta_{32}) cos\theta_{22} \end{bmatrix} \tag{3.45}$$

Next, the rotator, flexure and knee joint torque equations can be found from the force vector at the foot of leg 2, the distance vectors from the foot position to the joint positions and the unit vectors. Equations 3.46, 3.47, and 3.48 are used to calculate the joint torques, where W_2 is the normal force at the foot of leg 2.

$$M_{12_S} = \frac{1}{2}(dz^1_{P_2}(\sqrt{3}F_{Tx_2} + F_{Ty_2}) - (\sqrt{3}dx^1_{P_2} + dy^1_{P_2})W_2) \tag{3.46}$$

$$\begin{gathered} M_{23_S} = \tfrac{1}{2}(dz^2_{P_2}(F_{Tx_2} - \sqrt{3}F_{Ty_2}) - dx^2_{P_2}W_2 + \sqrt{3}dy^2_{P_2}W_2)cos\,(\theta_{22}) + \\ (dy^2_{P_2}F_{Tx_2} - dx^2_{P_2}F_{Ty_2})sin\,(\theta_{22}) \end{gathered} \tag{3.47}$$

$$\begin{gathered} M_{34_S} = \tfrac{1}{2}(dz^3_{P_2}(F_{Tx_2} - \sqrt{3}F_{Ty_2}) - dx^3_{P_2}W_2 + \sqrt{3}dy^3_{P_2}W_2)cos\,(\theta_{22}) + \\ (dy^3_{P_2}F_{Tx_2} - dx^3_{P_2}F_{Ty_2})sin\,(\theta_{22}) \end{gathered} \tag{3.48}$$

3.3.3 Actuator Torque for One Foot Pushup

This section will investigate the effects of d, link length ratio ($\alpha = \frac{r_3}{r_4}$), and F_T on the actuator torques. Similar to the three feet pushup analysis and two feet pushup analysis, first, the effects of d and α on the actuator torques when F_T equals zero will be considered independently. Then, d and α will be coupled and an optimization will be completed to determine an optimized α and d combination that will minimize the joint torques when F_T equals zero. The effects of F_T on the actuator torques will also be studied. A total link length (r_{tot}= r_3 + r_4) of 1.2 m, body link length, L_b, (=$L_0 + L_1 + L_2$, shown in Fig. 2.1) equal to 0.18 m, a friction coefficient, μ, of 0.3 and total body weight, W, of 28.42 N were chosen for the entire actuator torque analysis.

Effects of d on Actuator Torques

The effects of d on the actuator torques when α (= $\frac{r_3}{r_4}$) is equal to 0.6, and F_T is equal to zero was studied for both the bending and straight leg. Recall, that with the given parameters d ranges from $(r_4 - r_3) + L_b$ and $(r_3 + r_4 + L_b)$. Figs. 3.23 and 3.24 show the rotator, flexure and knee joint torques for the bending leg and straight leg.

As shown in Fig. 3.23(a), the flexure joint torque for the bending leg is lowest at h equal to h_{max} when d is smallest. Also, the maximum height is constrained to the value of d thus, for larger d values the maximum allowable height is smaller. The minimum maximum flexure joint torque occurs when d and h are small for the chosen parameters ($\alpha = 0.6$ and $F_T = 0$). Similar to the flexure joint torque of the bending leg, the minimum knee joint torque for the bending leg, shown in Fig. 3.23(b), also occurs when d is smallest and at its maximum height.

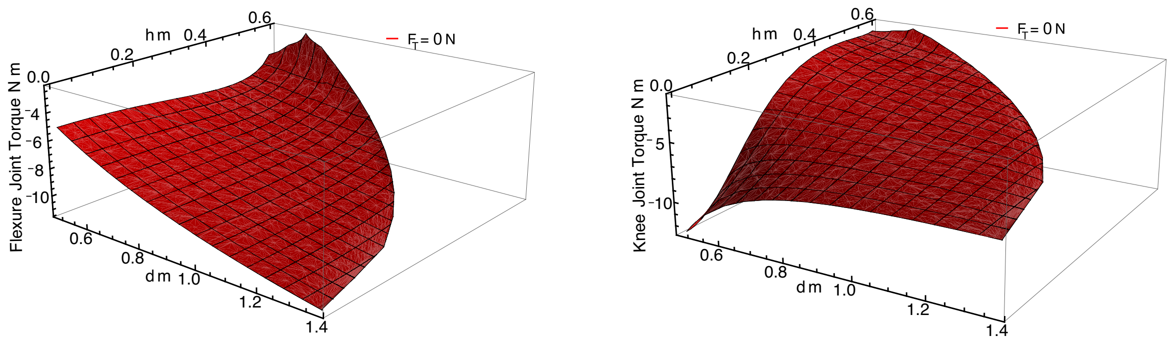

(a) Flexure joint torque (b) Knee joint torque

Figure 3.23: Bending leg joint torques for various d values and F_T =0 for the one foot pushup.

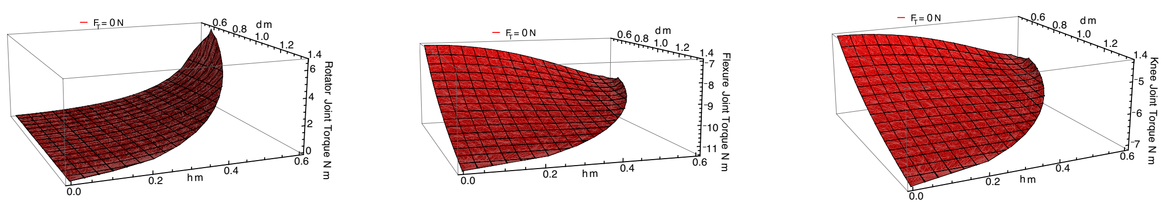

(a) Rotator joint torque (b) Flexure joint torque (c) Knee joint torque

Figure 3.24: Straight leg joint torques for various d values and F_T =0 for the one foot pushup.

Next, the straight leg joint torques were studied for different d values as the robot stands up using the one foot pushup. Similar to the two feet pushup, the rotator joint of leg 2 begins at zero for all values of d. As the robot stands the rotator joint torque increases. Thus, in order to minimize the rotator joint torque it is best if the final height of the robot is low, as shown in Fig. 3.24(a). Next, the flexure joint torque for leg 2 was studied, as shown in Fig. 3.24(b). The minimum maximum flexure joint torque for leg 2 occurs when d is small. The results of the knee joint torque as the body stands up with different d values for leg 2 are shown in Fig. 3.24(c). The knee joint torque follows a similar pattern to the flexure joint. Smaller d values yield lower joint torques and the minimum maximum knee joint torque yields the best d value.

Effects of Link Length Ratio on Actuator Torques

The effects of the link length ratio, α $(= \frac{r_3}{r_4})$, on the joint torques for the bending and straight leg were investigated given a d value of 0.65 m and F_T equal to zero, as shown in Figs. 3.25 and 3.26.

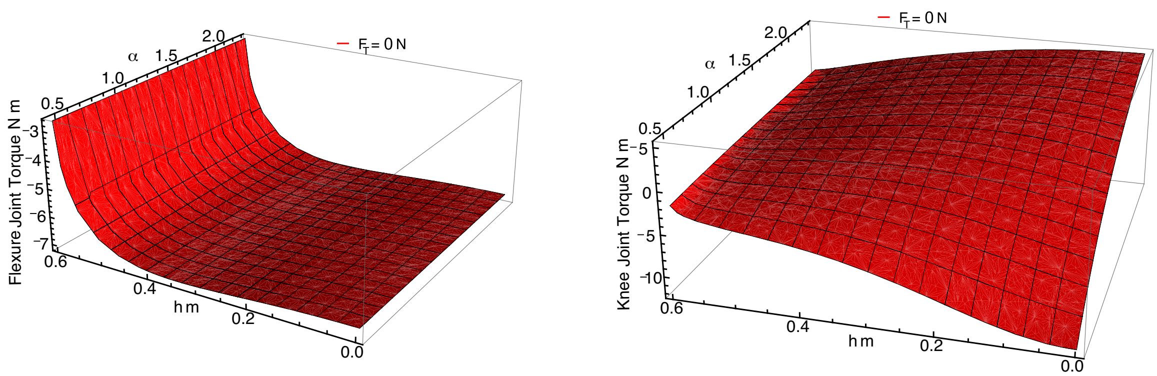

(a) Flexure joint torque (b) Knee joint torque

Figure 3.25: Bending leg joint torques for different link length ratios $(\alpha = \frac{r_3}{r_4})$ and F_T=0 for the one foot pushup.

For the bending and straight leg, it was found that α does not affect the rotator or flexure joint torques. However, the knee joint torques for the bending and straight legs do change as α changes. From Fig. 3.25(b), it was found that the minimum maximum knee joint torque for leg 1 occurs when α equals 1.5 and h equals 0.52. Also, from Fig. 3.26(c), the minimum maximum knee joint torque for leg 2 occurs when α equals 3 and h equals 0.

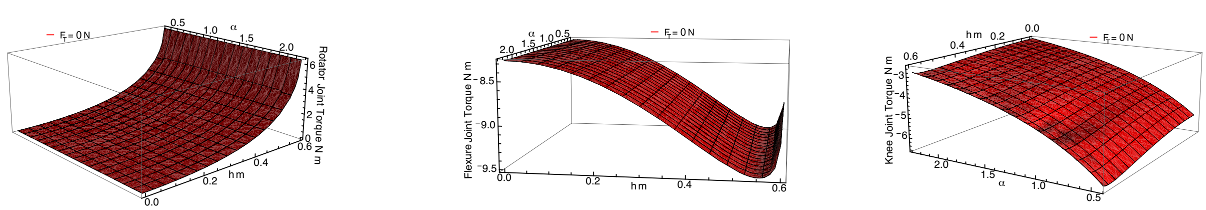

(a) Rotator joint torque (b) Flexure joint torque (c) Knee joint torque

Figure 3.26: Straight leg joint torques for different link length ratios $(\alpha = \frac{r_3}{r_4})$ and F_T=0 for the one foot pushup.

Actuator Torques Optimization for Various d and α Combinations

The same optimization approach used for the two feet pushup was implemented for the one foot pushup. Equation 3.49 is used to determine the cost value of the one foot pushup standing up strategy. The cost function is composed of the bending and straight joint torques. The goal is to calculated the minimum maximum cost for various d and α ranges. Thus, first the maximum cost as the robot stands for a pair of d and α was calculated.

$$Cost = {M_{23_B}}^2 + {M_{34_B}}^2 + {M_{12_S}}^2 + {M_{23_S}}^2 + {M_{34_S}}^2 \tag{3.49}$$

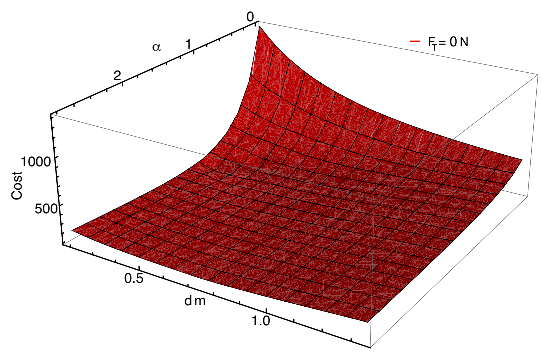

Figure 3.27: One foot pushup d and α optimization.

Once all the maximum values are found they can be plotted as shown in Fig. 3.27. For a given d value the minimum cost occurs when α is largest and for a given α the minimum cost occurs at lower d values. More specifically, for this example, it was found that the minimum cost occurs when d equals 0.29 m and α equals 1.01.

Effects of the Tangential Force on Actuator Torques

The effects of the tangential force on the actuator torques was also considered for the bending and straight leg (leg 1 and 2). The bending leg was first analyzed and the results are shown in Fig. 3.28. For both the flexure and knee joints of leg 1 the torque is minimized when the tangential force acts inwards towards the center of the body. The actuator torques are also maximized when the maximum tangential force acts outwards.

Next, the actuators of leg 2 were analyzed for different tangential forces. As, shown in Fig. 3.29(a), the rotator joint experiences less torque for a tangential forces acting outwards than a tangential force acting inwards towards the body. However, the flexure and knee joint torques do not act the same as the rotator joint. Instead, the same results as bending leg were found for leg 2. So, the flexure and knee joint torques of leg 2 are minimized with

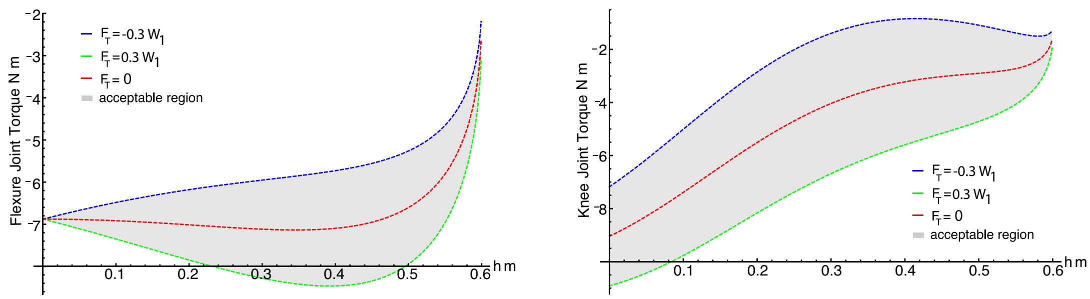

(a) Flexure joint torque (b) Knee joint torque

Figure 3.28: Bending leg joint torque region defined by a maximum and minimum F_T for the one foot pushup.

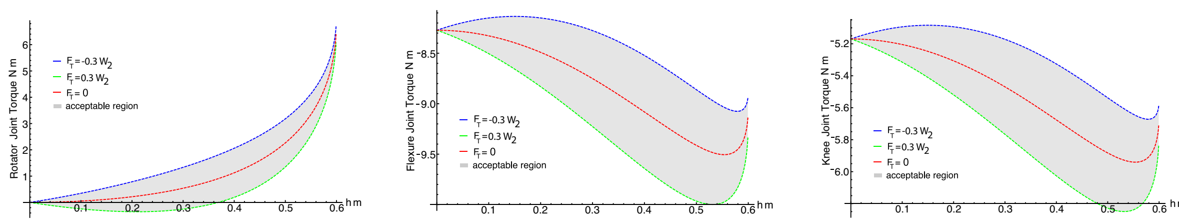

(a) Rotator joint torque (b) Flexure joint torque (c) Knee joint torque

Figure 3.29: Straight leg joint torque region defined by a maximum and minimum F_T for the one foot pushup.

tangential forces acting inwards towards the center of the body and maximized for tangential forces acting outwards.

3.3.4 Overall Conclusions of the One Foot Pushup

The one foot pushup is the third standing up strategy method considered for STriDER. It uses one leg to push the body upwards as the other two legs follow the direction of the body while keeping the feet at their initial foot positions. Fist, one leg positions its foot to a desired final foot position defined by d. Then, the bending leg lifts the body and the other two legs (legs 2 and 3) follow the body trajectory. Since legs 2 and 3 act the same, the analysis of the one foot pushup was divided in two parts: bending leg and straight leg. Like the three feet pushup and two feet pushup, the effects of three important parameters on the actuator torques as the robot stands up were investigated. These parameters included, a distance d defined by the distance between the projected center of the body on the ground and foot position, a thigh and shank link length ratio, α, and friction force F_T at the feet. The effects of all three parameters were considered given a total link length value of, r_{tot} equal to 1.2 m, L_b equal to 0.18m, and total body weight, W, of 28.42 N.

First, the effects of d and α were studied individually ignoring the tangential force (F_T=0). Then, d and α were coupled and a cost function was evaluated for F_T equal to zero. It was determined that for a given d value, the minimum cost occurs when α is largest and for a given α, the minimum cost occurs at lower d values. Similar to Donkers' findings [18], the cost function results for the one foot pushup (Fig. 3.27) showed that the peak forces decreased as d increased for small α values. However, this did not occur for large α values. As discussed in the two feet pushup section, the difference in results could be due to the fact that for STriDER all legs are the same length, unlike humans where the arms have different lengths than the lower body.

From the tangential force analysis, it was found that the flexure and knee joint torques of both the bending and straight legs are minimized for a maximum tangential force acting inwards towards the center of the body and maximized for a maximum tangential force acting outwards. However, the rotator joint torque of leg 2 acts in the opposite manner. Thus, for a maximum tangential force acting outwards, the rotator joint torque is minimized while for a maximum tangential force acting inwards the rotator joint torque is maximized.

3.4 Spiral Pushup

The spiral pushup method begins with the robot flat on the ground with all three legs extended outwards, as shown in Fig. 3.30(a). The feet are then positioned to a desired final foot position, as shown in Fig. 3.30(b). The final foot position is defined by a distance d (distance between the projected center of the body on the ground and foot position) and desired maximum body rotation about the $+Z_0$ axis. Once the feet are located at the desired final feet position, the body is lifted upwards by actuating the rotator joints and the legs pushing against the ground (Figs. 3.30(c) to 3.30(e)). The robot continues to lift and rotate about the $+Z_0$ axis until it reaches a maximum height, as shown in Fig. 3.30(f).

Note that the foot positions of the spiral pushup form an equilateral triangle. In fact, the configuration for all three legs in the spiral pushup standing up method is the same thus, a detailed analysis for only one leg is presented here as the other two legs will follow the same procedure. A kinematic and static force analysis is presented for the portion when the body begins to move upwards and twist and reaches its maximum height (Fig. 3.30(b) to Fig. 3.30(f)) for a range of d values, a range of allowable tangential friction forces between the feet and the ground, a range of maximum body rotations about the $+Z_0$ axis, and various link length ratios, α. The distance between the projected center of the body on the ground and final desired foot position is defined as d. As mentioned, a range of tangential contact force between the foot and the ground is defined by the friction coefficient and the normal contact force due to gravity. The body rotation about $+Z_0$ will range from zero (no rotation) to a desired maximum body rotation as the robot stands. In this example, the body rotates about the $+Z_0$ in a clockwise direction, thus the angles will be negative. The effects of these parameters on the actuator torques will be studied.

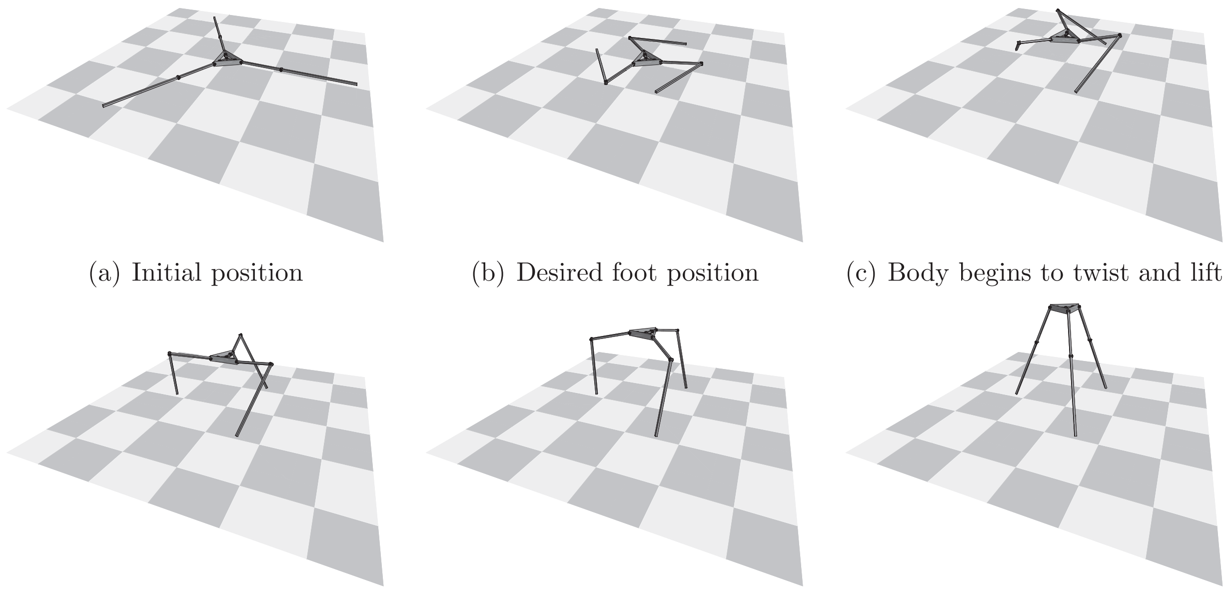

(a) Initial position (b) Desired foot position (c) Body begins to twist and lift

(d) Robot continues to stand up (e) Legs begin to straighten (f) Maximum height reached

Figure 3.30: The motion of the spiral pushup.

3.4.1 Kinematic Analysis for the Spiral Pushup

In order to obtain the rotator, flexure and knee joint angles as the robot stands using the spiral pushup method, a d value and maximum body rotation (θ_{Z_0max} about $+Z_0$ axis are defined. Fig. 3.31 shows a top view of the robot when the feet are located at their desired final foot positions. As mentioned, the final foot positions are calculated from d and θ_{Z_0max} using Equations 3.50 and 3.51. Recall that θ_{Z_0max} is negative since the body rotates in a clockwise direction. Also, the maximum allowable height for a given d value is defined in the same way as the three feet pushup method, using Equation 3.3. Note that L_b will equal 0.18 m for the entire standing up analysis.

$$P_x = dsin\left(\frac{\pi}{2} + \theta_{Z_0max}\right) \tag{3.50}$$

$$P_y = -dcos\left(\frac{\pi}{2} + \theta_{Z_0max}\right) \tag{3.51}$$

As the body height increases the current body rotation about the $+Z_0$ axis, θ_{Z_0}, can be calculated using Equation 3.52, where h is the current body height, θ_{Z_0max} is the maximum body rotation along the $+Z_0$ and is a constant (negative), and h_{max} is the maximum height when the thigh and shank links are aligned. In fact, the trajectory of the flexure joint forms a helix defined by the body height and $+Z_0$ rotation, as shown in Fig. 3.32.

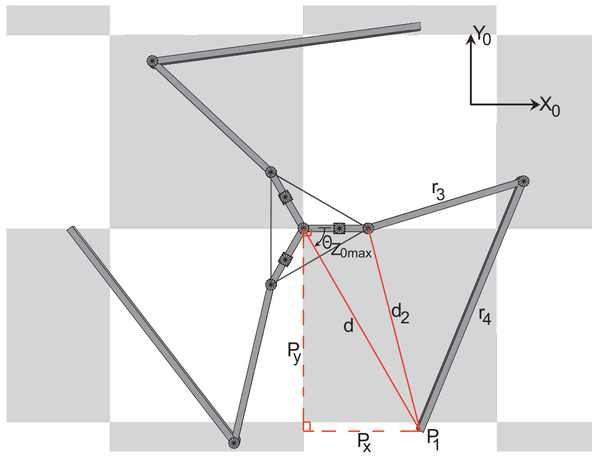

Figure 3.31: Top view of the initial position for spiral pushup kinematic and static force analysis.

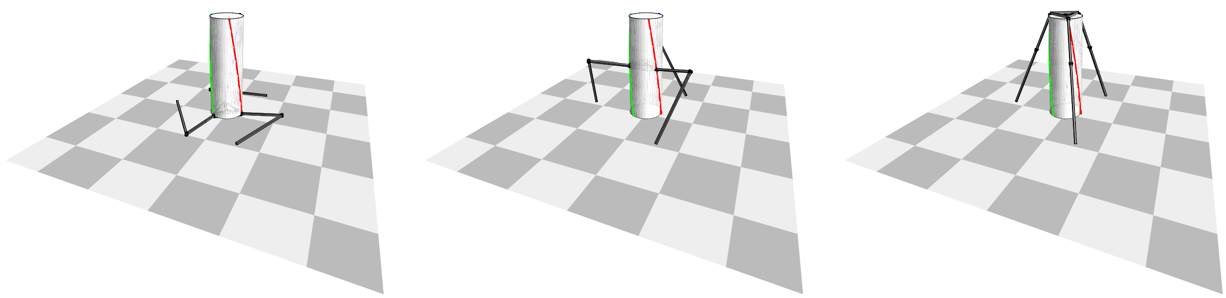

(a) Desired foot position (b) Body twists and lifts (c) Maximum height

Figure 3.32: The flexure joint trajectory follows a helical shape.

$$\theta_{Z_0} = h\frac{\theta_{Z_0max}}{h_{max}} \tag{3.52}$$

Since the global body position and orientation and the global foot positions are known, (assuming the global coordinates are located in the initial center of the body location) the rotator, flexure and knee joint angles can be calculated using the inverse kinematics procedure discussed in Section 2.3.

3.4.2 Static Force Analysis for the Spiral Pushup

The rotator, flexure and knee joint torques are calculated using a static force analysis. The actuator torques can be calculated using the general torque equation (Equation 3.20) discussed in Section 3.2.2. Recall that this equation requires a vector from the foot to the joint, a force vector at the feet and a unit vector at each joint to calculate torque. Thus, torque can be calculated by taking the cross product of a distance vector from the foot to the joint with a force vector at the foot and then taking the dot product of that result with the unit vector at the desired joint. The distance vector components (x, y, z) from the foot of leg 1 to the rotator, flexure and knee joints as the robot stands are found using Equations 3.53, 3.54, and 3.55, where P_x is the X_0 distance from the project center of the body to the foot position, P_y is the Y_0 distance from the project center of the body on the ground to the foot position, L_0 is the distance between the center of the body to the rotator joint, θ_{Z_0} is the body rotation about the Z_0 axis, r_3 is the thigh link length, θ_{21} is the rotator joint angle for leg 1, and θ_{31} is the flexure joint angle for leg 1.

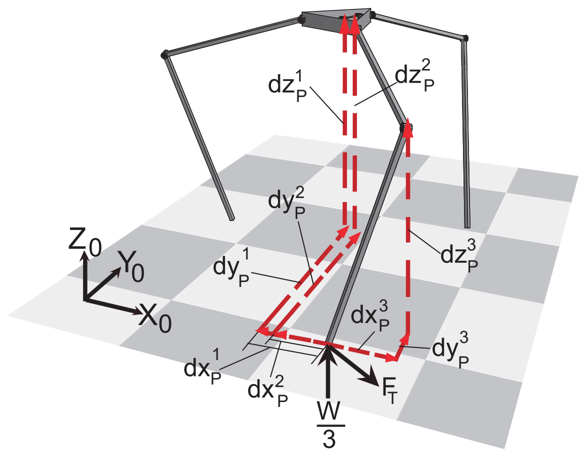

Figure 3.33: Foot to joint position distance labels.

$$\mathbf{d}_P^{11} = \begin{bmatrix} dx_P^{11} \\ dy_P^{11} \\ dz_P^{11} \end{bmatrix} = \begin{bmatrix} -P_x + L_0 cos\left(\theta_{Z_0}\right) \\ -P_y + L_0 sin\left(\theta_{Z_0}\right) \\ h \end{bmatrix} \tag{3.53}$$

$$\mathbf{d}_P^{21} = \begin{bmatrix} dx_P^{21} \\ dy_P^{21} \\ dz_P^{21} \end{bmatrix} = \begin{bmatrix} -P_x + L_b cos\left(\theta_{Z_0}\right) \\ -P_y + L_b sin\left(\theta_{Z_0}\right) \\ h \end{bmatrix} \tag{3.54}$$

$$\mathbf{d}_P^{31} = \begin{bmatrix} dx_P^{31} \\ dy_P^{31} \\ dz_P^{31} \end{bmatrix} = \begin{bmatrix} -P_x + cos\left(\theta_{Z_0}\right)\left(L_b + r_3 sin\left(\theta_{31}\right)\right) - r_3 cos\left(\theta_{31}\right) sin\left(\theta_{Z_0}\right) sin\left(\theta_{21}\right) \\ -P_y + sin\left(\theta_{Z_0}\right)\left(L_b + r_3 sin\left(\theta_{31}\right)\right) + r_3 cos\left(\theta_{31}\right) cos\left(\theta_{Z_0}\right) sin\left(\theta_{21}\right) \\ h - r_3 cos\left(\theta_{31}\right) cos\left(\theta_{21}\right) \end{bmatrix} \tag{3.55}$$

Also, the tangential force components (x and y) at the feet can be found from Equation 3.56, where W is the total weight of the robot and μ is the friction coefficient. There is also a normal force at each foot equal to $\frac{W}{3}$. Note that the determined tangential force at the foot is always parallel to the body link for each leg. Thus, the components of the tangential force are defined by the angle of rotation, θ_{Z_0}, of the body. Although other tangential forces exist at the foot, they are assumed to cancel each other out and will not be considered in this analysis. Fig. 3.33 shows the components of the direction vector for each joint and the chosen direction of the tangential force at the foot.

$$F_{T_1} = \begin{bmatrix} F_{T_{x_1}} \\ F_{T_{y_1}} \end{bmatrix} = \begin{bmatrix} \frac{\mu W cos(-\theta_{Z_0})}{3} \\ \frac{-\mu W sin(-\theta_{Z_0})}{3} \end{bmatrix} \tag{3.56}$$

From the general torque equation and the unit vector at the rotator joint found using forward kinematics, the rotator joint torque can be calculating using Equation 3.57,

$$M_{12} = \frac{1}{3} W \left[dy_P^{11} cos\left(\theta_{Z_0}\right) - dx_P^{11} sin\left(\theta_{Z_0}\right) \right] \tag{3.57}$$

where dx_P^{11}, dy_P^{21}, dz_P^{11} are the x, y and z vector components from the foot position of leg 1 to the rotator joint, θ_{Z_0} is the body rotation about the $+Z_0$ axis in the clockwise direction, and W is the total weight of the body. Note that because the chosen tangential force and the rotator joint have the same unit vector, F_T will does not affect the torque at the rotator joint.

Next, the flexure joint torque can be calculated using Equation 3.58,

$$\begin{aligned} M_{23} = \tfrac{1}{3} cos\left(\theta_{21}\right) \left[-3dz_P^{21} F_T + dx_P^{21} W cos\left(\theta_{Z_0}\right) + dy_P^{21} W sin\left(\theta_{Z_0}\right) \right] + \\ F_T sin\left(\theta_{21}\right) \left[dy_P^{21} cos\left(\theta_{Z_0}\right) - dx_P^{21} sin\left(\theta_{Z_0}\right) \right] \end{aligned} \tag{3.58}$$

where dx_P^{21}, dy_P^{21}, dz_P^{21} are the x, y and z vector components from the foot position of leg 1 to the flexure joint, θ_{Z_0} is the body rotation about the $+Z_0$ axis in the clockwise direction, θ_{21} is the rotator joint angle for leg 1, and W is the total weight of the body.

Lastly, the knee joint torque can be calculated using Equation 3.59,

$$\begin{aligned} M_{34} = \tfrac{1}{3} cos\left(\theta_{21}\right) \left[-3dz_P^{31} F_T + dx_P^{31} W cos\left(\theta_{Z_0}\right) + dy_P^{31} W sin\left(\theta_{Z_0}\right) \right] + \\ F_T sin\left(\theta_{21}\right) \left[dy_P^{31} cos\left(\theta_{Z_0}\right) - dx_P^{31} sin\left(\theta_{Z_0}\right) \right] \end{aligned} \tag{3.59}$$

where dx_P^{31}, dy_P^{31}, dz_P^{31} are the x, y and z vector components from the foot position for leg 1 to the knee joint, θ_{Z_0} is the body rotation about the $+Z_0$ axis in the clockwise direction, θ_{21} is the rotator joint angle for leg 1, and W is the total weight of the body.

3.4.3 Actuator Torque for Spiral Pushup

As previously mentioned, a friction force was added to account for different tangential forces, F_T. A maximum friction coefficient, μ, of 0.3 was chosen for this analysis and the total weight of the robot was set to 28.42 N. A tangential force, F_T, can be chosen for any value less than the normal force times the friction coefficient. Since only one leg is being analyzed the maximum tangential force is one third of the weight of the body times μ. The maximum magnitude of the F_T is 2.84 N and can act in both the positive and negative direction, $-2.84N \leq F_T \leq 2.84N$. The minimum magnitude of the F_T is equal to zero. The positive and negative values of F_T account for an outwards and inwards force at the feet. The effects of F_T, d, θ_{Z0max}, and link ratios ($\alpha = \frac{r_3}{r_4}$) on the actuator torques will be studied in this section. A given total link length (r_{tot}=r_3 + r_4) of 1.2 m was chosen for the analysis and d_2 (shown in Fig. 3.31) can be calculated from Equation 3.60 using the law of cosines.

$$d_2 = \sqrt{((L_b^2 + d^2) - (2L_b^2 d cos\left(-Z_{0max}\right))} \tag{3.60}$$

Effects of d on actuator torques

The effects of different d values on the actuator torques as the robot stands using the spiral pushup were studied. The following parameters were used; r_3 = 0.45 m, r_4=0.75 m, and θ_{Z0max}= $-\frac{\pi}{3}$. Recall that, L_0, L_1, and L_2 will equal 0.1m, 0 m, and 0.08 m, for all of the standing up strategy analysis. The minimum and maximum allowable d values were found using Equations 3.61 and 3.62.

$$\begin{gathered} d_{min} = (L_0 + L_1 + L_2)\, cos\left(-Z_{0max}\right) + \\ \sqrt{-{L_0}^2 - 2L_0L_2 - {L_2}^2 + {r_3}^2 - 2r_3r_4 + {r_4}^2 + (L_0 + L_2)^2 cos\left(-\theta_{Z0max}\right)^2} \end{gathered} \tag{3.61}$$

$$\begin{gathered} d_{max} = (L_0 + L_1 + L_2)\, cos\left(-Z_{0max}\right) + \\ \sqrt{-{L_0}^2 - 2L_0L_2 - {L_2}^2 + {r_3}^2 + 2r_3r_4 + {r_4}^2 + (L_0 + L_2)^2 cos\left(-\theta_{Z0max}\right)^2} \end{gathered} \tag{3.62}$$

Fig. 3.34 shows the actuator torque results for d values ranging from d_{min} to d_{max}. Note that as the value of d increases the allowable maximum height of the body decreases since the stance of the robot is larger. As shown in Fig. 3.34(a), the rotator joint torque increases as d increases. This trend is the same for the flexure and knee joints, as shown in Figs. 3.34(b) and 3.34(c). Thus, it may be concluded that the actuator torques increase as the d increases for the spiral pushup. However, although a smaller d value will yield less torque at the actuators the robot will become more unstable since the support triangle formed by the foot contact points is smaller.

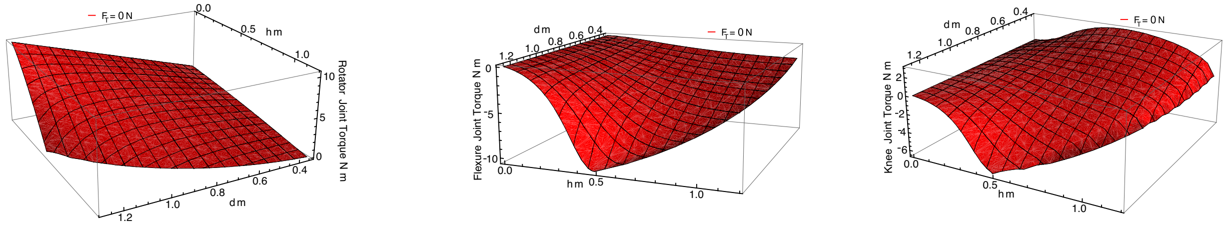

(a) Rotator joint torque (b) Flexure joint torque (c) Knee joint torque

Figure 3.34: Actuator torque results for various d values for the spiral pushup method.

Effects of θ_{Z_0max} on actuator torques

The effects of the maximum body rotation about the $+Z_0$ axis was also studied for the spiral method as the body stands. The maximum body rotation, θ_{Z_0max}, shown in Fig. 3.31, is assumed to be negative for all examples since the robot will be rotating in a clockwise direction. The following parameters were chosen for this analysis; r_3 = 0.45 m, r_4=0.75 m, and d = 0.65 m. The minimum θ_{Z_0max} value was set to zero. Note, that when θ_{Z_0max} equals zero the motion of the robot is the same as the three feet pushup method. Thus, the three feet pushup is a special case of the spiral pushup. The maximum θ_{Z_0max} value was set to $\frac{-2\pi}{3}$. The actuator torque results for various θ_{Z_0max} values are shown in Fig. 3.35.

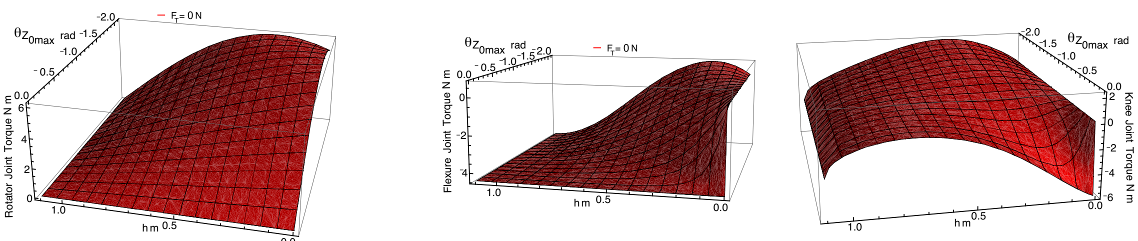

(a) Rotator joint torque (b) Flexure joint torque (c) Knee joint torque

Figure 3.35: Actuator torque results for different θ_{Z_0max} values for the spiral pushup method.

The rotator joint torque for different θ_{Z_0max} values is shown in Fig. 3.35(a). Note that when θ_{Z_0max} equals zero the rotator joint torque also equals zero, thus it agrees with the three feet pushup method. Also, as θ_{Z_0max} increases the rotator joint torque also increases. The results for the flexure joint torque for various θ_{Z_0max} values are shown in Fig. 3.35(b). When θ_{Z_0max} equals zero the results are the same as *Case* 1 of the three feet pushup since the same parameters were chosen. Note that for all cases the final flexure joint torque is the same because a set d value and α value was defined thus, the same maximum height is reached. Similar to the flexure joint torque, the knee joint torque, shown in Fig. 3.35(c), is the same for all θ_{Z_0max} value when the robot reaches its maximum height. Also, the initial knee joint torque is maximum when θ_{Z_0max} equals zero.

Effects of link length ratio on actuator torques

The effects of the link length ratio, α ($\frac{r_3}{r_4}$), on the actuator torques were studied for the spiral pushup standing method. Fig. 3.36 shows the actuator torque results as the body moves upward for different link length ratios. Note that the rotator and flexure joint torques do not change as α changes. However, the knee joint torque is affected by α, as shown in Fig. 3.36(c). The optimal link length ratio yields the minimum maximum torque as the robot stands. From the given parameters the α that will yield the minimum maximum knee joint torque is equal to 1.01.

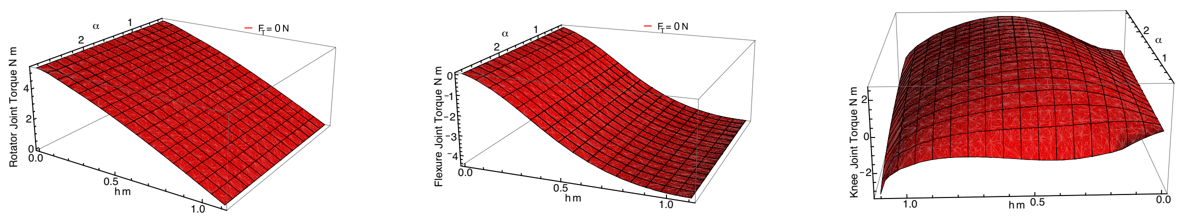

(a) Rotator joint torque (b) Flexure joint torque (c) Knee joint torque

Figure 3.36: Actuator torque results for different α values for the spiral pushup method.

Actuator Torques Optimization for Various d, α, and θ_{Z_0max} Combinations

An optimization was completed for the spiral pushup to determined the coupled affects of d and θ_{Z_0max} and d and α. Equation 3.63 was used to determine the cost value for the spiral pushup stranding up strategy. The cost function is used to find the maximum value as the robot stands for different parameter combinations. For example, d and θ_{Z_0max} were firs coupled and α was set to 0.6.

$$Cost = {M_{12}}^2 + {M_{23}}^2 + {M_{34}}^2 \tag{3.63}$$

The cost results were plotted, as shown in Fig. 3.37(a) and the minimum maximum cost occurs when d equals 0.44 m and θ_{Z_0max} equals $\frac{-\pi}{6}$. This approach would be beneficial for determining the optimal operation values for an already designed robot that will use the spiral method to stand up. Next, d and α were coupled and θ_{Z_0max} was set to $\frac{-\pi}{3}$. The cost results are shown in Fig. 3.37(b). The minimum maximum cost for this case occurs when d is equal to 0.39 m and α equal to 0.61.

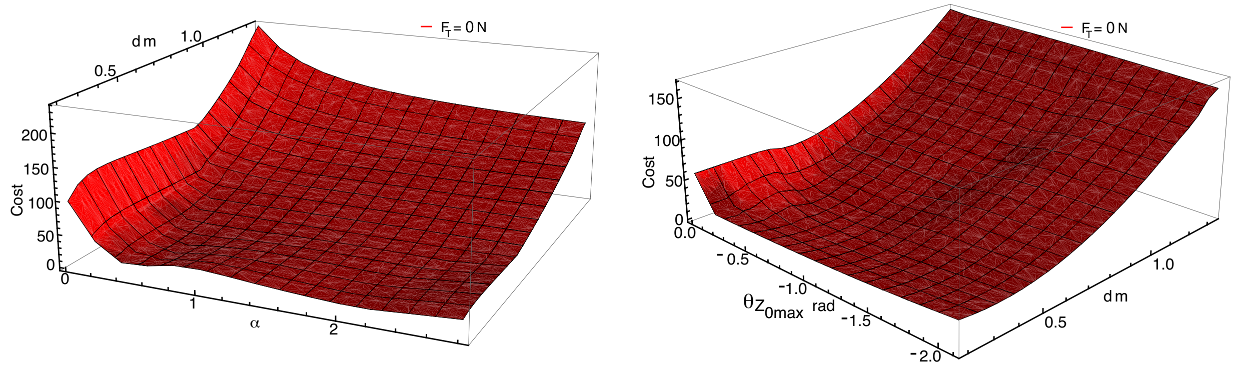

(a) Various d and α values (θ_{Z_0max}=$\frac{-\pi}{3}$)

(b) Various d and θ_{Z_0max} values ($alpha$ = 0.6)

Figure 3.37: Spiral pushup optimization d, α, and θ_{Z_0max}.

Effects of the tangential force on actuator torques

The effects of a friction force at the feet on the actuator torques was studied for the spiral method as the robot stands. As mentioned, a range of $-2.84N \leq F_T \leq 2.84N$ was considered given a maximum magnitude of 2.84 N ($\frac{\mu W}{3}$) acting in positive and negative directions at the feet. The chosen parameters were $r_3 = 0.45$ m, r_4=0.75 m, $d = 0.65$ m, and θ_{Z_0max}= $-\frac{\pi}{3}$. Fig. 3.38 shows the rotator, flexure and knee joint torque results for the defined F_T range.

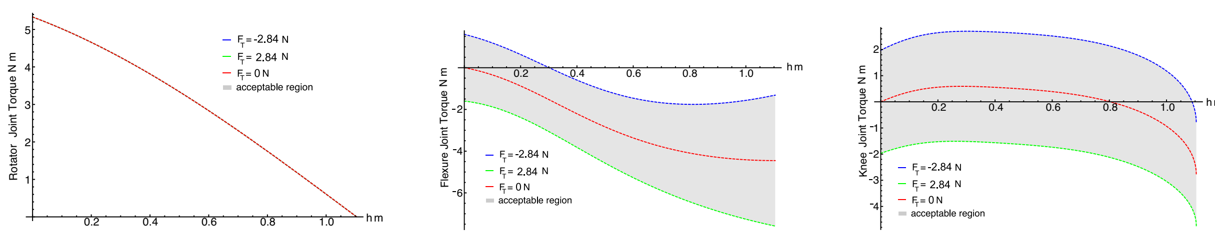

(a) Rotator joint torque

(b) Flexure joint torque

(c) Knee joint torque

Figure 3.38: Actuator torque results for various F_T values for the spiral pushup.

Note, that the final pose of the three feet pushup and spiral method are the same (Figs. 3.30(f) and 3.2(f)). Thus, since the same parameters for the spiral pushup and *Case* 1 of the three feet pushup were chosen the final joint torques will be the same. Also, as shown in Fig. 3.38(a), F_T does not affect the rotator joint torque since the unit vector at the rotator joint and the tangential force vector are in the same direction. The magnitude of the flexure joint torque is less for a tangential force acting inwards towards the center of the body than a tangential force acting outwards, as shown in Fig. 3.38(b). However, for the knee joint torque, as shown in Fig. 3.34(c), the minimum torque will occur for a tangential force between 0 and -2.84 N.

3.4.4 Overall Conclusions of the Spiral Pushup

The spiral pushup is another standing up strategy considered for STriDER. It uses its three legs to push the body upwards and simultaneously rotates the body by actuating the rotator joints. The feet are first positioned to their desired final position defined by d and θ_{Z_0max}. d is the distance between the projected center of the body to the ground and the foot position and θ_{Z_0max} is the maximum allowable body rotation about the $+Z_0$ axis. Since the configuration for all three legs in the spiral standing up method is the same, only one leg was analyzed. Similar to the other standing up methods, several important parameters were changed and their effects on the actuator torques were investigated. These parameters included, d, θ_{Z_0max}, the thigh and shank link length ratio, α, and the friction force at the feet, F_T. The effects of all four parameters were studied given a total link length value, r_{tot} $(= r_3 + r_4)$ of 1.2 m, L_b equal to 0.18m, and a body weight, W, of 28.42 N.

First, the effects of d, θ_{Z_0max}, and α on the actuator torques were studied individually when F_T was set equal to zero. For a fix value of θ_{Z_0max}, α, F_T equal to zero, and varying d, it was found that lower d values yield lower actuator torques. Then d and α were fixed and θ_{Z_0max} was varied. For this analysis it was found that as θ_{Z_0max} increases the rotator joint experience higher torques, but the flexure and knee joint experience lower torques. In fact, when θ_{Z_0max} equals zero the results are the same as the three feet pushup so, the three feet pushup is a special case of the spiral pushup. An optimization analysis was also completed by varying d and θ_{Z_0max} together for a set value α and F_T equal to zero. The procedure for the optimization was to determined the maximum cost for each d and θ_{Z_0max} combination as the robot stands using the spiral pushup. Once the maximum points were gathered and plotted the minimum maximum cost yields the optimal parameters. From this optimization, it was found that the minimum maximum cost occurs when d equals 0.44 m and θ_{Z_0max} equals $\frac{-\pi}{6}$. This approach is beneficial when a robot has already been designed and the optimal operation parameters (i.e d and θ_{Z_0max}) are desired.

Next, d, θ_{Z_0max}, and F_T were fixed and α was varied. From this analysis, it was determined that neither the rotator nor the flexure joints are affected by the link length ratios. However, the knee joint torque does vary as α changes. From the given parameters ($d = 0.65$ m, θ_{Z_0max} $= \frac{-\pi}{3}$, and $F_T = 0$), the alpha that yields the minimum maximum knee joint torque is equal to 1.01. An optimization was also completed for various d and α combination when θ_{Z_0max} equals $\frac{-\pi}{3}$, and F_T equals zero. It was found that the minimum maximum cost occurs when d equals 0.39 and α equals 0.61.

The last parameter that was analyzed was the tangential force at the feet, F_T. Recall that the tangential force is defined by the friction coefficient and normal force at the feet. After some analysis, it was determined that the rotator joint is not affect by F_T. Also, the flexure and knee joint torques experience higher torques for a tangential force acting outwards than a tangential force acting inwards towards the center of the body. In fact, the maximum actuator torques occurs when the maximum F_T acts outwards.

3.5 Feet Slipping Pushup

The feet slipping pushup begins with the robot flat on the ground with all three legs extended outwards, as shown in Fig. 3.39(a). Next, the legs begin to slip and lift the body upwards until the feet reach a desired final position defined by d (Fig. 3.39(b) to 3.39(f)). Large joint torque requirements are expected in order to implement this method. In fact, the flexure joint actuators create the motion needed to slide the feet inwards and force the body up by pushing the feet against the ground. During the feet slipping pushup, the robot is always statically stable since the projected center of gravity lies inside the support triangle formed by the three foot contact points. Note that as the feet move inwards, the symmetrical motion always forms a equilateral triangle with the foot positions.

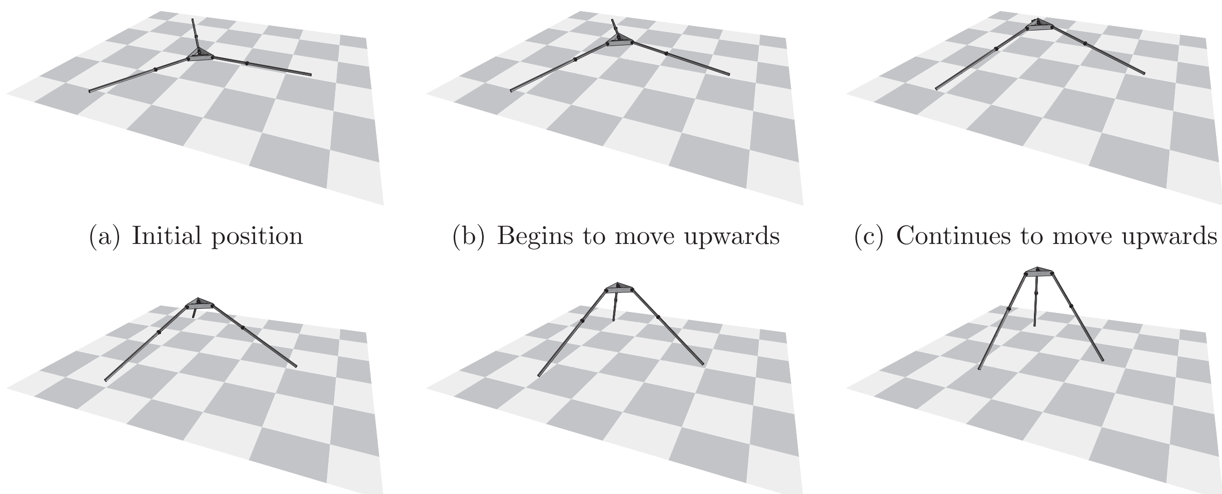

(a) Initial position (b) Begins to move upwards (c) Continues to move upwards

(d) Continues to move upwards (e) Continues to move upwards (f) Desired feet position reached

Figure 3.39: The motion of the feet slipping pushup.

The configuration for all three legs of the feet slipping pushup is the same thus, only one leg will be analyzed since the other two will follow the same procedure. A kinematic and static force analysis will be presented for the feet slipping pushup when F_T is equal to zero. Although setting F_T equal to zero is not realistic, it will help study the effects of d and α on the actuator torques. A range of d values and various link length ratios ($\alpha = \frac{r_3}{r_4}$) will be investigated in the analysis. For this method, d is defined as the distance between the projected center of the body on the ground to the final desired foot positions. Thus, the minimum d value is the length of the body link, L_b, and the maximum d value is the added length of the thigh, shank and L_b. The link length ratio, α, can range from zero ($\alpha = r_4$) to ∞ ($\alpha = r_3$). The effects of both d and α will be studied for the feet slipping pushup method. Next, a tangential force equal to $\frac{\mu W}{3}$ will be added to the feet. Note, that the friction force will always oppose the moving motion thus, it will always point outwards, as shown in Fig. 3.40.

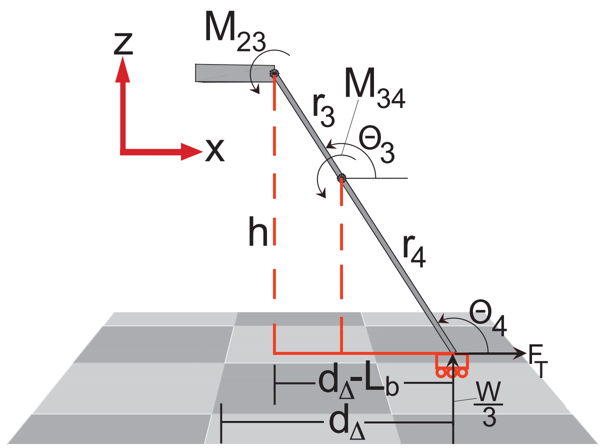

Figure 3.40: One leg free body diagram for feet slipping pushup.

3.5.1 Kinematic Analysis for the Feet Slipping Pushup

Because of the simplicity of the feet slipping pushup, the joint angles can be found using geometry. As shown in Fig. 3.40, the joint angles θ_3 and θ_4 are equal since the thigh and shank links are aligned during the entire motion of the feet slipping pushup. Thus, θ_4 can easily be calculated from Equation 3.64, where h is the height of the body and r_{tot} is the sum of the thigh and shank link lengths. The maximum height of the body is defined by a desired final foot position, d, and r_{tot} and calculated using Equation 3.3. Note that d_Δ is the changing distance between the projected center of the body on the ground and foot position as the body stands and that it will equal d once the feet reach a desired final position.

$$\theta_4 = \theta_3 = \pi - ArcSin\left(\frac{h}{r_{tot}}\right) \tag{3.64}$$

3.5.2 Static Force Analysis for the Feet Slipping Pushup

The flexure and knee joint torques as the robot stands using the feet slipping pushup method is presented in this section. As shown in Fig. 3.40 and calculated using Equation 3.65, d_Δ changes as the body moves upwards and reaches its desired final foot position defined by d. The flexure joint torque is calculated from Equation 3.66 where d_Δ changes for different h values. The knee joint torque is calculated from Equations 3.67.

$$d_\Delta = \sqrt{{r_{tot}}^2 - h^2} + L_b \tag{3.65}$$

$$M_{23} = \frac{-W\left(d_{\Delta} - L_b\right)}{3} - F_T h \tag{3.66}$$

$$M_{34} = \frac{-W r_4 cos\left(-\theta_4 + \pi\right)}{3} - F_T r_4 sin\left(-\theta_4 + \pi\right) \tag{3.67}$$

3.5.3 Actuator Torque Results for Feet Slipping Pushup

This section will investigate the effects of d and α on the flexure and knee joint torques when F_T equals zero. Note that F_T is set equal to zero to better understand the relationship between d and α on the actuator torques. Then, the effects of F_T on the flexure and knee joint torques will be studied.

Effects of d and Link Length Ratio on Actuator Torques

The effects of d and α on the flexure and knee joint torques are shown in Fig. 3.41. The knee and flexure joint torques were calculated for various d and α values. From Fig. 3.41(a) it can be concluded that in order to minimize the knee joint torque it is best if α is as large as possible and d is as small as possible. Note that when d is as small as possible the legs are aligned straight downwards so, the support triangle is very small and the stability of the robot is jeopardized. Fig. 3.41(b) shows the flexure joint results for different d and α combinations. It was found that the flexure joint torque is not affected by α and that smaller d values yield lower torques at the flexure joint.

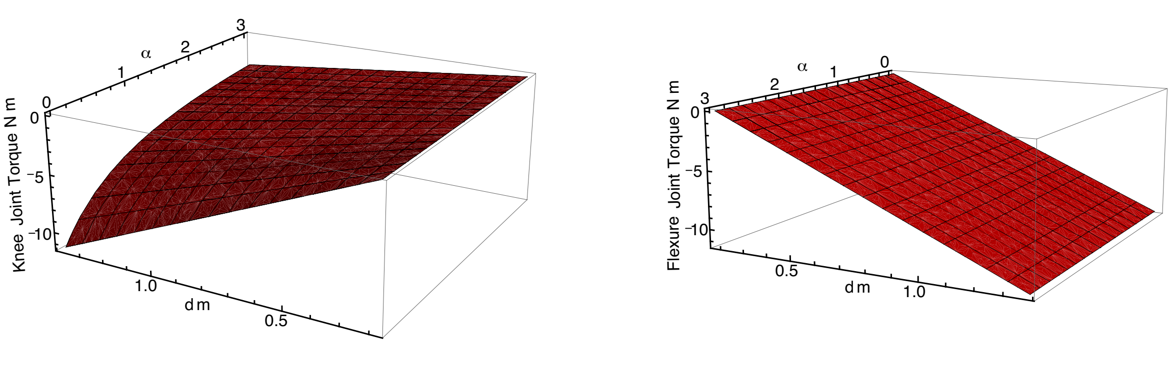

(a) Knee joint torque

(b) Flexure joint torque

Figure 3.41: Joint torques for different d and α values for the feet slipping pushup.

Effects of the Tangential Force on Actuator Torques

The effects of F_T on the flexure and knee joint torques is shown in Fig. 3.42. For this analysis the final desired d was set to 0.65 m and the link length ratio, α, was set to 0.6. As shown in Figs. 3.42(a) and 3.42(b), the knee and joint torques both increase as the tangential force F_T increases. Recall that in this case, the tangential force is constant and equal to $\frac{\mu W}{3}$. Thus, in this case the friction coefficient, μ, has a large effect on the actuator torques. Also, the flexure joint torques are greater than the knee joint torques, as would be expected.

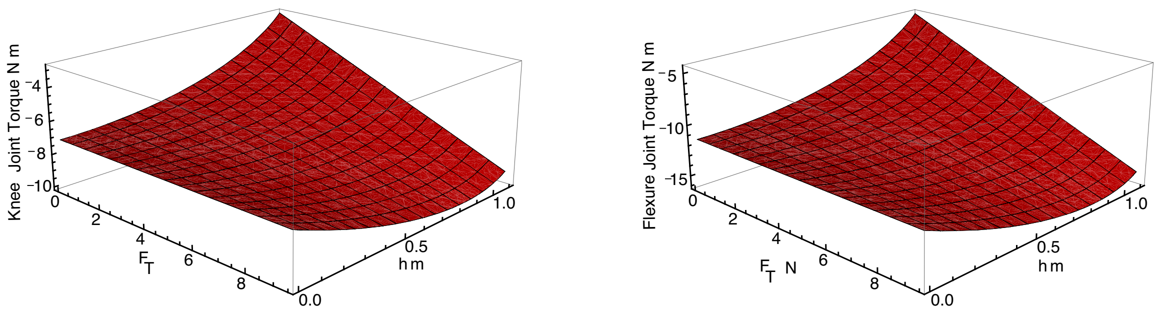

(a) Knee joint torque

(b) Flexure joint torque

Figure 3.42: Joint torques for different F_T values (d= 0.6 m and α= 0.6) for the feet slipping pushup.

3.5.4 Overall Conclusions of the Feet Slipping Pushup

The feet slipping pushup is the last standing up strategy presented in this thesis. It symmetrically uses its three legs to slide the feet along the ground and lift the body while keeping the thigh and shank links aligned. A d value was defined as the distance between the projected center of the body and the final desired foot positions. It was found that a larger link length ratio, α, would minimize the knee joint torques and that a small d value would minimize the flexure joint torques. Thus, for the feet slipping method it is best to have the largest possible link length ratio and have the robot's feet slide inwards closest to the center of the body as possible. Note that the closer the feet are to the center of the body, the support triangle becomes smaller and the robot becomes less stable.

It was also found that as the tangential force F_T increases the actuator torques also increase. For this method since the feet are sliding, F_T, is equal to a constant $\frac{\mu W}{3}$, defined by a the friction coefficient and always opposes the direction of the motion. Thus, in this case F_T always faces outwards. Although this is method seems like an acceptable solution for

STriDER to stand, it is not practical. This method would work well in low friction surfaces, such as ice, but not in rough surfaces.

3.6 Standing Up Experiments

Experiments were conducted to validate the standing up strategies. For each standing up method, torque readings were recorded for various joints at twenty different heights for seven trials. All torque values were recorded from static positions thus, the values were not recorded continuously as the robot stood up. The same link lengths and testing parameters were chosen for all of the experiments. These parameters included; a thigh link length, r_3, equal to 0.495 m, a shank link length, r_4, equal to 0.56 m, and a d value of 0.67 m.

The actuators used on STriDER were Dynamixel RX-28 and RX-64 DC motors. These motors allow the user to control position and speed and give load torque feedback with a resolution of 1024 steps. However, the torque feedback fluctuates greatly due to various variables thus, the readings are not very accurate. Ideally, external torque sensors should be used at each joint to adequately record torque values. Although the results of the experiments cannot be used to directly compare the analytical and experimental data, experiments were conducted to determined actuator troque trends for each standing up strategy. Once all motor joint trends were compiled, a conclusion was made to determined which of the five strategies is the most efficient for the tested prototype.

3.6.1 Three Feet Pushup Experiments

Fig. 3.43 shows various positions as STriDER stands using the three feet pushup method. As noted, the actuator torques were recorded from the motor feedbacks at twenty different heights for seven trials. The average of the seven trials was used to determine the actuator torque trends as the robot stands.

The results of the three feet pushup experiments are shown in Fig. 3.44. As shown in Fig. 3.44(a), the flexure joint torque followed a close trend for all seven trials. At first, the flexure joint experiences a large change in torque and then slowly decreases. This validates why it is difficult for the robot to stand from a height of zero.

The knee joint torque, shown in Fig. 3.44(b), however, does not follow such a close trend. It is important to note that although the motor torque readings were not as consistent as it would have been liked, they still can show an adequate trend. The maximum knee joint torque occurs near the end as the robot stands. However, after comparing the flexure joint and knee joint experimental results, the flexure joint experiences the largest torque. Also, the changes in torque show the effects of the tangential force on the actuator torques.

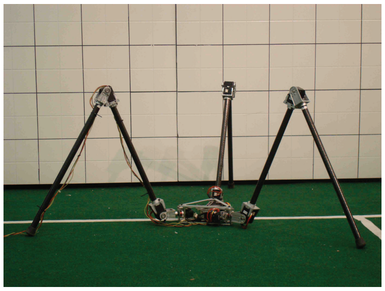

(a) Desired foot position

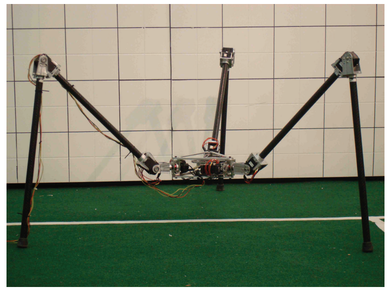

(b) Begins to move upwards

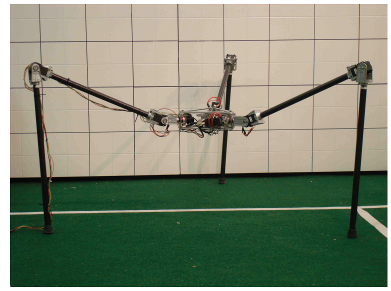

(c) Continues to move upwards

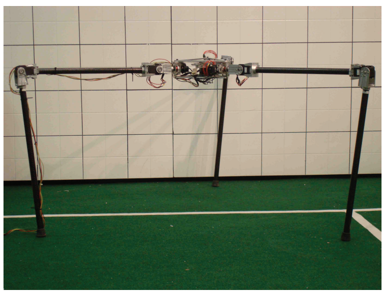

(d) Continues to move upwards

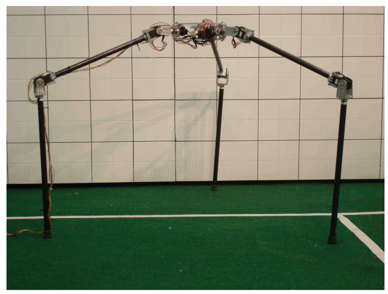

(e) Continues to move upwards

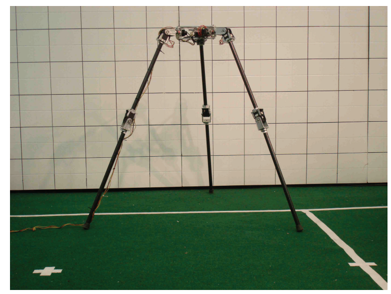

(f) Maximum height reached

Figure 3.43: Experiments of the three feet pushup.

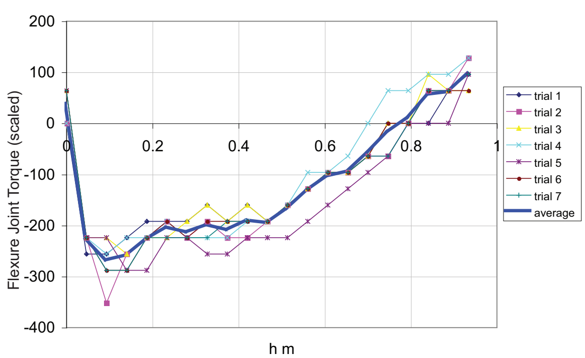

(a) Flexure joint torque

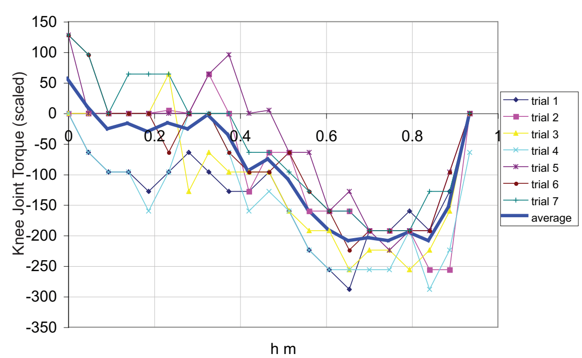

(b) Knee joint torque

Figure 3.44: Three feet pushup joint torque experiment results (r_3= 0.495 m, r_4=0.56 m, d = 0.67 m).

3.6.2 Two Feet Pushup Experiments

Various static positions of STriDER using the two feet pushup are shown in Fig. 3.45. Note that for this method two legs push the body upwards while the middle leg remains straight. Also, the foot positions do not change as the robot stands and they do not form and equilateral triangle. Lastly, the robot is always statically stable as is stands up using this strategy.

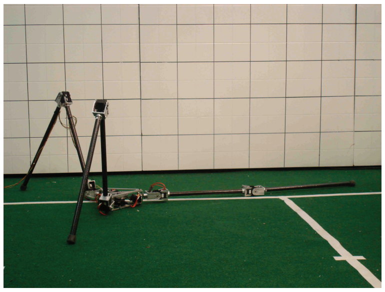

(a) Desired foot position

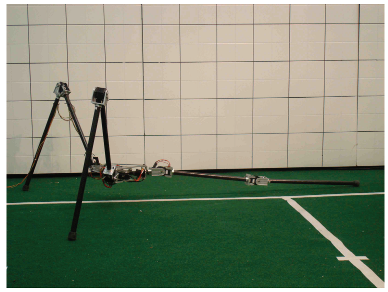

(b) Begins to move upwards

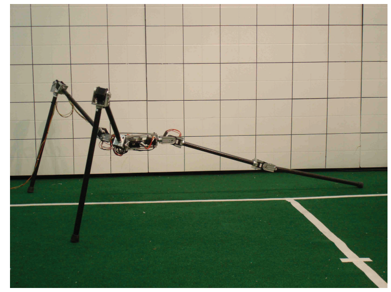

(c) Continues to move upwards

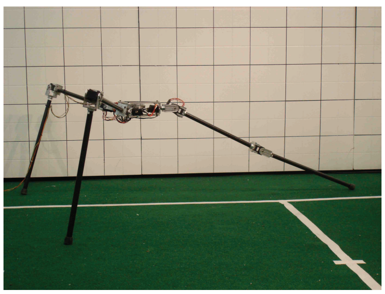

(d) Continues to move upwards

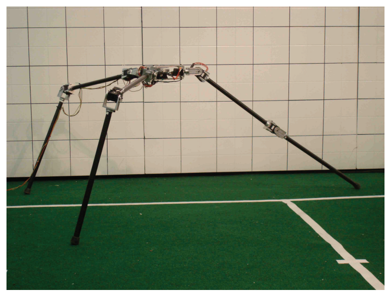

(e) Continues to move upwards

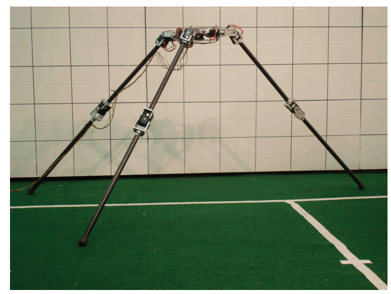

(f) Maximum height reached

Figure 3.45: Experiments of the two feet pushup.

The results of the two feet pushup experiments are shown in Fig. 3.46 and 3.47. Similar, to the analytical analysis, the experiments were divided in two parts: leg 1 and leg 2. Leg 1 is the leg that remains straight as the robot stands, and leg 2 bends and pushes the body upwards as discussed in Section 3.2.

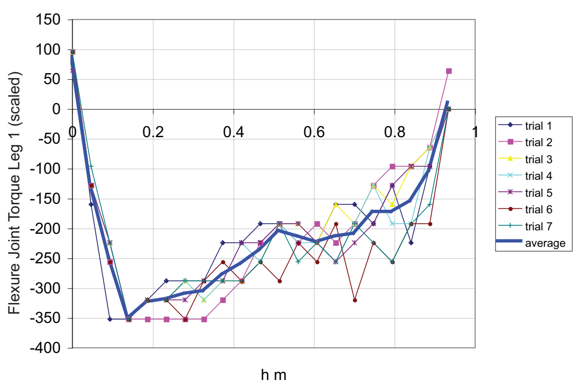

(a) Flexure joint torque

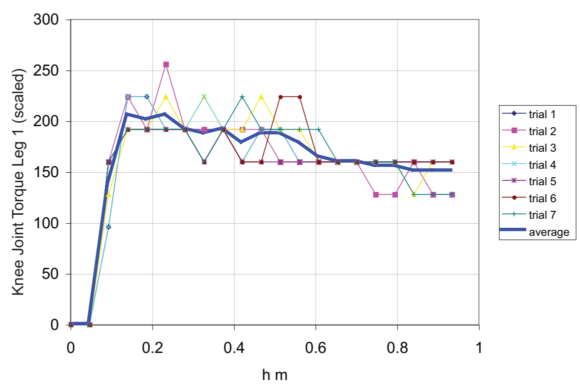

(b) Knee joint torque

Figure 3.46: Two feet pushup joint torque experiment results leg 1(r_3= 0.495 m, r_4=0.56 m, d = 0.67 m).

The flexure joint torque of the straight leg, shown in Fig. 3.46(a), experiences relatively high torques as the robot stands. The flexure joint torque rapidly increases to a maximum value and then decreases until the robot reaches its maximum height. The knee joint of leg 1, shown in Fig. 3.46(b), first rapidly increases and then slowly decreases. Note that the flexure joint torque has a larger magnitude at the majority of the heights than the knee joint for leg 1.

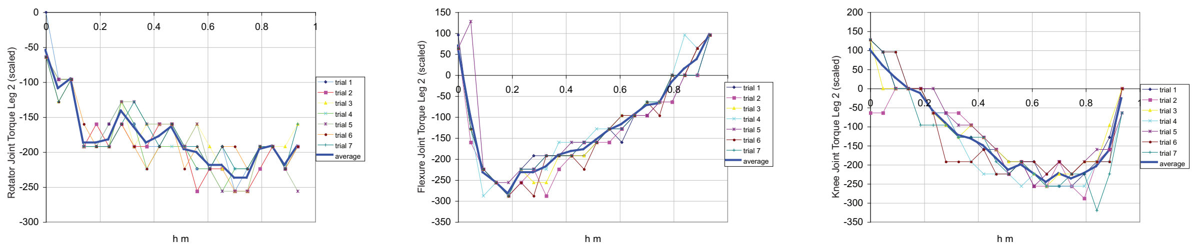

(a) Rotator joint torque (b) Flexure joint torque (c) Knee joint torque

Figure 3.47: Two feet pushup joint torque experiment results leg 2(r_3= 0.495 m, r_4=0.56 m, d = 0.67 m).

The rotator joint torque of the bending leg is shown in Fig. 3.47(a). It was found that as the robot stands, the rotator joint experiences much higher torques. Next, the flexure joint torque was recorded and the results are shown in Fig. 3.47(b). As shown, the flexure joint torque for leg 2 rapidly increases, then slowly decreases, reaches zero and then slowly increases in magnitude again. The knee joint torque of leg 2 is shown in Fig. 3.47(c). In this case, the torque decreases, reaches zero, increases and then final decreases until it reaches a maximum height.

After analyzing the straight and bending leg experimental results, it was found that the maximum torque occurs at the flexure joint of the straight leg, as expected from the analysis.

3.6.3 One Foot Pushup Experiments

Fig. 3.48 shows STriDER standing up using the one foot pushup method. As noted in Section 3.3, for this strategy the middle leg's foot is moved to its desired final foot position defined by d while the other two legs do not bend. After some initial experiments is was determined that the actuator torques were to large for the motors to handles and they were braking. Thus, the knees of the straight leg were bent in order to complete the experiments and reduce the actuator torques as the robot lifted using a modified one foot pushup.

The results of the one foot pushup experiments are shown in Figs. 3.49 and 3.50. Similar to the two feet pushup experiments, the one foot pushup was also divided in two parts: bending and straight leg experiments. First, the flexure joint torques were recorded at twenty different heights for seven trials, as shown in Fig. 3.49(a). The flexure joint torque decreases until

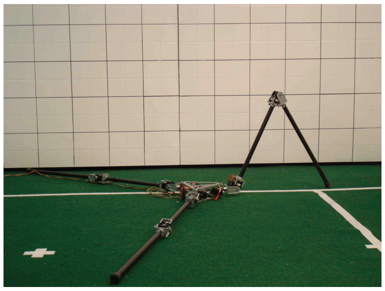

(a) Desired foot position

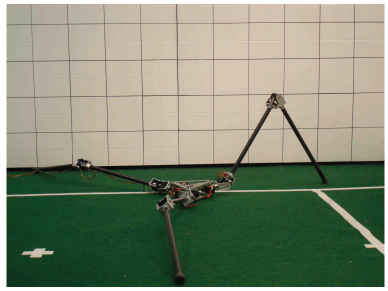

(b) Begins to move upwards

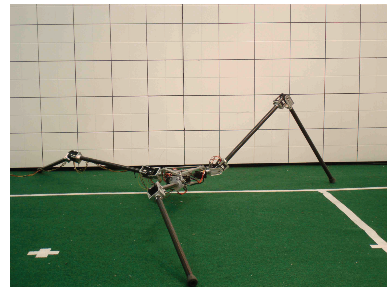

(c) Continues to move upwards

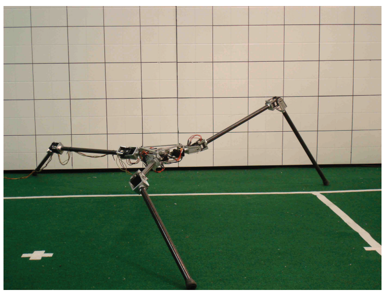

(d) Continues to move upwards

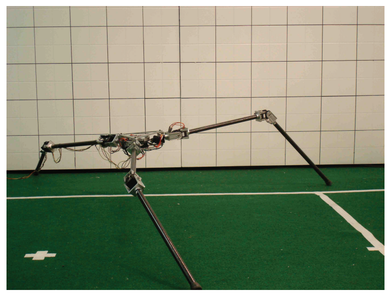

(e) Continues to move upwards

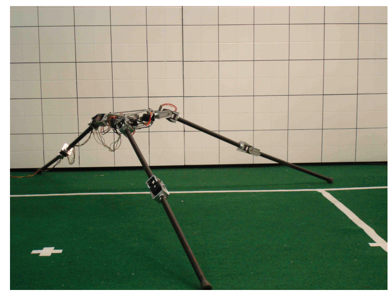

(f) Maximum height reached

Figure 3.48: Experiments of the one foot pushup.

it reaches zero, and then increases until it reaches a maximum torque. After the maximum flexure joint torque for leg 1 is reached, the joint torque decreases in magnitude. Next, the knee joint torques were recorded for leg 1, as shown in Fig. 3.49(b). The knee torque increases in magnitude, then decreases, reaches zero and finally increases until the robot reaches its maximum height.

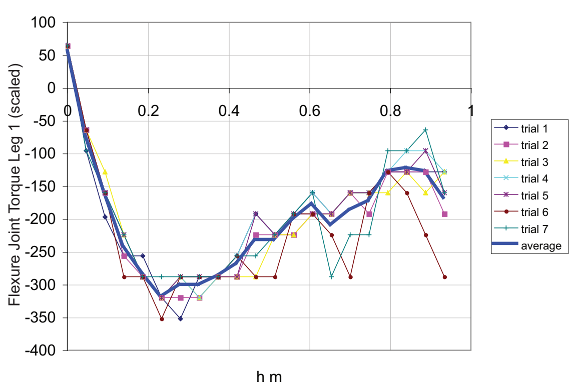

(a) Flexure joint torque

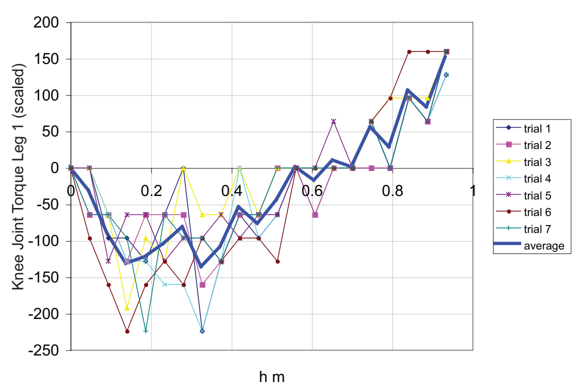

(b) Knee joint torque

Figure 3.49: One foot pushup joint torque experiment results eg 1(r_3= 0.495 m, r_4=0.56 m, d = 0.67 m).

The experiment results of the rotator joint for leg 2 are shown in Fig. 3.50(a). The rotator joint torque increases until the maximum height is reached. Next, the flexure joint results are presented in Fig. 3.50(b). As shown, the flexure joint torque increases and then remains close to constant. Finally, the results of the knee joint torque experiments for leg 2 are shown in Fig. 3.50(c). In this case, the knee joint torque increases, reaches a maximum, decreases until it reaches zero and then increases until the maximum height it reached.

For the one foot pushup case, the maximum torque occurs at the rotator joint of leg 2.

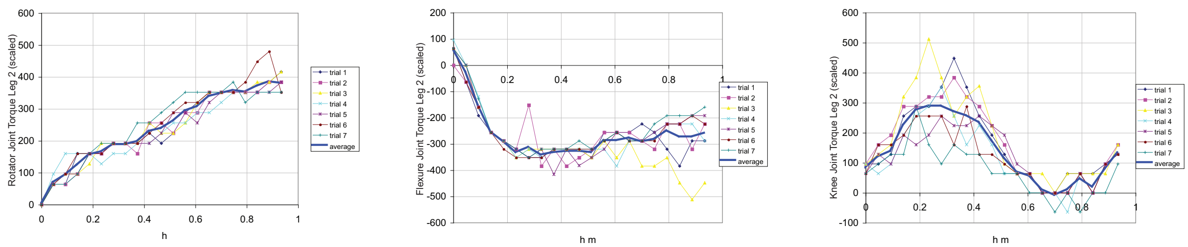

(a) Rotator joint torque (b) Flexure joint torque (c) Knee joint torque

Figure 3.50: One foot pushup joint torque experiment results leg 2(r_3= 0.495 m, r_4=0.56 m, d = 0.67 m).

3.6.4 Spiral Pushup Experiments

Several static positions of the spiral pushup are shown in Fig. 3.51. As previously discussed in Section 3.4, all three legs act the same for this method. First the feet are placed in their desired final positions, forming an equilateral triangle. Then, the body is lifted upwards by pushing the feet against the ground and rotating about the $+Z_0$ axis.

The results of the spiral pushup experiments are shown in Fig. 3.52. In addition to parameters listed above, a maximum body rotation of $\frac{-\pi}{6}$ was chosen for the spiral pushup experiments. The rotator joint results, presented in Fig. 3.52(a), show that the rotator joint experiences a large change in torque as the robot initially stands up but then decreases for the remainder of the body lifting. Next, the flexure joint torque, shown in Fig. 3.52(b), shows that the flexure joint torque varied some for the seven different trials. The trends shows that at first the flexure joint torque slightly increases, slightly decreases until it reaches close to zero, and then increases to a maximum torque value, and finally decreases. Finally, the knee joint torques were recorded for the knee joint, as the robot stands using the spiral pushup method, as shown in Fig. 3.52(c). These results show that the seven trials followed a very similar trend. The torque begins to decrease until it reaches zero, then increases in magnitude until the maximum torque is reached. Once the maximum torque is reached, the torque decreases in magnitude and the maximum height is achieved. From the experiments, it can be concluded that the maximum joint torque occurs at the knee joint torque.

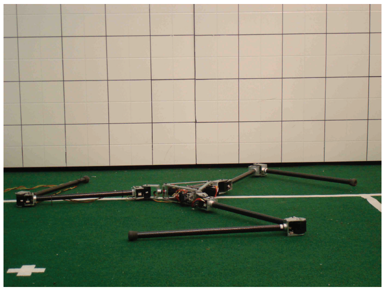

(a) Desired foot position

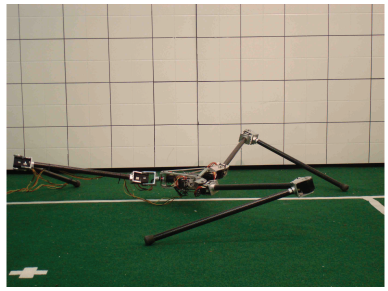

(b) Begins to move upwards

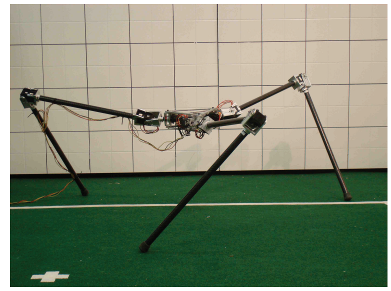

(c) Continues to move upwards

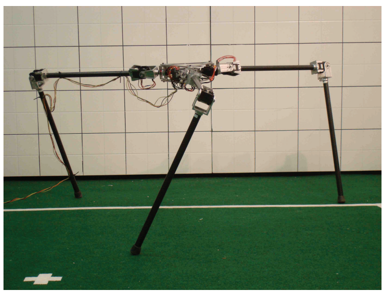

(d) Continues to move upwards

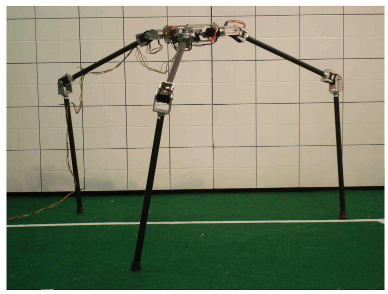

(e) Continues to move upwards

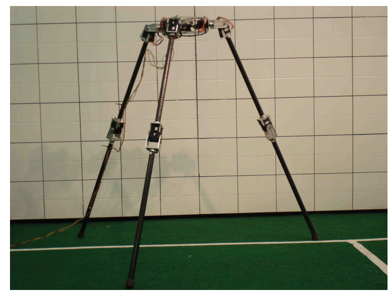

(f) Maximum height reached

Figure 3.51: Experiments of the spiral pushup.

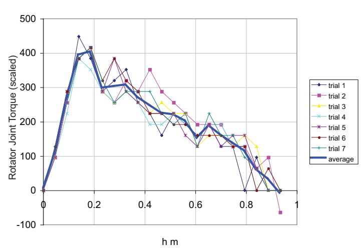

(a) Rotator joint torque

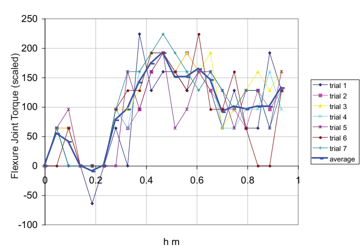

(b) Flexure joint torque

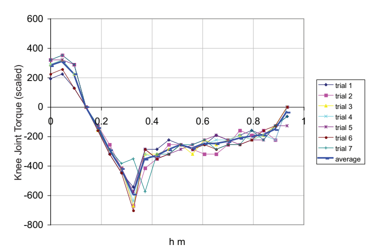

(c) Knee joint torque

Figure 3.52: Spiral pushup joint torque experiment results (r_3= 0.495 m, r_4=0.56 m, d = 0.67 m).

3.6.5 Feet Slipping Pushup Experiments

Fig. 3.53 shows six static positions for the feet slipping pushup strategy. Since torque readings could not be recorded as the robot was standing, the results of the feet slipping pushup experiments are not accurate. As mentioned in Section 3.5, the tangential force, F_T, for the this method always opposes the direction of motion. However, in this case since the torque values were recorded at static instances the values are not correct, but they will still be used to compare with the other strategies.

The results of the feet slipping pushup experiments are shown in Fig. 3.54. The flexure joint

(a) Desired foot position

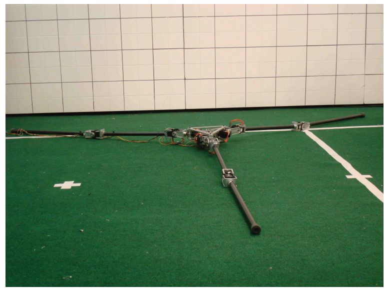

(b) Begins to move upwards

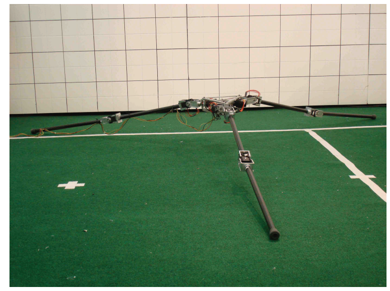

(c) Continues to move upwards

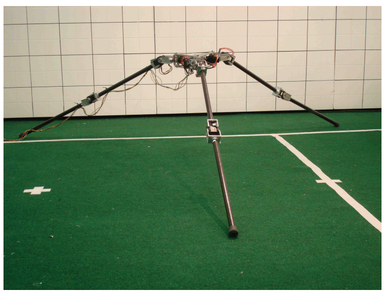

(d) Continues to move upwards

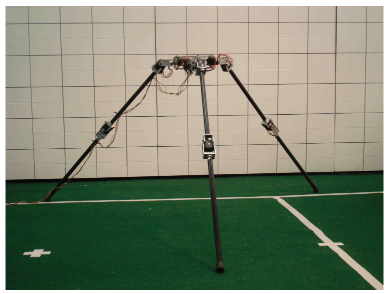

(e) Continues to move upwards

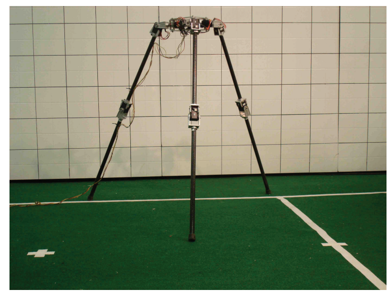

(f) Maximum height reached

Figure 3.53: Experiments of the feet slipping pushup.

torque trend, shown in Fig. 3.54(a), shows that as the robot stands the torque increases in magnitude until it reaches a maximum value and then decreases until it reaches zero. Once the torque reaches zero, it increases until the maximum height of the robot is reached. The knee joint torque results are shown in Fig. 3.54(b). It was found that the knee joint torque increases in magnitude, plateaus and then decreases. The maximum torque occurs at the flexure joint, as expected from the analysis.

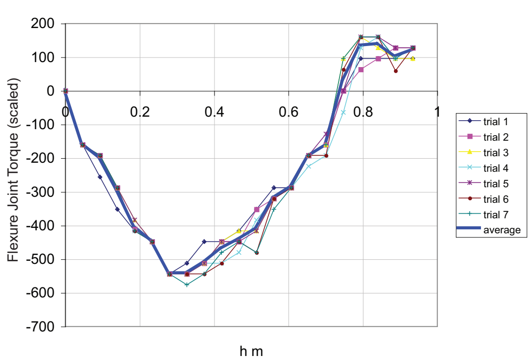

(a) Flexure joint torque

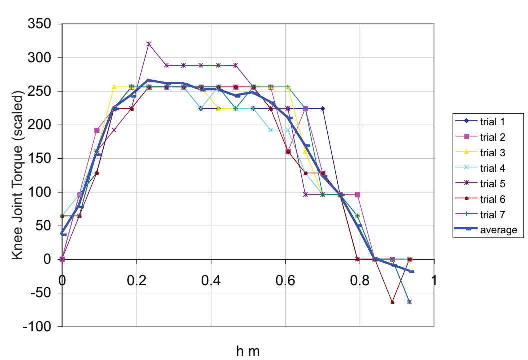

(b) Knee joint torque

Figure 3.54: Feet slipping pushup joint torque experiment results (r_3= 0.495 m, r_4=0.56 m, d = 0.67 m).

3.6.6 Overall Conclusions of Standing Up Experiments

Standing up experiments were conducted to validated the analytical model and to determine the most efficient strategy for a specific prototype of STriDER. Seven trials were preformed for each method and static torque readings were recorded at twenty different heights. The same parameters were chosen for each experiment and the following values were used; thigh link length, r_3, equal to 0.495 m, shank link length, r_4, equal to 0.56 m, and d equal to 0.67 m. For each experiment, the maximum torque value was recorded and are listed in Table 3.4. From the results, it may be concluded that for the tested prototype the three feet pushup is the most efficient standing up strategy in terms of maximum joint torque requirements. On the other hand, the spiral pushup is the least efficient.

Table 3.4: Standing up experimental results

Standing Up Strategy	|Maximum Torque|
Three Feet Pushup	269
Two Feet Pushup	352
One Foot Pushup	384
Spiral Pushup	594
Feet Slipping Pushup	544

From the experiments it was found that it was most difficult for the robot to stand when the body is flat on the floor. Thus, once the robot reached a certain height the maximum torque values greatly decreased. Also, from the torque analysis it was expected that the three feet pushup would be the most efficient strategy since all three legs distribute the forces and torques evenly. Thus, the analytical and experimental results agreed. However, the actual torque values cannot be directly compared due to the inaccuracy of the torque feedback of the actuators and the varying tangential forces.

It is important to note that for all of the presented analysis a friction coefficient, μ, of 0.3 was chosen. However, experiments were conducted on a surface that has a friction coefficient close to 0.9. Thus, in this case, the boundary formed by the maximum tangential forces in both the positive and negative direction is much larger than the one presented in the analysis. Therefore, the experimental results will most likely fall within the allowable boundary defined by the minimum and maximum tangential force. Also, the recorded torque trend for each actuator is greatly affected by F_T. Thus, since F_T cannot be controlled it is difficult to truly compare the analytical and experimental results because only position control was used and not torque control.

Future work will implement force control on the actuators to directly compare the analytical and experimental results and to optimize F_T to minimize torque. Also, a simple way to compare the experiments and analytical model using position control is to eliminated the friction forces by adding rollers at the feet. However, adding rollers at the feet is not practical for real case scenarios when STriDER needs to walk using its tripedal gait.

3.7 Overall Conclusions of Standing Up Strategies

Five standing standing up strategies unique to STriDER were investigated. These strategies included a three feet pushup, two feet pushup, one foot pushup, spiral pushup, and feet slipping pushup. Although STriDER is inherently stable with its tripod stance it is important for the robot to be able to stand up if it falls while walking or external forces act on it. For each strategy various parameters were studied and their effects on the actuator torques were analyzed. The parameters included, d, the distance between the projected center of the body on the ground and the foot positions, α, the thigh and shank link length ratio, and F_T, the tangential force at the feet. As noted, the range of tangential contact force between the foot and the ground is defined by the friction coefficient and the normal force due to gravity. As long as the tangential contact forces at the feet are between the minimum and maximum allowable values, and the force balance is satisfied then, the tangential forces can be adjusted by force control of the actuators of the the robot. Also, for all of the standing up strategy analysis a total allowable link length, r_{tot} $(= r_3 + r_4)$, was set to 1.2 m, L_b $(= L_0 + L_1 + L_2)$ was set to 0.18 m and total body weight, W, was equal to 28.42 N.

Several of the findings from human standing and human pushup analysis discussed in Section 1.2.5 were implemented in this work. For example, in [12] it was concluded that static loads dominate joint forces and torques as a subject rises from a sit position; however, dynamics becomes more important as the speed increases. Thus, for the study of STriDER's standing up strategies, dynamics was ignored and the analysis was solely statically based, assuming the robot was not standing up at high speeds. Also in [15], the process of standing from a chair was divided into several phases. Although STriDER's standing up methods were not specifically defined by different phases, common initial and final positions were defined. For example, similar initial and final conditions were considered (i.e. all strategies begin with the robot flat on the ground with the legs extended straight outwards and end when the robot reaches a maximum allowable height). In [14], cost functions were evaluate to determined optimal human standing up trajectories. For STriDER, cost functions were evaluated for each standing up strategy to determined optimal design and operation parameters. Also, the effects of hand positions on the torque of the elbow joint for human pushup was investigated in [17]. They found that the peak forces at the human elbow joint decreased as the distance between the hands increased. This idea directly related to studying the effects of d on the actuator joints of STriDER.

For each strategy the effects of d and α were investigated individually with F_T equal to zero. Then, the effect of F_T on the actuator torques was investigated for specified d and α values. From the analysis it was found that the rotator and flexure joints are not affected by α. Also, d had a large effect on the actuator torques. For most strategies, smaller d values yield lower actuator torques. This conclusion does not agree with the research findings. This difference could occur because in STriDER's case all three legs are the same length. However, for average males the arm length (shoulder to fingertip) is approximately 0.44 percent of the total height and the lower body (hip to feet) is about 0.53 of the total height, as found in [20].

Also, depending on the range of d and the range of α, the results sometimes did agree with Donkers. For example in the two feet pushup analysis, it was found that for small d value ranges and for small α, the knee joint (same as human elbow) peak torque did decrease as d increased. Finally, for most standing up strategies it was concluded that tangential forces acting inwards yield lower actuator torques than tangential forces acting outwards. Due to the many variable effects on the actuator torques, it was found that it was best to evaluate a cost function to determine optimal design and operation parameters.

Lastly, experiments were conducted to determined the most efficient standing up standing up strategy for a specific prototype. Although the recorded torque values from the actuator feedback were not as accurate as desired, torque trends were determined for each method. In fact, actuator torques were recorded for twenty static positions and seven trials for all five standing strategies. From the experiments, it was determined that the three feet pushup yields the lowest maximum torque as STriDER stands thus, it is the most efficient.

Chapter 4

Considerations for Gait Planning Strategies Based on Kinematics

Many factors and constraints contribute to the development of STriDER's path planning strategies and gait generation. To correctly generate a gait both kinematics and dynamics must be considered. Although dynamics plays a major role in gait generation, the following sections discuss possible considerations for gait planning strategies solely based on kinematics.

4.1 Stability

The robot's static stability is important during a step, as the novel tripedal gait requires the robot to become statically unstable forcing the robot to fall forward and swing its middle leg in between the stance legs and catch the fall. However, when all three feet are touching the ground, the robot must be statically stable by keeping the projected center of gravity point in the support triangle, formed by the three foot positions. Thus, the location of the projected center of gravity point plays an important role in the generation of a gait. A detailed discussion of a quantitative static stability margin is discussed below.

4.1.1 Static Stability Criteria

A specific quantitative static stability margin (SSM) was developed to assess the stability of STriDER. Stable, unstable and marginally stable cases are discussed in this section. The stability margin was quantified based on the distance between the projected center of gravity of the robot on the ground and the incenter of the the support triangle formed by the three feet contact points. Table 4.1 summarizes the SSM range for stable, unstable and marginally

Table 4.1: SSM range

Static Stability Condition	**SSM Range**
Stable	$1 > SSM > 0$
Marginally Stable	$SSM = 0$
Unstable	$-\infty > SSM < 0$

stable cases.

Stable Stability Margin

First, the CG_P point, shown in Fig. 4.1, is the center of gravity point projected in the negative Z_0 direction to the triangular plane formed by the robot's three foot contact points in 3D space. When the CG_P lies inside the support triangle, the SSM is calculated for a stable condition as shown in Equation (4.1),

$$SMM = Min\left[\frac{d_1}{r}, \frac{d_2}{r}, \frac{d_3}{r}\right] \tag{4.1}$$

where d_1, d_2, and d_3 is the distance from point CG_P to each side of the support triangle and r is the radius of the support triangle's incircle, as shown in Fig. 4.1. The center of the support triangle, labeled I in Fig. 4.1, was chosen as the center of the incircle of the support triangle since it is the point that represents the maximum equal distance from each side of the triangle.

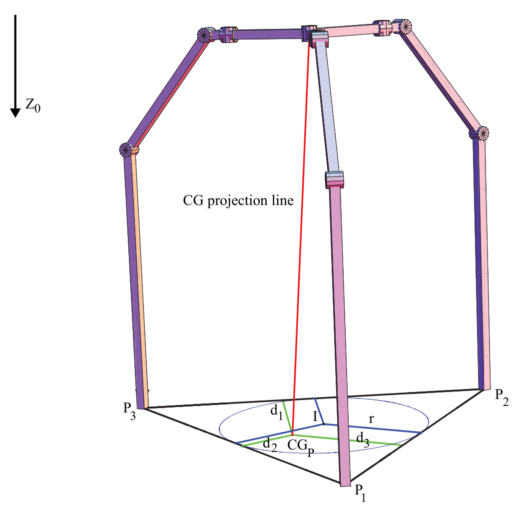

Figure 4.1: Stable configuration with SM=0.555

The robot is most stable when the projected center of gravity point lies on point I, thus the SSM is equal to 1. As the point CG_P moves closer to the sides of the triangle the SSM decreases and once CG_P lieso n any of the sides, the SM is equal to 0. Note that when the projected center of gravity point, CG_P, lies on any of the support triangle's sides it is marginally stable.

4.1.2 Unstable Stability Margin

If the point CG_P lies outside the support triangle the robot is statically unstable, as shown in Fig. 4.2. As the CG_P point continues to move further outside the support triangle the SSM increases in magnitude in the negative direction. In this case, the static stability margin depends upon the region, defined by the lines connecting point I to the three foot positions, P_1, P_2, and P_3, in which CG_P lies, as shown in Fig. 4.3.

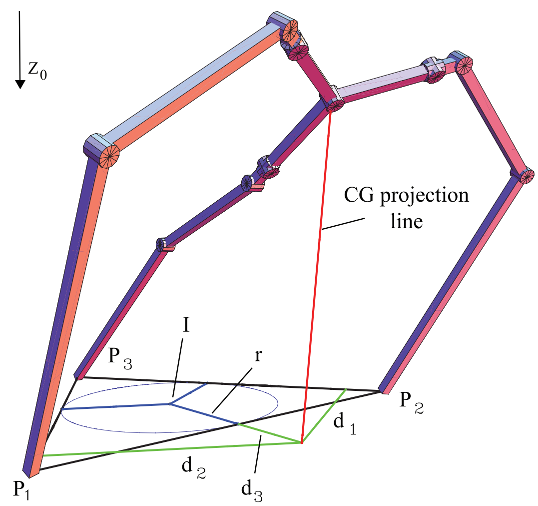

Figure 4.2: Unstable configuration with a SM=-0.723.

Therefore the angles, θ_{CG}, θ_2, and θ_3, are defined as that between lines $\overline{IP_1}$ and $\overline{ICG_P}$ and $\overline{IP_1}$ and $\overline{IP_2}$ respectively as in Fig. 4.3. The static stability margin is then given as Equation (4.2),

$$SMM = \begin{cases} -\frac{d_3}{r} & 0 \leq \theta_{CG} < \theta_2 \\ -\frac{d_1}{r} & \theta_2 \leq \theta_{CG} < \theta_3 \\ -\frac{d_2}{r} & \theta_3 \leq \theta_{CG} < 2\pi \end{cases} \tag{4.2}$$

where r, d_1, d_2, and d_3 are defined as before.

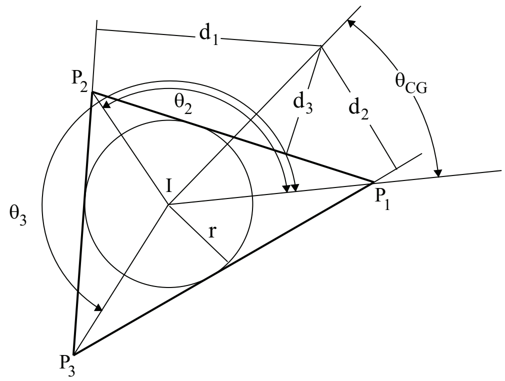

Figure 4.3: SSM definition when CG_P lies outside the support triangle.

4.2 Dynamics

Dynamics plays a key role in producing the gait for walking robots. STriDER can be modeled as a planar four-link inverted pendulum in the sagittal plane by treating the two stance legs as a single link connected to the ground by a revolute joint, as shown in Fig. 4.4 [1]. In this figure, the angle between the link representing the stance legs and the ground is called the tilting angle.

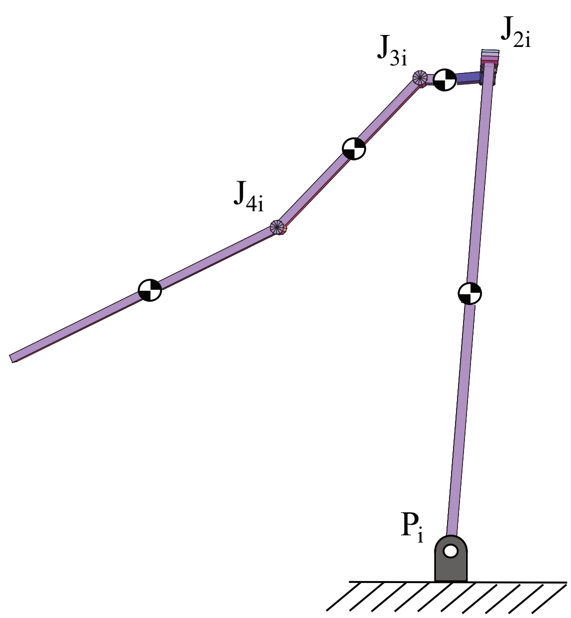

Figure 4.4: Inverted four link pendulum [6].

Since there is no active actuator between the foot and the ground, STriDER is inherently an under-actuated mechanical system. Assuming no slipping on the ground, the tilting angle during a gait is affected by the coupled dynamics of the other links in the system. The rotation of the body or any of the other actuated links will drive the unactuated links. In [8], self-excited control is utilized to enable a three-link planar robot to walk naturally on level ground. Utilizing this concept of self-excitation, STriDER's passive dynamic gait was produced in [1, 3]. [10] proved the existence of limit-cycle motion of multi-link planar robots by using differential flatness and dynamic-based optimization. This methodology will be utilized in generating the gait for STriDER in future research where all of the joints of the robot are actively controlled to control the unactuated tilting angle of the robot. In this thesis, all joint angles of STriDER are calculated based on kinematics only to illustrate the concept of a single-step gait and to emphasize the importance of the kinematic constraints for the system.

4.3 Height of the body

The height of the body must also be considered when taking a step which is defined as the distance from the center of the body (point B in Fig. 2.1) to the ground in the negative Z_0 direction. The body's maximum height depends on the geometry of the support triangle. Thus, the height of the body when all links of the stance legs are aligned from the center of the body to the stance leg foot position is the maximum height during that step with that specific support triangle's geometry. However, the maximum possible height for any geometry is the total length of the thigh and shank link. The minimum height must allow the swing leg to swing underneath the body as the body rotates 180 degrees without scuffing the ground. The height of the body also affects the speed of the fall. The higher the body the slower the fall of the robot and the lower the body position the faster the fall of the robot.

4.4 Body twisting motion during a step

During a step, two pivot lines must be considered; one is the pivot line formed by aligning the stance legs hip abductor joints that allows the body to rotate 180 degrees called the *body pivot line*, while the other is the pivot line formed by the two stance leg's foot contact point that allows the entire robot to pivot called the *stance leg pivot line*. When the *body pivot line* and *stance leg pivot line* are parallel while the robot takes a step, the kinematic analysis is greatly simplified and collision between the swing leg and stance legs is prevented. However, for uneven terrains it might be beneficial for the pivot lines to be skewed, as it may aid the swing leg in avoiding obstacles.

STriDER has to align two of its rotator joints to prepare for each step. A top view of the support triangle formed by the foot contact points, P_1, P_2, and P_3 is shown in Fig. 4.5. $\overline{P_2P_3}$ is the *stance leg pivot line* and P_1 is the initial location of the swing leg foot contact point. Line f is formed by points P_1 and P_2 and line e is formed by points P_1 and P_3. Region I

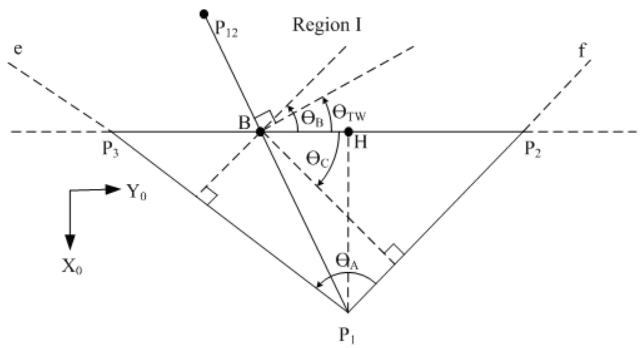

Figure 4.5: Top view of the support triangle.

is the boundary created between line *f*, line e and $\overline{P_2P_3}$. For the case presented here, it is assumed that initially, the *body pivot line* is parallel to the *stance leg pivot line* and point P_{12} is the final swing leg foot contact position which must lie in Region I. Since P_1 and P_{12} form a straight line going through Region I, the body has to twist its facing angle and make its projected pivot line perpendicular to $\overline{P_1P_{12}}$. The twisting motion of the body is controlled with the stance legs and during the twisting the plane of the body is parallel with the ground. The twisting angle θ_{TW}, as shown in Fig. 4.5, is defined as the rotation of the *body pivot line* about its midpoint in $\pm Z_B$ directions, where Z_B is the z-axis of the body coordinate system shown in Fig. 2.1. θ_{TW} can be determined from the coordinates of P_1, P_2, P_3 and P_{12}, and satisfies the following constraints:

$$-\theta_C < \theta_{TW} < \theta_B \tag{4.3}$$

$$\theta_A = \theta_B + \theta_C \tag{4.4}$$

$$\theta_B = ArcTan\left(\frac{\overline{P_3H}}{\overline{HP_1}}\right) \tag{4.5}$$

$$\theta_C = ArcTan\left(\frac{\overline{P_2H}}{\overline{HP_1}}\right) \tag{4.6}$$

Note that θ_B and θ_C are two extreme cases when the final foot position P_{12} lies on line e or *f*.

The twisting angle of the body is an important factor for the turning strategy of STriDER on various terrains. A large turning angle per step can increase the mobility of STriDER in complicated environments [25].

4.5 Swing leg's clearance and landing position

The swing leg's foot path is also an important variable to consider as the robot takes a step. The swing leg's foot should not scuff the ground during the swing portion of the gait thus, the knee must be bent at certain angles to prevent the foot from touching the ground. Also, when considering a single step an allowable region for the subsequent swings leg's foot contact position must be constrained, as mentioned in Section 4.4.

4.6 Foundations for a single step gait generation

This section lays out the foundation and guidelines for future work on a single step gait generation based on both kinematics and dynamics. Several of the constraints addressed in Sections 4 should be considered when taking a single step. The objective is to achieve a single step from an initial swing leg foot position, P_1, to a desired final swing leg foot position P_{12} (within Region I), on an even ground, as shown in Fig. 4.5.

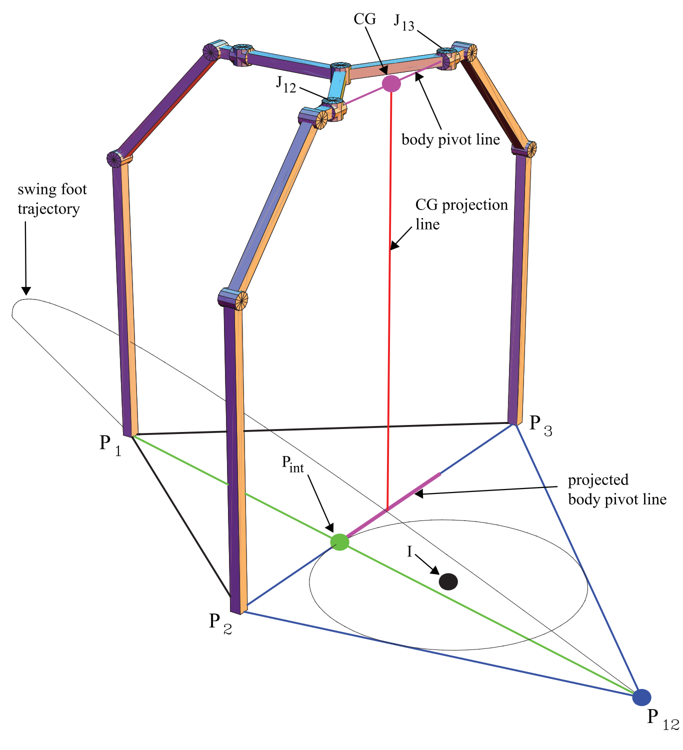

Figure 4.6: Gait simulation labels

In Fig. 4.6, the center of gravity can be assumed to be located in the midpoint of the *body pivot line* formed by global positions of the hip abductor joints J_{12} and J_{13}. The swing foot projected path line, $\overline{P_1P_{12}}$, is formulated from an initial swing leg foot position, P_1, to a final foot position, P_{12}. The *stance leg pivot line*, $\overline{P_2P_3}$, is defined as the line connecting the stance leg's foot contact points, P_2 and P_3. P_{int}, is the intersection point of lines $\overline{P_1P_{12}}$ and $\overline{P_2P_3}$. First, the robot may begin its gait at marginally stable state, where the projected center of gravity point lies on the *stance leg pivot line*, $\overline{P_2P_3}$, as shown in Fig. 4.6 and discussed in Section 4.1.1. The robot must then shift so the projected center of gravity point, CG_P, coincides with P_{int}, the intersection of lines $\overline{P_1P_{12}}$ and $\overline{P_2P_3}$. Then, as mentioned in Section 4.4, the body must twist so the projected *body pivot line* is perpendicular to $\overline{P_1P_{12}}$. The robot is now in position to fall forward and reach its desired final foot location. The rotation of the body or any other actuated links will force the robot to fall forward to initiate the swing portion of the step. Also, the body should be set at a height below the maximum height but high enough so the swing leg would have adequate room to swing in between the stance legs.

Chapter 5

Conclusions and Recommendations

5.1 Conclusions

This thesis presented investigations of standing up strategies and consideration for gait planning based on kinematics for a novel three-legged walking robot called STriDER (Self-excited Tripedal Dynamic Experimental Robot). Although the robot is inherently stable with its tripod stance, it can still fall down if it trips while walking or if unexpected external forces act on the robot. Thus, five different standing up strategies were investigated. The unique structure of STriDER makes standing up challenging for a number of reasons; the relatively high height of the robot and long length of the limbs require high torque at the actuators due to its large moment arms and the number of limbs (three) does not allow extra support and stability in the process of standing up, to name a few. The five standing up methods investigated included; a three feet pushup, two feet pushup, one foot pushup, spiral pushup, and feet slipping pushup. The primary goal of each study was to minimize the torque at the joints by changing three main parameters. These parameters included; a value of d which describes the foot placement position, defined by the distance between the projected center of the body on the ground to the desired final foot position, the thigh and shank link length ratio, α, and a tangential force at the feet, F_T, which occurs due to friction, defined by the normal force and friction coefficient.

Also, several factors for gait planning were discussed as the robot takes a step including; stability, dynamics, the body's maximum and minimum allowable heights, the swing leg's foot clearance to the ground, and the range of the subsequent swing foot contact positions.

5.1.1 Conclusions for Standing Up Strategies

Overall conclusions for each standing up strategy are presented below.

Three Feet Pushup

First, the three feet pushup was analyzed. This strategy begins with all three legs extended straight outwards. Then, the feet of the robot are placed at a desired foot position, defined by d and once the feet reach their desired position, the body is lifted by pushing the feet against the ground. It was found that for a given link length ratio, α, an optimal d value, d_{opt} can be calculated using Equation 3.12. Also, for a given d value, the largest α will yield a minimum maximum knee joint torque. It was also found that the flexure joint torque is not affected by different link length ratios and a minimum d value will yield the lowest flexure joint torque. Finally, the tangential forces, F_T, analysis showed that a tangential force acting inwards towards the center of the body will yield lower actuator torques than a tangential force acting outwards.

Two Feet Pushup

Next, the two feet pushup was analyzed. This method uses two of its legs to stand the robot while the third leg reminds straight. First, two of the feet of the robot are placed to a desired final foot position and the body is then lifted upwards by pushing against the ground. Since two of the legs act the same and the third remains straight, the analysis of the two feet pushup was divided in two parts: straight leg and bending leg. From a cost function it was determined that for a given link length ratio, α, a minimum allowable d would minimize the actuator torques. Also, for a given d value, a maximum α would minimize the actuator torques. The tangential force, F_T, analysis showed that for the rotator joint torque of the bending leg a tangential force acting outwards minimizes the torque; however, once the thigh link is parallel to the tangential force vector at the feet then, any tangential force will yield the same torque. Once that position has passed, a tangential force acting inwards towards the body will minimize the rotator joint torque for the bending leg. Lastly, the flexure and knee joint torques for both the straight and bending leg are minimized when the tangential force at the feet acts inwards toward the center of the body.

One Foot Pushup

The one foot pushup was the third standing up strategy method considered for STriDER. It uses one leg to push the body upwards as the other two legs follow the direction of the body while keeping the feet at their initial feet positions. First, one leg positions its foot to a desired final foot position defined by d. Then, the bending leg lifts the body and the other two legs follow the body trajectory. Since the straight legs act the same, the analysis of the one foot pushup was divided in two parts: bending leg and straight leg. It was determined that for a given d value the minimum cost occurs when α is largest and for a given α, the minimum cost occurs at lower d values. From the tangential force analysis, it was found that the flexure and knee joint torques of both the bending and straight legs are minimized for a maximum tangential force acting inwards towards the center of the body and maximized for a maximum tangential force acting outwards. However, the rotator joint torque of the straight leg acts in the opposite manner.

Spiral Pushup

The spiral pushup was another standing up strategy considered for STriDER. It uses its three legs to push the body upwards and simultaneously rotates the body by actuating the rotator joints. The feet are first positioned to their desired final position defined by d and θ_{Z_0max}, where θ_{Z_0max} is the maximum allowable body rotation about the $+Z_0$ axis. For a fixed value of θ_{Z_0max}, α, F_T equal to zero, and varying d, it was found that lower d values yield lower actuator torques. When d and α were fixed and θ_{Z_0max} was increased the rotator joint experienced higher torques, but the flexure and knee joint experienced lower torques. An optimization analysis was also completed by varying d and θ_{Z_0max} together for a set value α and F_T equal to zero. The procedure for the optimization was to determined the maximum cost for each d and θ_{Z_0max} combination as the robot stands using the spiral pushup. This approach is beneficial when a robot has already been designed and the optimal operation parameters (i.e d and θ_{Z_0max}) are desired. The rotator nor the flexure joints are affected by the link length ratios; however, the knee joint torque does vary as α changes. An optimization was also completed for various d and α combination for a given θ_{Z_0max} value and F_T equal to zero. After some analysis, it was determined that the rotator joint is not affect by F_T. Also, the flexure and knee joint torques experienced higher torques for a tangential force acting outwards than a tangential force acting inwards towards the center of the body.

Feet Slipping Pushup

The feet slipping pushup was the last standing up strategy presented in this thesis. It symmetrically uses its three legs to slide along the ground and lift the body while keeping the thigh and shank links aligned. For the feet slipping method it is best to have the largest possible link length ratio and have the robot's feet slide inwards closest to the center of the body as possible. Although this is method seems like an acceptable solution for STriDER to stand, it is not practical. This method would work well in frictionless surfaces, such as ice, but not in rough surfaces.

Experiments

Standing up experiments were also conducted to determine the most efficient strategy for a specific prototype of STriDER. Seven trials were preformed for each method and static torque readings were recorded at twenty different heights. To adequately compare the experimental results, the same parameters were chosen for each standing up strategy. For each experiment, the maximum torque value was recorded and from the results, it may be concluded that for the tested prototype the three feet pushup was the most efficient standing up strategy. On the other hand, the spiral pushup was the least efficient. This conclusion also agrees with the analytical results of the standing up strategies. However, in order to truly validated the analytical results with experiments force control should be implemented since in real scenarios the tangential forces cannot be controlled. Also by adding rollers at the feet the analytical results for no friction cases can be compared with the experimental results.

5.1.2 Conclusions for Gait Planning Considerations

Five major considerations for gait planning were investigated including; stability, dynamics, height of the body, body twisting motion, and swing leg clearance and landing position. As discussed, the robot's static stability is important during a step, as the novel tripedal gait requires the robot to become statically unstable forcing the robot to fall forward and swing its middle leg in between the stance legs and catch the fall. Thus, a quantitative static stability margin was developed to asses the stability of the robot. STriDER can be modeled as a planar four-link inverted pendulum in the sagittal plane by treating the two stance legs as a single link connected to the ground by a revolute joint. In fact, STriDER is inherently an under-actuated mechanical system. The minimum height must allow the swing leg to swing underneath the body as the body rotates 180 degrees without scuffing the ground. The height of the body also affects the speed of the fall. During a step, two pivot lines must be considered; one is the pivot line formed by aligning the stance legs hip abductor joints that allows the body to rotate 180 degrees called the *body pivot line*, while the other is the pivot line formed by the two stance leg's foot contact point that allows the entire robot to pivot called the *stance leg pivot line*. When the *body pivot line* and *stance leg pivot line* are parallel while the robot takes a step, the kinematic analysis is greatly simplified and collision between the swing leg and stance legs is prevented. However, for uneven terrains it might be beneficial for the pivot lines to be skewed, as it may aid the swing leg in avoiding obstacles. Finally, the swing leg's foot path was also considered as the robot takes a step. The swing leg's foot should not scuff the ground during the swing portion of the gait thus, the knee must be bent at certain angles to prevent the foot from touching the ground. Also, when considering a single step an allowable region for the subsequent swings leg's foot contact position must be constrained.

5.2 Overall Recommendations

After analyzing five different standing up strategies, completing experiments and investigating issues for gait planning specific to STriDER, a number of recommendations can be made. From the standing up strategy analysis and experimental results it can be concluded that the most efficient standing up method is the three feet pushup. Thus, when standing on a flat surface it is recommended to use the three feet pushup while keeping the three feet positions as close as possible to the center of the body in order to minimize joint torques. Note that the length ratio between the thigh and the shank really should be decided based on walking performance rather than for standing up. However, the results from this analysis will give insight into the effect of limb length ratio to the motor torque requirements which will still be useful in the design process. If standing up on an incline, however, it is possible that it could be more beneficial to use the two feet pushup. Future work should investigate the effects of different surfaces and terrain geometry when standing up. In fact, strategies that take advantage of dynamics of the robot could be investigated. One of these strategies might include a whipping motion where one leg swings above the body and in return forces the body and the other two legs to rise due to the inertia of this motion. Thus, as the body begins to rise the stance legs push against the ground and the middle whipping leg catches the fall. Also, in order to adequately test the standing up methods, different link lengths and other parameters should be tested during experiments. In the design process, if possible, the range of motion at the joints should be maximized to enable the foot placement positions closer to the center of the body to minimize the motor torque requirements when standing up, and motors with large torque should be used to sustain the required high torques at each joint. In addition, by decreasing the weight of the robot, the task of standing up could be made easier. Also, to accurately record the actuator torques as the robot stands during experiments, torque sensors should be used instead of the inaccurate method of using the motor current information to estimate the torque.

In regards to gait planning, a number of additional considerations could be investigated. More specifically, dynamics should be considered in future work since to correctly generate a gate both kinematics and dynamics must be considered. The strategies and effects on stability for flat terrains, uneven terrain and changes in elevation should be studied. Motion planning for uneven terrains should also be considered in future research. First, gaits for walking and changing directions can be developed by knowing the geometry of uneven surfaces in advance. Then, maps for unknown terrains can be formed by sequentially compiling foot positions for each step. Ultimately, the goal is to establish gaits for unknown surface geometries using reactive approaches.

Bibliography

[1] J.R. Heaston. Design of a novel tripedal locomotion robot and simulation of a dynamic gait for a single step. Masters thesis, Virginia Polytechnic and State University, 2006.

[2] D.W. Hong and D.F Lahr. Synthesis of the body swing rotator joint aligning mechanism for the abductor joint of a novel tripedal locomotion robot. *ASME Mechanisms and Robotics Conference*, September 2007.

[3] J.R. Heaston and D.W. Hong. Design of a novel tripedal locomotion robot and simulation of a dynamic gait for a single step. *ASME Mechanisms and Robotics Conference*, September 2007.

[4] D.W. Hong. Biologically inspired locomotion strategies: Novel ground mobile robots at romela. *2006 URAI International Conference on Ubiquitous Robots and Ambient Intelligence*, October 2006.

[5] P. Ren, I. Morazzani, and D.W. Hong. Forward and inverse displacement analysis of a novel three-legged mobile robot based on the kinematics of in-parallel manipulators. *31st ASME Mechanisms and Robotics Conference*, September 2006.

[6] I. Morazzani, D. Lahr, D.W. Hong, and P. Ren. *Novel Tripedal Mobile Robot and Considerations for Gait Planning Strategies Based on Kinematics.* Springer Verlang, 2007.

[7] T. McGeer. Passive dynamic walking. *International Journal of Robotics Research*, 9(2):62–82, April 1990.

[8] Takahashi Ono and T. Shimada. Selfex-cited walking of a biped mechanism. *International Journal of Robotics Research*, 20(12):953–966, 2001.

[9] Sangwan V. and Agrawal S.K. Differentially flat design of bipeds ensuring limit cycles. *Proceedings of IEEE International Conference on Robotics and Automation*, April 2007.

[10] S.K. Agrawal and V. Sangwan. Design of under-actuated open-chain planar robots for repetitive cyclic motions. *ASME International Design Engineering Technical Conferences and Computers and Information in Engineering Conference*, September 2006.

[11] M.W. Spong and G. Bhatia. Further results on control of the compass gait biped. *International Conference on Intelligent Robots and Systems*, pages 1933–1938, October 2003.

[12] Erin B. Hutchinson, Patrick O. Riley, and David E. Krebs. A dynamic analysis of the joint forces and torques during rising from chair. *IEEE Transactions on Rehabilitation Engineering*, 2(2):49–55, June 1994.

[13] K. M. Kerr, J. A. White, D. A. Barr, and R. A. B. Mollan. Analysis of the sit-stand-sit movement cycle in normal subjects. *Clinical Biomechanics*, 12(4):236–245, 1997.

[14] Jernej Kuzelicki, Milos Zefran, Helena Burger, and Tadej Bajd. Synthesis of standing-up trajectories using dynamic optimization. *Science Direct*, November 2003.

[15] Margaret Schenkman, Richard A Berger, Patrick O Riley, Robert W Mann, and W Andrew Hodge. Whole-body movements during rising to standing from sitting. *Physical Therapy*, 70(10):51–64, 1990.

[16] A Kralji, Jaeger RJ, and Munih M. Analysis of standing up and sitting down in humans: definitions and normative data presentation. *Journal of Biomechanics*, 023(11):1123–38, 1190.

[17] Kai-Nan An, Margaret J. Donkers, Edmund Y.S. Chao, and Bernard F. Morrey. Intersegmental elbow joint load during pushup. *Biomedical Sciences Instrumentation*, pages 69–74, 1992.

[18] Margaret J. Donkers, Kai-Nan An, Edmund Y.S. Chao, and Bernard F. Morrey. Hand position affects elbow joint load during pushup exercise. *Journal of Biomechanics*, 26(6):625–632, 1993.

[19] Kai-Nan An, Sarah L. Korinek, T. Kilpela, and S. Edis. Kinematic and kinetic analysis of pushup exercise. *Biomedical Sciences Instrumentation*, pages 53–57, 1990.

[20] David A. Winter. *Biomechanics and Motor Control of Human Movement*, volume 3rd. John Wiley and Sons, Inc., 2005.

[21] J.R. Heaston, D.W. Hong, I. Morazzani, P. Ren, and G. Goldman. Strider: Self-excited tripedal dynamic experimental robot. *IEEE International Conference on Robotics and Automation*, April 2007.

[22] M.W. Spong and M. Vidyasagar. *Robot Dynamics and Control*. John Wiley and Sons, Inc., 1989.

[23] D.W Hong and R.J. Cipra. Visualization of the contact force solution space for multi-limbed robots. *Journal of Mechanical Design*, 128(1):295–302, 2006.

[24] D.W. Hong and R.J. Cipra. Optimal contact force distribution for multi-limbed robots. *Journal of Mechanical Design,*, 128(3):566–573, 2006.

[25] M.E Worley, P. Ren, C. Sandu, and D.W. Hong. The development of an assessment tool for the mobility of lightweight autonomous vehicles on coastal terrain. *SPIE Defense and Security Symposium*, April 2007.